

High Energy Physics Division Semiannual Report of Research Activities

Semiannual Report Of research Activities

High Energy Physics Division
Argonne National Laboratory

ARGONNE IS OPERATED BY THE UNIVERSITY OF CHICAGO FOR THE U.S. DEPARTMENT OF ENERGY OFFICE OF SCIENCE



About Argonne National Laboratory

Argonne is operated by The University of Chicago for the U.S. Department of Energy Office of Science, under contract W-31-109-Eng-38. The Laboratory's main facility is outside Chicago, at 9700 South Cass Avenue, Argonne, Illinois 60439. For information about Argonne and its pioneering science and technology programs, see www.anl.gov.

Availability of This Report

This report is available, at no cost, at <http://www.osti.gov/bridge>. It is also available on paper to U.S. Department of Energy and its contractors, for a processing fee, from:

U.S. Department of Energy
Office of Scientific and Technical Information
P.O. Box 62
Oak Ridge, TN 37831-0062
phone (865) 576-8401
fax (865) 576-5728
reports@adonis.osti.gov

Disclaimer

This report was prepared as an account of work sponsored by an agency of the United States Government. Neither the United States Government nor any agency thereof, nor The University of Chicago, nor any of their employees or officers, makes any warranty, express or implied, or assumes any legal liability or responsibility for the accuracy, completeness, or usefulness of any information, apparatus, product, or process disclosed, or represents that its use would not infringe privately owned rights. Reference herein to any specific commercial product, process, or service by trade name, trademark, manufacturer, or otherwise, does not necessarily constitute or imply its endorsement, recommendation, or favoring by the United States Government or any agency thereof, Argonne National Laboratory, or The University of Chicago.

Argonne National Laboratory
9700 South Cass Avenue
Argonne, Illinois 60439

**HIGH ENERGY PHYSICS DIVISION
SEMIANNUAL REPORT OF
RESEARCH ACTIVITIES**

January 1 - June 30, 2004

Prepared from information gathered and edited by
The Committee for Publications and Information:

Members: P. Malhotra
J. Norem
R. Rezmer
R. Wagner

October 2004

Abstract

This report describes the research conducted in the High Energy Physics Division of Argonne National Laboratory during the period of January 1 through June 30, 2004. Topics covered here include experimental and theoretical particle physics, advanced accelerator physics, detector development, and experimental facilities research. Lists of Division publications and colloquia are included.

Table of Contents

I.	EXPERIMENTAL RESEARCH PROGRAM	1
A.	EXPERIMENTS WITH DATA	1
	1. Medium Energy Polarization Program	1
	2. Collider Detector at Fermilab	6
	a) Physics	6
	b) Operations	9
	3. The CDF Upgrade Project	10
	a) Run IIb Preparation.....	10
	4. ZEUS Detector at HERA	12
	a) Physics Results.....	12
	b) HERA and ZEUS Operations	17
B.	EXPERIMENTS IN PLANNING OR CONSTRUCTION	18
	1. MINOS Main Injector Neutrino Oscillation Search	18
	2. ATLAS Detector Research & Development.....	24
	a) Overview of ANL ATLAS Tile Calorimeter Activities	24
	3. ATLAS Calorimeter Engineering Design and Analysis.....	24
	a) Calorimeter EBA Pre-Assembly.....	26
	b) Work in Collaboration with ATLAS Technical Coordination	27
	c) Services Design and Installation.....	30
C.	NEW PROJECTS AND DETECTOR DEVELOPMENT	32
	1. Computational Projects.....	32
	a) ATLAS Computing.....	32
	2. Detector Development for the Linear Collider	33
	a) Monte Carlo Simulation Studies.....	33
	b) Development of Resistive Plate Chambers as Active Medium of a Digital Hadron Calorimeter	34
	3. Electronics Support Group.....	39
	4. Experiment to Measure the θ_{13} Neutrino Mass-Mixing Parameter.....	42
	a) NO ν A (NuMI Off-axis ν_e Appearance) Experiment.....	42
	b) A New Reactor Neutrino Experiment.....	46
	5. Cosmic Ray Experiments.....	51
	a) VERITAS.....	51
	b) Auger.....	52
II.	THEORETICAL PHYSICS PROGRAM	53
A.	THEORY	53
	1. Higgs Boson Production in Weak Boson Fusion at Next-to-Leading Order	53
	2. Constraints on the Light Gluino Mass from a Global Analysis of Hadronic Data	55
	3. Transverse Momentum Distribution of Upsilon Production	56
	4. Aspen Winter Meeting, 2004.....	57

5.	Theory Workshop on Supersymmetry, Higgs Bosons, and Extra Dimensions	58
6.	Lattice Computation of Spin Correlations in NRQCD Color-Octet Matrix Elements.....	59
7.	Lattice QCD	60
8.	Electroweak Baryogenesis and Dark Matter in the nMSSM.....	62
9.	Noncommutativity and the Ultrahigh-Energy Cosmic Ray & TeV Photon Paradoxes	64
III.	ACCELERATOR RESEARCH AND DEVELOPMENT	66
A.	ARGONNE WAKEFIELD ACCELERATOR PROGRAM	66
1.	The Argonne Wakefield Accelerator Facility Status.....	69
2.	Development of externally-driven, 11.424 GHz, dielectric-loaded structures and high-power tests at NRL.	
B.	MUON COLLIDER EFFORT	70
a)	Development of the Breakdown Model	70
b)	Booster Improvements at Fermilab	70
IV.	PUBLICATIONS	72
A.	Books, Journals, and Conference Proceedings	72
B.	Major Articles Submitted for Publication.....	76
C.	Papers or Abstracts Submitted to Conferences.....	79
D.	Technical Reports and Notes	82
V.	COLLOQUIA AND CONFERENCE TALKS	84
VI.	HIGH ENERGY PHYSICS COMMUNITY ACTIVITIES	90
VII.	HIGH ENERGY PHYSICS DIVISION RESEARCH PERSONNEL.....	94

I. EXPERIMENTAL RESEARCH PROGRAM

I.A. EXPERIMENTS WITH DATA

I.A.1. Medium Energy Polarization Program

The medium-energy polarization group is primarily interested in the polarized proton program at the Relativistic Heavy Ion Collider (RHIC) at Brookhaven. This is a continuation of our more than a quarter century of work on spin physics. In support of the RHIC polarization program, we have been involved in polarization development studies at the Alternating Gradient Synchrotron (AGS, the injector for RHIC) for more than a decade. In more recent years we have also collaborated on the construction, installation, and commissioning of an endcap electromagnetic calorimeter (EEMC) for the STAR detector to enhance capabilities for jet, π° , and direct-photon detection. We were primarily responsible for the construction of the EEMC shower maximum detector (SMD), which will be essential for π°/γ discrimination at high energies.

The early part of 2004 was dominated by the RHIC run, with Au+Au collisions at $\sqrt{s_{NN}} = 200$ and 63 GeV from January through early April followed by polarized proton running through May 15. This was the first run following the installation of the remaining 2/3 of the EEMC detector elements and of the first 1/3 of the MAPMT electronics for readout of the SMD and the pre- and post-shower layers. The remaining MAPMT electronics are being installed during the 2004 summer shutdown. The ANL group played an important role in calibration and commissioning of the SMD and in the development of many online histograms to monitor the performance of the EEMC.

The proton run was primarily a beam development run. It was immediately preceded by a shutdown period of a few days for installation of the polarized gas jet target. Our group assisted with the operation of this target, which was successfully used to calibrate the proton beam polarizations at 24 and 100 GeV. The calibrations will be repeated with higher precision in 2005. During the proton run, the accelerator physicists made great progress. One significant accomplishment was the development of a new accelerator tune for RHIC which increased the beam polarization at the top energy. Another was the commissioning of a warm helical partial Siberian snake which replaced the solenoidal partial snake partially funded by ANL over ten years ago.

Although the run focused on beam development, STAR acquired 400 nb⁻¹ of longitudinally polarized proton collisions. These data will be valuable for understanding the performance and calibration of the SMD, and Jaki Hostler, an undergraduate student from Berea College, has joined our group at Argonne during the summer of 2004 to assist with these studies. The Argonne group also plans to use these data to test π° reconstruction algorithms. We expect that these data will provide an initial measurement

of the double-spin asymmetry for π^0 production, which has sensitivity to different models of the gluon polarization within the proton. At a meeting of the EEMC group in May, we agreed that Bob Cadman of ANL and a postdoctoral fellow from Indiana University would work on independent analyses of these data. This is a modification of our earlier plans to study direct-photon production in d+Au data taken in 2003 to probe the modification of the gluon distribution in nuclei. Although we remain interested in that topic, our colleagues have found problems with the 2003 data from the barrel electromagnetic calorimeter (the EEMC did not have electronics for the SMD modules in 2003). Because of these difficulties, it is not clear whether it is worthwhile to attempt to extract photon cross sections from those data.

We also continued to support the polarization development in the AGS. Our primary contribution has been through the operation and maintenance of the so-called E880 polarimeter in the AGS, now being used to calibrate the Coulomb-Nuclear Interference polarimeter which was installed in the AGS before the 2003 run. We have been working on absolute calibrations of the E880 polarimeter to resolve apparent discrepancies in the low-energy analyzing powers, and during the 2004 run we completed an absolute calibration at $G\gamma = 12.5$ ($p \sim 6.5$ GeV/c).

Members of our group also served as detector operator, shift leader, and period coordinator at STAR during the RHIC run this year. Hal Spinka of ANL continued to serve as co-convenor of the STAR spin physics working group.

With the end of the run our focus turned to the future. For example, we have begun to look for a role for our group in a proposed tracking upgrade which will allow measurement of parity violating asymmetries in real W boson production. This measurement is sensitive to the flavor dependence of quark and anti-quark helicities in the proton. As part of this effort Hal Spinka and Dave Underwood plan to work on upgrading STAR simulation software to improve the characterization of the time projection chamber electronics immediately in front of the EEMC. This is relevant both to the tracking upgrade and to our understanding of already existing EEMC data, and at the May meeting the EEMC group agreed this was an important task. The simulation of the SMD response will also be improved as part of this effort. This work will follow up on the efforts of a Master's degree student from Ball State University, Chris McClain, who has been supported by our group to work on SMD simulations. He will continue working through the summer to finish his thesis on this topic.

Eight STAR (-related) papers were published in this period, and an additional six were submitted for publication. Four Crystal Ball papers were also published. A summary of some of these papers is given below.

One of the physics articles (“Cross Sections and Transverse Single-Spin Asymmetries in Forward Neutral-Pion Production from Proton Collisions at $\sqrt{s} = 200$ GeV;” Phys. Rev. Lett. **92**, 171801 (2004)) reports measurements of the production of forward high energy π^0 s from transversely polarized pp collisions. The prototype EEMC consisting of 3×4 towers and a SMD was located to cover $\eta \sim 3.4 - 4.0$ for these data. The derived cross section is generally consistent with next-to-leading order perturbative QCD calculations, as shown in Fig. 1. The analyzing power for

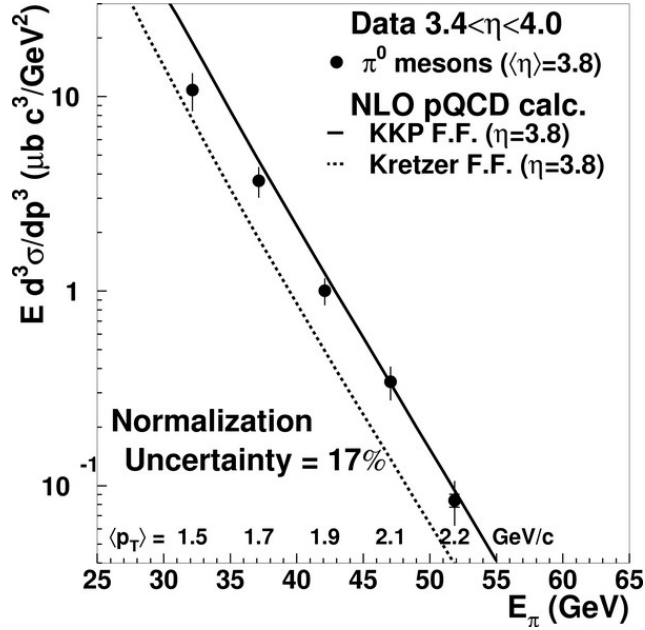


Figure 1. Inclusive π^0 production cross section as a function of π^0 energy. The average transverse momentum is correlated with the energy, as the prototype EEMC was located at a fixed η . The inner error bars are statistical, and are smaller than the symbols for most points. The outer error bars combine these with the energy dependent systematic errors. The curves are next-to-leading order pQCD calculations.

inclusive, identified π^0 -production and for total energy in the prototype EEMC is presented in Fig. 2 for an assumed average beam polarization of 0.16. It is small at x_F below 0.3, and becomes positive and large at higher x_F , similar to the trend in the FNAL E704 data at $\sqrt{s} \sim 19$ GeV. This is the first significant spin result seen for particles produced with $p_T > 1$ GeV/c at a polarized proton collider.

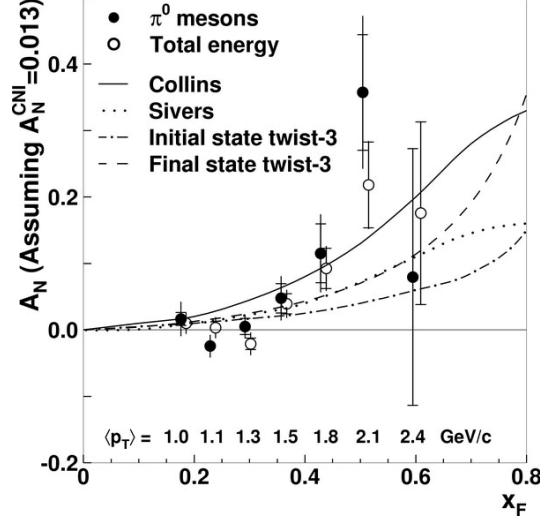


Figure 2. Analyzing powers versus Feynman x . The solid circles are for identified π^0 s, and the open circles for the total energy, shifted by $x_F + 0.01$. The inner error bars are statistical, and the outer combine these with point-to-point systematic errors. The curves are from pQCD models evaluated at $p_T = 1.5 \text{ GeV/c}$.

A set of four published STAR papers describe identified particle production in heavy ion collisions. One (“ ρ^0 Production and Possible Modification in Au + Au and p + p Collisions at $\sqrt{s_{NN}} = 200 \text{ GeV}$,” Phys. Rev. Lett. **92**, 092301 (2004)) reports results on $\rho^0 (770) \rightarrow \pi^+ \pi^-$ production in p + p interactions and the first direct measurement in heavy ion (peripheral Au + Au) collisions. The reconstructed mass seems to increase slightly as a function of p_T and to decrease with multiplicity; see Fig. 3. Similar mass shifts have

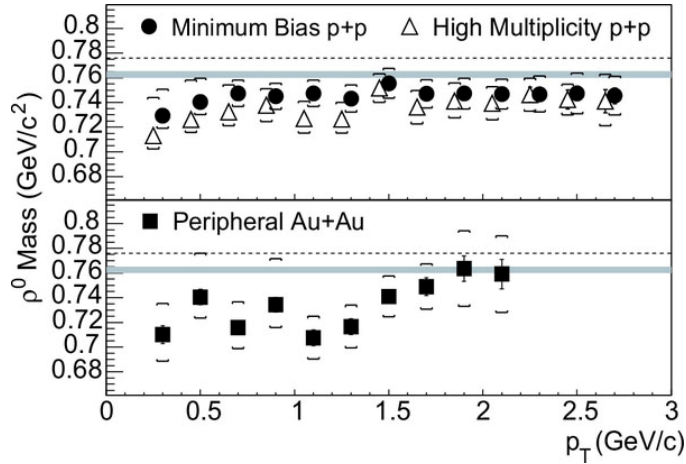


Figure 3. The ρ^0 mass as a function of transverse momentum for minimum bias p + p (filled circles), high multiplicity p + p (open triangles), and peripheral Au + Au (filled squares) collisions. The error bars indicate the estimated systematic uncertainty. The ρ^0 mass was obtained by fitting the data to a relativistic p-wave Breit-Wigner function times a factor which accounts for phase space. The dashed lines represent the average of the ρ^0 mass measured in $e^+ e^-$ and the shaded areas indicate the ρ^0 mass measured in p + p collisions.

been seen previously in $e^+ e^-$ and $p + p$ interactions. Another paper (“Multistrange Baryon Production in Au + Au Collisions at $\sqrt{s_{NN}} = 130$ GeV,” Phys. Rev. Lett. **92**, 182301 (2004)) presents transverse mass spectra ($m_{\perp} = \sqrt{p_T^2 + m^2}$) and midrapidity yields for Ξ s and Ω s. They are identified by their decays to $\Lambda\pi$ and ΛK , respectively, with the Λ decay to $p + \pi$. Some spectra are shown in Fig. 4. The other two papers are “Identified Particle Distributions in pp and Au + Au Collisions at $\sqrt{s_{NN}} = 200$ GeV,” Phys. Rev. Lett. **92**, 112301 (2004) and “Kaon Production and Kaon to Pion Ratio in Au + Au Collisions at $\sqrt{s_{NN}} = 130$ GeV,” Phys. Lett. **B595**, 143 (2004).

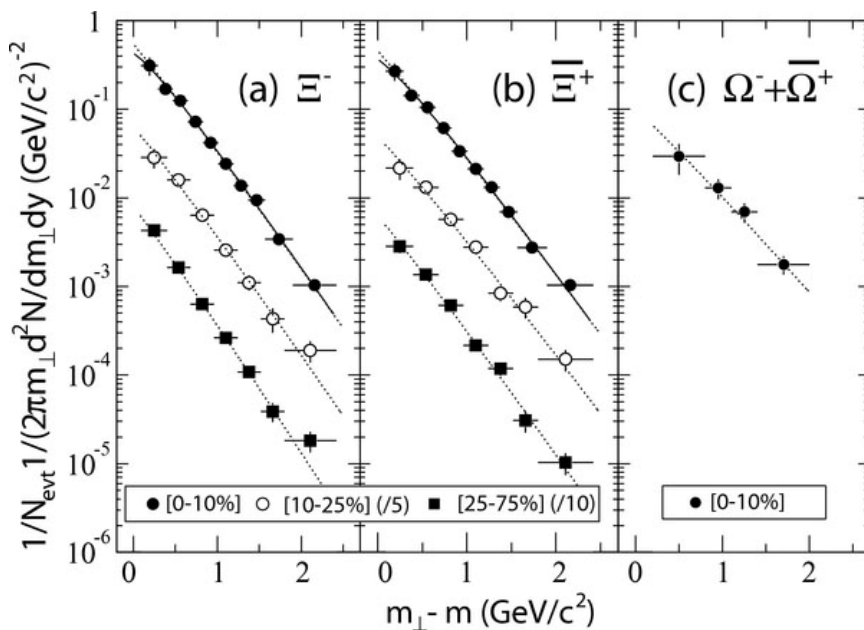


Figure 4. Transverse mass spectra for Ξ and Ω baryons at three centrality classes (0 – 10, 10 – 25, and 25 – 75%). Points are drawn at the bin centers, and the horizontal bars indicate the bin sizes. The dashed curves are Boltzmann fits, and the solid curves are hydrodynamically inspired model fits to the spectra.

The remaining STAR papers include two on particle flow (“Azimuthal Anisotropy at the Relativistic Heavy Ion Collider: the First and Fourth Harmonics,” Phys. Rev. Lett. **92**, 062301 (2004) and “Particle-Type Dependence of Azimuthal Anisotropy and Nuclear Modification of Particle Production in Au + Au Collisions at $\sqrt{s_{NN}} = 200$ GeV,” Phys. Rev. Lett. **92**, 052302 (2004)). Finally, a paper (“Estimating Relative Luminosity for RHIC Spin Physics,” Nucl. Instrum. Meth. **A530**, 536 (2004)) was published showing that the standard formula used at CDF and D0 to correct luminosity monitor counts for high rates is biased, but this bias is acceptably small ($< 10^{-4}$) for anticipated RHIC polarized proton running conditions.

Four papers were also published from results with the Crystal Ball detector at Brookhaven. “Differential Cross Section of the Charge-Exchange Reaction $\pi^- p \rightarrow \pi^0 n$ in the Momentum Range From 148 to 323 MeV/c” (Phys. Rev. **C69**, 055206 (2004)) reports 160 new data points for this reaction at 8 momenta. Typical statistical uncertainties are 2 – 6 %, and systematic errors are estimated to be 3 – 6 %. These results nearly double the data base for these measurements in this momentum interval. A second paper, “ γ Scaling in Quasifree Pion-Single-Charge Exchange,” (Phys. Rev. **C69**, 064612 (2004)) analyzes the results in terms of a single quasifree elastic collision (γ scaling). The angular dependence of the data is used to separate the spin and nonspin isovector responses. Finally, the remaining two articles (“Measurement of $\pi^- p \rightarrow \pi^0 \pi^0 n$ From Threshold to $p_\pi = 750$ MeV/c,” Phys. Rev. **C69**, 045202 (2004) and “Reaction $K^- p \rightarrow \pi^0 \pi^0 \Lambda$ from $p_K = 514$ to 750 MeV/c,” Phys. Rev. **C69**, 042202(R) (2004)) analyze these two reactions to search for evidence of a $f_0(600)$ or σ meson. The Dalitz plots in both cases are highly nonuniform, and suggest that the final states are dominantly produced via $\pi^0 \Delta^0(1232)$ and $\pi^0 \Sigma^0(1385)$, respectively.

(H. M. Spinka and R. V. Cadman)

I.A.2. Collider Detector at Fermilab

a) Physics

During the spring we collected total data samples surpassing 400 pb^{-1} . Signs of ageing were found in the drift chambers; this was eventually mitigated by adding a small amount of oxygen to the Argon/ethane. About 90 pb^{-1} was collected with the inner layers of the drift chamber running at reduced voltage. The first 200 to 250 pb^{-1} were used in a wide variety of analyses.

The analysis of low transverse momentum J/Ψ production which Tom LeCompte has been pushing along with a b to J/Ψ cross section was blessed and is approaching publication. There is no longer any ambiguity in interpreting the b cross section, and indeed, the b cross section which historically has been regarded as being in excess of QCD predictions is now completely compatible with the latest QCD predictions

Masa Tanaka and Barry Wicklund continue the investigation of systematic effects in lifetimes as measured in semileptonic modes, which are systematically shorter than fully reconstructed mode measurements. Understanding the semileptonic sample will be a key to being able to do precise tagged mixing studies. Bob Wagner is investigating the $J/\Psi\eta$ decay mode. While B_s mixing may take a while to understand, there is a preliminary indication of separation into different lifetime states, shown in Fig 1.

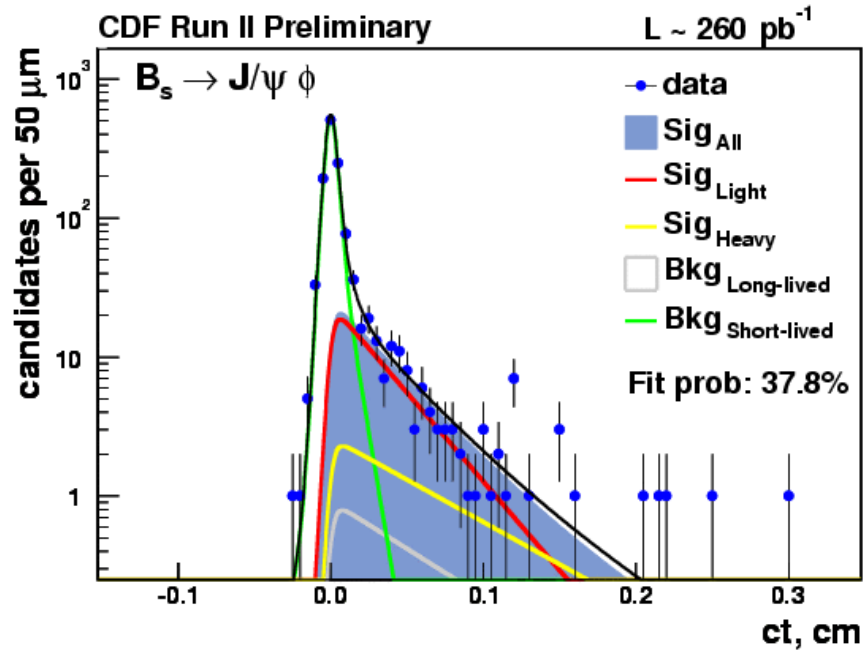


Figure 1. Lifetime for B_s candidates is analyzed in terms of separate heavy and light states which are separated angular distributions picking out CP states. The lifetime difference inferred is larger than expected.

Larry Nodulman is working with a group predominantly from Toronto and Duke on the run 2 W mass measurement. An attempt was made to get to a blessed result for summer conferences but problems with z view alignment and the RESBOS simulation built into the fitting proved daunting. The electron and muon first round W/Z cross section analysis, shown Fig. 2, is no longer preliminary.

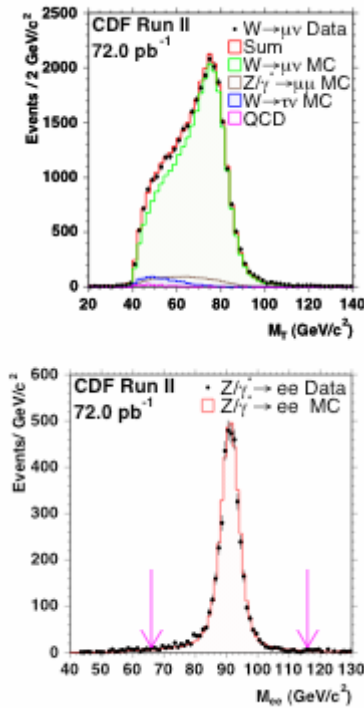


Figure 2. Transverse mass for the muon W sample and the electron Z sample as submitted for publication of the W and Z cross section results.

Steve Kuhlmann and Bob Blair continue to work with the QCD and exotics photon analysis group. The exotics group has used the Z lineshape to set limits on possible Z' production, shown in Fig. 3.

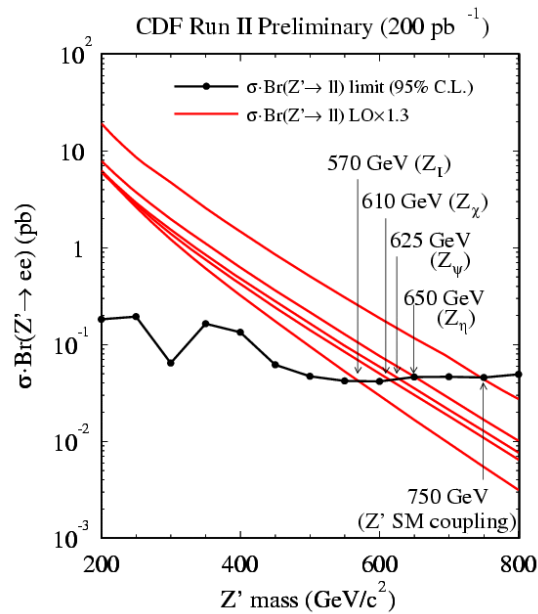


Figure 3. As the high side tail of the Z peak in electron pairs is well behaved, limits on possible Z' production can be inferred.

Tom, Masa and Barry have continuing subgroup leadership roles in b physics. Larry has been appointed to head the internal review for lepton plus jets top mass measurement with templates.

b) Operations

Data taking operations continued through the spring. Luminosity continued to improve. The COT wire age problem was stopped and eventually recovered allowing normal full operation to resume with full function restored. Luminosity delivered and recorded is shown in Fig. 4. The COT status is illustrated in Fig. 5.

Masa Tanaka became a deputy head of operations. Larry Nodulman continued as calorimeter co-leader, Karen Byrum continued to lead the shower maximum support, and Karen, Masa and Steve Kuhlmann were active in supporting the Level 2 Trigger. Bob Wagner continued servicing central EM PMTs.

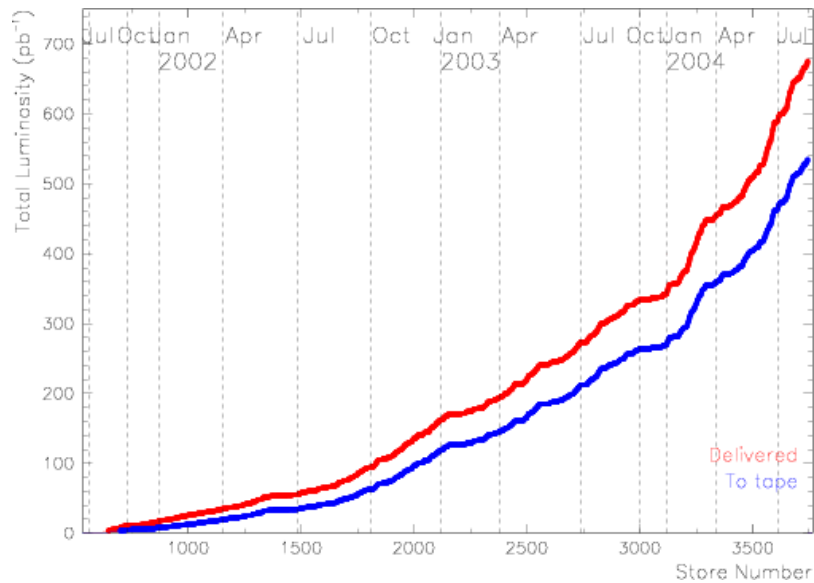


Figure 4. Accumulated luminosity delivered to and recorded by CDF in Run II.

Larry continued to provide offline and online calibrations for the central EM calorimeter as well as cross checks of the other calorimeters. Some adjustment of strategy was needed to calibrate the reduced COT data.

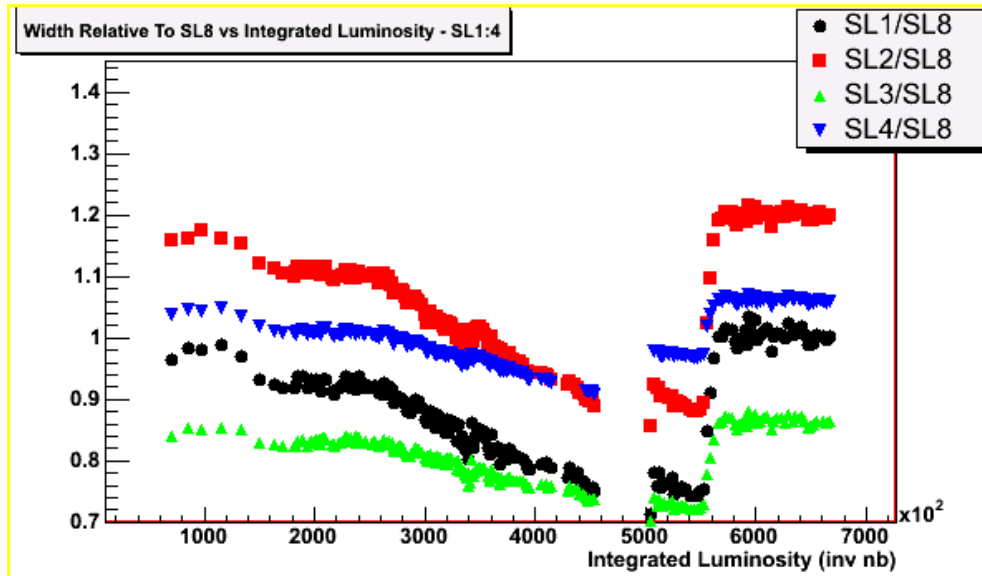


Figure 5. Pulse width (charge) ratios for the inner superlayers of COT with respect to the outermost layer. The gap represents a period of HV reduced or off. After the gap faster flow with recirculation was installed, and the introduction of oxygen is apparent.

Several members of the HEP division have been actively supporting the Tevatron program at Fermilab, Jim Norem helping with the booster, Wei Gai helping with electron cooling.

I.A.3. The CDF Upgrade Project

a) Run IIb Preparation

Mass production of preradiator panels got started and half of the panels were produced and tested using the MINOS scanner, see Fig. 6. Production of crack panels was ready to get started. The STAR cosmic ray test stand was used to confirm the light

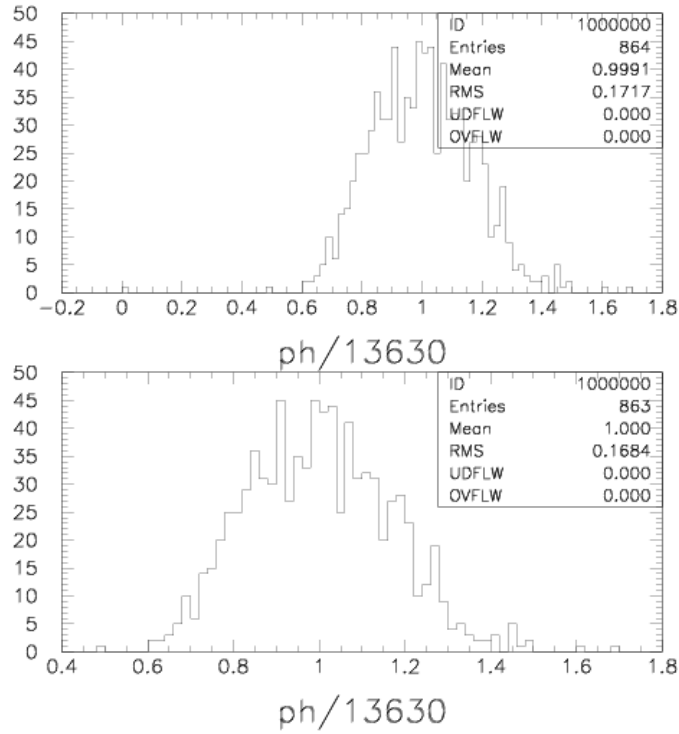


Figure 6. Peak current for pads of the first 16 preradiator panels tested on the MINOS scanner. Top plot includes one broken fiber zero tower.

yield for minimum ionizing particles, shown in Fig. 7. The production schedule looked good for having parts ready to install in fall shutdown. The scaffolding design for

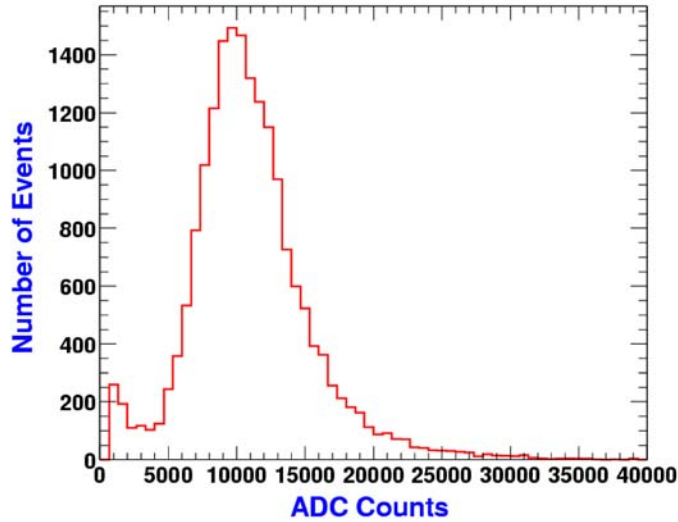


Figure 7. Minimum ionizing peak seen in a preradiator tile during a long cosmic ray run on the STAR stand.

installation in the pit, Fig. 8, had promise that although getting inside would not be easy, once in, installing panels would be much more convenient than replacing crack chambers in the assembly hall before Run II. A large workforce of collaborators and volunteers was being planned to do the installation.

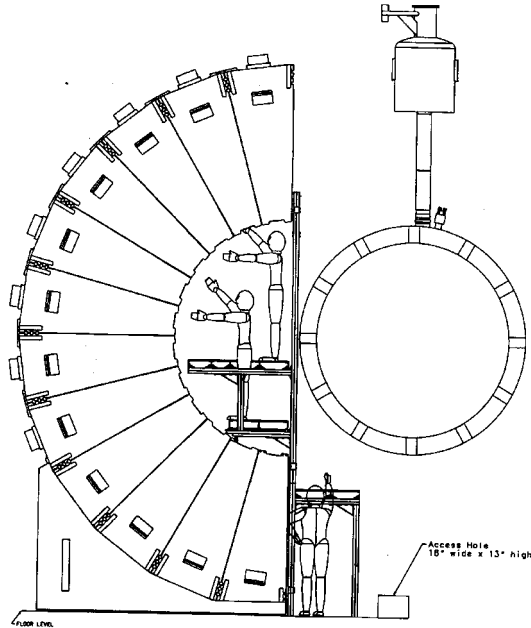


Figure 8. Scaffolding designed for installation on the front face of the CDF central calorimeter.

(L. Nodulman)

I.A.4. ZEUS Detector at HERA

a) Physics Results

Six papers were published in this period and six more manuscripts were submitted for publication. In the following, we shall summarize some of the published papers.

i) *Measurement of $D^{*\pm}$ Production in Deep Inelastic $e^\pm p$ Scattering at HERA*

Inclusive production of $D^{*\pm}$ (2010) mesons in deep inelastic scattering has been measured with the ZEUS detector at HERA using an integrated luminosity of 81.9 pb^{-1} . The decay channel $D^{*+} \rightarrow D^0 \pi^+$ with $D^0 \rightarrow K^- \pi^+$ and corresponding antiparticle decay were used to identify D^* mesons. Differential D^* cross sections with $1.5 < Q^2 < 1000 \text{ GeV}^2$ and $0.02 < y < 0.7$ in the kinematic region $1.5 < p_T(D^*) < 15 \text{ GeV}$ and $|\eta(D^*)| < 1.5$ are compared to different QCD calculations incorporating different parameterizations of the parton densities in the proton. The data show sensitivity to the gluon distribution in the proton and are reasonably well described by next-to-leading order QCD with the ZEUS NLO QCD fit used as the input parton density in the proton. The observed cross section is extrapolated to the full kinematic region in $p_T(D^*)$ and $\eta(D^*)$ in order to determine the open-charm contribution $F_2^{\text{cc}}(x, Q^2)$, to the proton structure function, F_2 . Figure 1 compares the measured open-charm structure function F_2^{cc} at values of x between 0.00003 and 0.03 as a function of Q^2 with the results of the ZEUS NLO QCD fit. The agreement between data and prediction is satisfactory. Since, at low Q^2 , the uncertainties of the data are comparable to those from the QCD fit, the measured differential cross sections in y and Q^2 should be used in future fits to constrain the gluon density.

ii) *Bose-Einstein Correlations in One- and Two-Dimensions in Deep Inelastic Scattering*

Bose-Einstein correlations in one- and two-dimensions have been studied in deep inelastic ep scattering events using an integrated luminosity of 121 pb^{-1} . The correlations are independent of the virtuality of the exchanged photon, Q^2 , in the range $0.1 < Q^2 < 8000 \text{ GeV}^2$. There is no significant difference between the correlations in the current and target regions of the Breit frame for $Q^2 > 100 \text{ GeV}^2$. The two-dimensional shape of the particle-production source was investigated, and a significant difference between the transverse and longitudinal dimensions of the source is observed. This difference also shows no Q^2 dependence. The results demonstrate that Bose-Einstein interference, and hence the size of the particle-production source, is insensitive to the hard subprocess at the interaction vertex.

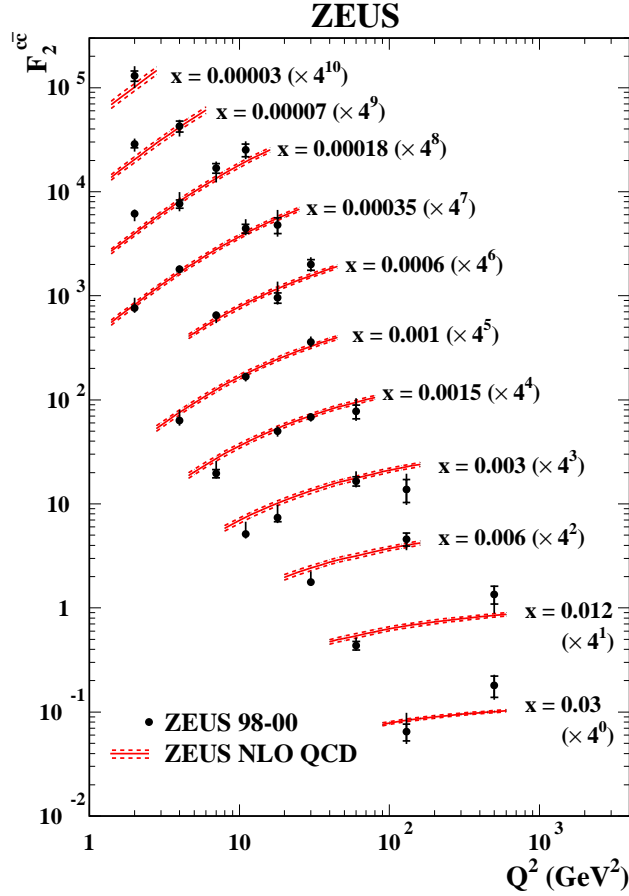


Figure 1. The measured F_2^{cc} at x values between 0.00003 and 0.03 as a function of Q^2 compared to the ZEUS NLO QCD fit to inclusive deep inelastic scattering data. The lower and upper curves show the fit uncertainty propagated from the experimental uncertainties of the fitted data.

iii) *Bose-Einstein Correlations in One- and Two-Dimensions in Deep Inelastic Scattering*

Bose-Einstein correlations in one- and two-dimensions have been studied in deep inelastic ep scattering events using an integrated luminosity of 121 pb^{-1} . The correlations are independent of the virtuality of the exchanged photon, Q^2 , in the range $0.1 < Q^2 < 8000 \text{ GeV}^2$. There is no significant difference between the correlations in the current and target regions of the Breit frame for $Q^2 > 100 \text{ GeV}^2$. The two-dimensional shape of the particle-production source was investigated, and a significant difference between the transverse and longitudinal dimensions of the source is observed. This difference also shows no Q^2 dependence. The results demonstrate that Bose-Einstein interference, and hence the size of the particle-production source, is insensitive to the hard subprocess at the interaction vertex.

iv) *The dependence of Dijet Production on Photon Virtuality in ep Collisions at HERA*

The dependence of dijet production on the virtuality of the exchanged photon, Q^2 , has been studied by measuring dijet cross sections in the range $0 \leq Q^2 \leq 2000 \text{ GeV}^2$ using an integrated luminosity of 38.6 pb^{-1} . The cross sections were measured for jets with transverse energy $E_T^{\text{jet}} > 7.5$ and 6.5 GeV and pseudorapidities in the photon-proton centre-of-mass frame in the range $-3 < \eta^{\text{jet}} < 0$. The variable x_γ^{obs} , a measure of the photon momentum entering the hard process, was used to enhance the sensitivity of the measurement to the photon structure. The Q^2 dependence of the ratio of low- to high- x_γ^{obs} events is shown in Figure 2 compared to next-to-leading order QCD calculations. The calculations are found to generally underestimate the low- x_γ^{obs} contribution relative to that at high x_γ^{obs} . In contrast, Monte Carlo models based on leading-logarithmic parton showers, using a partonic structure for the photon which falls smoothly with increasing Q^2 , provide a qualitative description of the data.

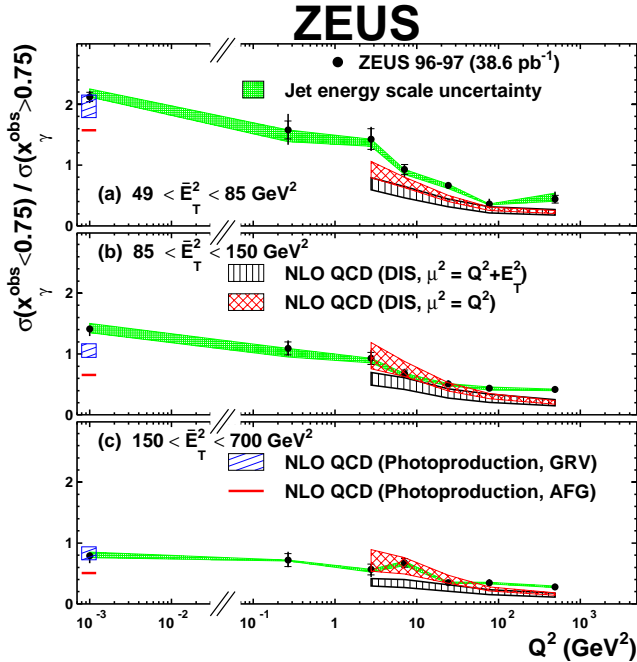


Figure 2. Measured ratio $R = \sigma(x_\gamma^{\text{obs}} < 0.75) / \sigma(x_\gamma^{\text{obs}} > 0.75)$ as a function of Q^2 in different regions of average jet transverse momentum. The NLO QCD calculations of DISASTER++ with $\mu^2 = Q^2 + (E_T^{\text{jet}})^2$ and $\mu^2 = Q^2$ as well as the Frixiere and Ridolfi predictions for the photoproduction region are shown.

v) *Isolated Tau Leptons in Events with Large Missing Transverse Momentum at HERA*

A search for events containing isolated tau leptons and large missing transverse momentum, not originating from the tau decay, has been performed using 130 pb^{-1} of integrated luminosity. The search looked for isolated tracks coming from hadronic tau decays. Observables based on the internal jet structure were exploited to discriminate between tau decays and quark- or gluon-induced jets. Three tau candidates were found,

while $0.40^{+0.12}_{-0.13}$ were expected from Standard Model processes, such as charged current deep inelastic scattering and single W^\pm -boson production. To search for heavy-particle decays, a more restrictive selection was applied to isolate tau leptons produced together with a hadronic final state with high transverse momentum. Two candidate events survive, while 0.20 ± 0.05 events are expected from Standard Model processes. Figure 3 shows the event display of one of the surviving tau candidates.

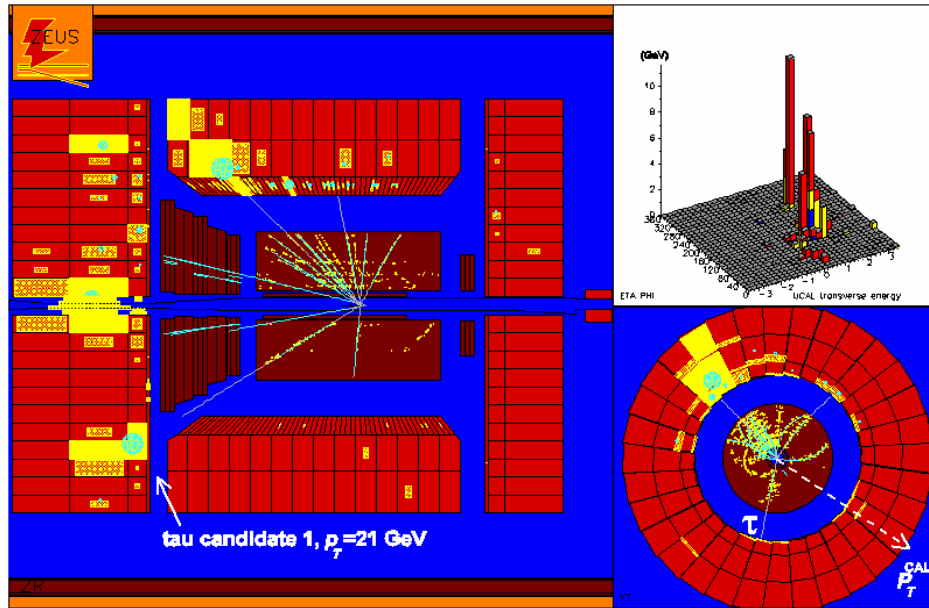


Figure 3. Tau candidate event with tau transverse momentum $p_T^{\text{tau}} = 21$ GeV. The energy deposition in the calorimeter is proportional to the size and density of the shading in the calorimeter cells. The lego plot shows the calorimeter energy deposition projected into the $\{\eta, \phi\}$ -plane. In the x-y view, only the energy deposition in the barrel calorimeter is shown. The dashed arrow in the x-y view indicates the direction of the missing transverse momentum in the calorimeter, p_T^{cal} .

vi) *Search for QCD-Instanton Induced Events in Deep Inelastic ep Scattering at HERA*

A search for QCD-instanton-induced events in deep inelastic scattering has been performed using data corresponding to an integrated luminosity of 38 pb^{-1} . A kinematic range defined by cuts on the photon virtuality, $Q^2 > 120 \text{ GeV}^2$, and on the Bjorken scaling variable, $x > 10^{-3}$, has been investigated. The QCD-instanton-induced events were modeled by the Monte Carlo generator QCDINS. Figure 4 shows the kinematics of an instanton-induced event, where I stands for instanton. A background-independent, conservative 95% confidence level upper limit for the instanton cross section of 26 pb is obtained, to be compared with the theoretically expected value of 8.9 pb.

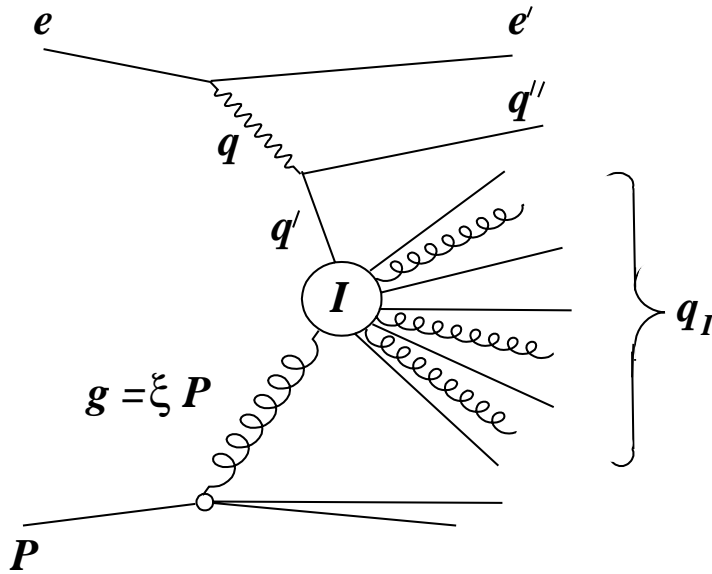


Figure 4. Kinematics of QCD-instanton induced events, where I denotes the instanton.

b) HERA and ZEUS Operations

The first half of 2004 was dedicated to the delivery of luminosity for the colliding beam experiments. The machine constantly improved its performance reaching peak luminosities of $3.7 \cdot 10^{31} \text{ cm}^{-2}\text{s}^{-1}$ and delivering an average of $0.44 \text{ pb}^{-1}/\text{day}$. The operational efficiency on a day-to-day basis was satisfactory; however, several more serious problems, such as coasting beams and grounding problems of the proton ring, surfaced. These problems are being addressed and will ultimately lead to an improved performance of the machine.

The background conditions which have prevented machine operation with high beam currents in the past, have drastically improved after the shutdown and are not anymore considered a concern. While the machine was commissioned and operated with positrons after the 2003 shutdown, the decision of switching over to electrons after the machine shutdown in summer 2004 has now been finalized.

The ZEUS detector is performing well. The new components, i.e. the Micro-vertex detector and the forward Straw Tube Tracker, are being integrated fully into the ZEUS tracking system. Tracks have been reconstructed with segments in the Micro-vertex detector, the Straw Tube Tracker and the Central Tracking Detector

(J. Repond)

I.B. EXPERIMENT IN PLANNING OR CONSTRUCTION

I.B.1. MINOS - Main Injector Neutrino Oscillation Search

The phenomenon of neutrino oscillations allows the three flavors of neutrinos to mix as they travel through space or matter. The MINOS experiment will use a Fermilab muon neutrino beam to study neutrino oscillations with higher sensitivity than any previous experiment. MINOS is optimized to explore the region of neutrino oscillation parameter space (values of the Δm^2 and $\sin^2(2\theta)$ parameters) suggested by atmospheric neutrino experiments. To accomplish this, the experiment compares the rates and characteristics of neutrino interactions in a 980-ton “near” detector, close to the source of neutrinos at Fermilab, and a 5400-ton “far” detector, 735 km away in the underground laboratory at Soudan, Minnesota. The MINOS detectors are steel-scintillator sandwich calorimeters with toroidally magnetized 1-inch thick steel planes. The detectors use extruded plastic scintillator with fine transverse granularity (4-cm wide strips) to provide both calorimetry (energy deposition) and tracking (topology) information. The neutrino beam and MINOS detectors are being constructed as part of the NuMI (Neutrinos at the Main Injector) Project at Fermilab.

Argonne physicists and engineers have been involved in many aspects of MINOS construction during the past decade: scintillator-module factory engineering, near-detector scintillator-module fabrication, near-detector front-end electronics, near- and far-detector installation and the construction and installation of neutrino beamline components. The group has played a major role in the calibration of near-detector electronics in a charged-particle test beam at CERN, as part of the MINOS CalDet program. Figure 1 shows the excellent agreement obtained between the energy resolutions measured at CalDet and the expected values, for both electrons and charged pions. Argonne physicists are now working with groups from Indiana University and the University of Minnesota to measure the ratio of positive and negative cosmic-ray muon fluxes with data from the MINOS far detector. Finally, the group has begun to devote considerable effort to the design of next-generation neutrino experiments, as described in the Detector Development section of this report.

MINOS detector work was highlighted by several important achievements during the first half of 2004. At Soudan, the far detector continued to record high quality data on cosmic-ray muons and atmospheric-neutrino interactions, with an average duty cycle exceeding 90%. As described in previous reports, the magnetization of steel planes in the MINOS far detector enables a unique search for CPT symmetry violation in atmospheric neutrino oscillations. During a five-year exposure, which began in 2003, the

experiment will search for CPT-violating differences in the oscillations of muon neutrinos and muon antineutrinos. The MINOS far detector is the only atmospheric neutrino experiment able to distinguish between positive and negative muons from charged current neutrino interactions.

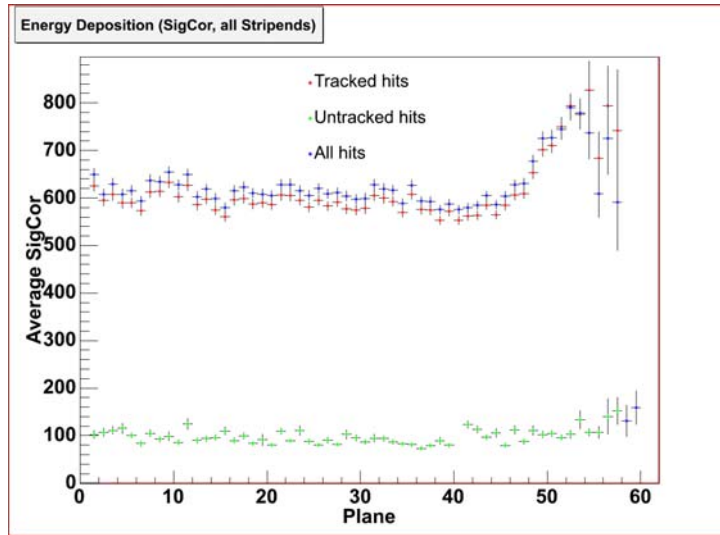
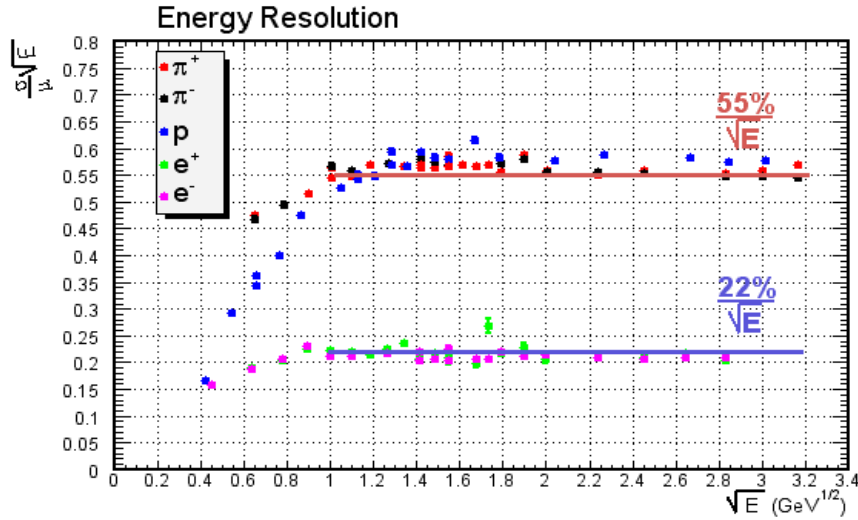


Figure 1. MINOS detector energy resolution. The top graph shows a comparison between the energy resolutions obtained from the MINOS CalDet test beam exposure at CERN (data points) and the expected performance (horizontal lines), for charged pions (upper curve) and electrons (lower curve). The bottom graph shows the energy deposition along stopping muon tracks as they move through the planes of the CalDet detector. MINOS will use stopping cosmic-ray muons to obtain the relative energy calibrations of the near and far detectors. (Figures are taken from the May 2004 presentation of MINOS collaborator Mike Kordosky, from Texas-Austin, at the Denver APS meeting.)

During 2004 the Argonne group has continued to focus its effort at Fermilab, where the installation of MINOS near detector planes began in April and is scheduled for completion in late summer. Argonne physicists and engineers have played an important part in the installation and commissioning of the near detector electronics and data acquisition systems. The Argonne electronics group completed the fabrication of front-end electronics in 2003 and finished the associated checkout in early 2004. The group's work to implement various electronics modifications needed to complete detector commissioning is slowing winding down. The near detector has now recorded its first cosmic ray events and is making routine use of light injection and other calibration systems for commissioning studies as additional detector planes are mounted. Figure 2 shows the MINOS Collaboration data-acquisition team in front of the partially completed detector.



Figure 2. MINOS near detector installation. The Argonne-Oxford-Rutherford-Sussex data acquisition team poses in front of the partially installed near detector. A fully instrumented detector plane, with five Argonne-built scintillator-strip modules is shown. The magnet coil will be installed through the central hole (with the survey fiducial mark) after all planes have been mounted.

The MINOS Collaboration presented preliminary results from its first physics analyses at two major conferences in the first half of 2004: the annual meeting of the American Physical Society in Denver and the Neutrino 2004 conference in Paris. The

highlight of these presentations was the first MINOS observation of atmospheric neutrino events, which is the subject of two MINOS Ph.D. theses (on upward-going muons by Brian Rebel at Indiana University and on fully-contained events by Caius Howcroft at the University of Cambridge). Other MINOS talks at these meetings described test beam results on detector energy resolution, observation of the moon shadow in cosmic-ray muon data from the far detector (see Figure 3) and the expected sensitivity of the search for CPT violation in atmospheric neutrino oscillations.

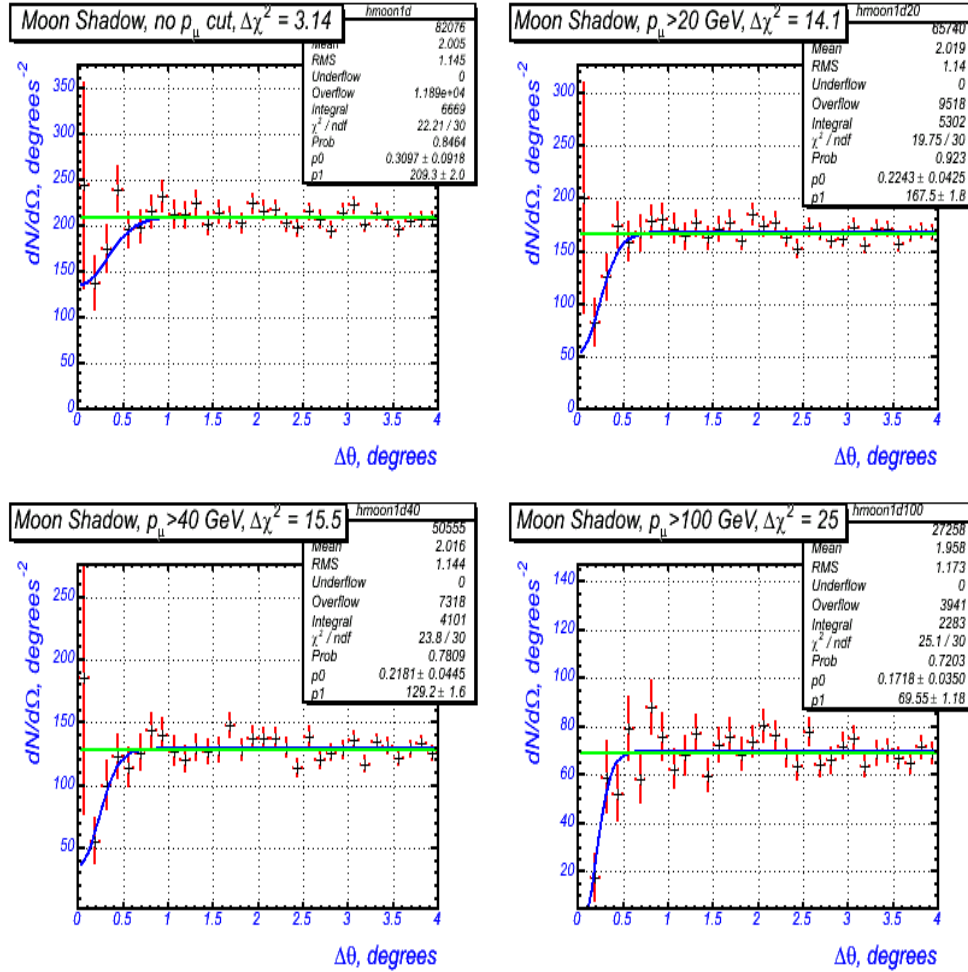


Figure 3. Moon shadow from MINOS far detector cosmic ray muon data. The good angular resolution and precise alignment of the MINOS far detector is demonstrated by its ability to detect the deficit of cosmic-ray muon flux in the direction of the Moon. The track density per solid angle is plotted against the angle between each track and the direction of the Moon. The four plots show the dependence of the signal significance on muon energy, as measured by curvature in the magnetized steel detector planes. The $\Delta\chi^2$ values shown for each graph refer to the differences in fit quality for fits to a constant value and a “dip” function. (This analysis was performed by MINOS collaborator Sergei Avvakumov from Stanford.)

At its June 2004 meeting, the MINOS Collaboration devoted considerable and discussion time to the question of whether the Soudan 2 detector should be restarted to enhance the sensitivity of the MINOS experiment to $\nu_{\mu} \rightarrow \nu_e$ oscillations. The detector was turned off and placed in “mothball” status in July 2001 to save operating funds. At the end of the meeting the MINOS Collaboration decided not to restart the Soudan 2 detector, which will likely be decommissioned and removed during the second half of 2004.

As the MINOS detector work ramp-down began in 2002, Argonne physicists started work on the construction and testing of NuMI neutrino beam components at Fermilab. This work spans a range of activities. One physicist is the Deputy Level 3 Manager for Neutrino Beam Devices and is also responsible for preparation of the work cell facility, which will be used to repair highly radioactive beamline components. Other group members worked on remote-control rigging procedures, vibration measurements of the production target and magnetic focusing horns, horn magnetic-field measurements and the readout and integration of target hall instrumentation. Achievements in these areas during the first half of 2004 are summarized in the paragraphs below.

The most complex part of the work cell is the remotely controlled lift-table system, which is used inside a shielded enclosure to attach or detach a target or horn from its support module. In late 2003 and early 2004 the lift table system was used to practice the attachment of Horn 1, Horn 2 and the neutrino-production target assembly to their support modules in an above-ground test setup. In a parallel effort, the preassembly of the work cell shielding enclosure was completed in the New Muon Lab at Fermilab early in 2004. The structure was then disassembled and moved underground, where it was reassembled along with the lift table system. It was then used to attach Horns 1 and 2 to their support modules prior to initial installation in the target chase. Figure 4 is a photograph of Horn 1 and its support module being moved from the work cell to the target chase.

Argonne physicist Bob Wagner finished cooling-water vibration measurements of the NuMI production target in early 2004, completing the program of target stability studies. All tests have indicated that target vibrations induced by horn pulsing, cooling-air and cooling-water are quite small and do not require any design changes. Bob is now working on the installation of cameras and other equipment needed for remote control of the target hall bridge crane. These will be used to move radioactive shield blocks and the target and horn subassemblies if faults occur in these components after initial operation of the high intensity proton beam. Failed components, still attached to their support modules, will be moved into the work cell, where they will be repaired or replaced. These “hot handling” procedures will be tested under realistic conditions during the final installation of the target and horn assemblies in the target chase in late 2004.

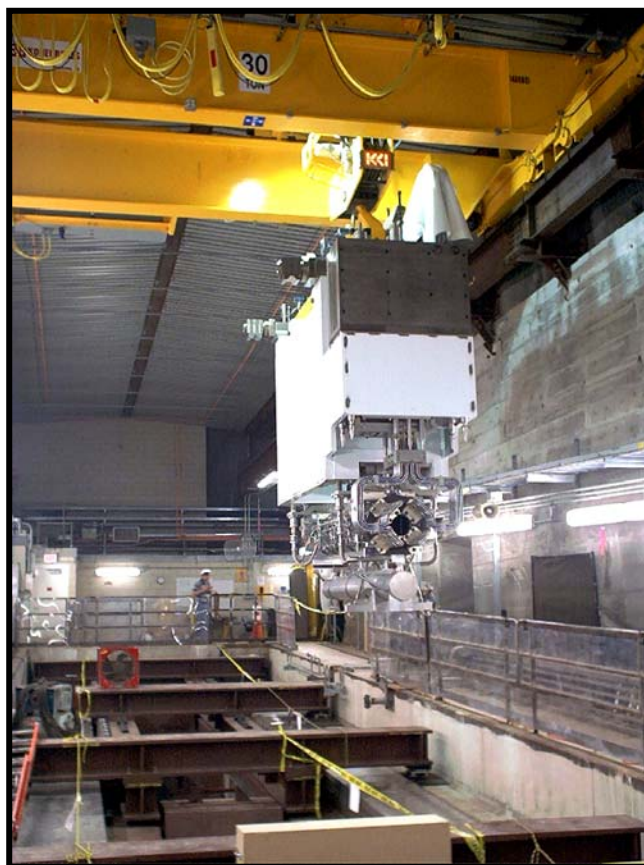


Figure 4. NuMI Horn 1 being rigged into place. In June 2004 the NuMI beamline focusing Horn 1 was attached to its support module in the underground work cell for the first time. The assembly was then moved from the work cell to the heavily shielded target chase with the bridge crane. The 26-ton (white-painted object in the photo) support module contains the feed-through connections for the high-current stripline (visible on the end of the horn facing the camera), cooling water, transverse position control and instrumentation. The cylindrical cooling-water reservoir tank is visible below the horn. Both Horns 1 and 2 were installed in the target chase by the end of June. The horn and target assemblies will be fully tested in late fall with all target chase shielding in place. The horn and target assemblies will then be individually removed by remote control and placed in the work cell during the “hot handling” practice. They will be reinstalled, by remote control, shortly before the Main Injector proton beam is transported to the NuMI production target for the first time at the end of 2004.

In 2004 Argonne physicists and engineers also continued work on the preparation of the electronics used to read out target hall instrumentation. Argonne’s instrumentation readout responsibilities include the thermocouples that measure temperatures at many locations in the target hall, the beam-loss monitors used for horn-crosshair alignment measurements, the readout of the precise positions of remotely movable devices, and the radiation-hard instrumentation cabling. Argonne work on the design of signal conditioning electronics, which is used to interface instrumentation signals to the ACNET data acquisition system, also continued during this period.

(D.S. Ayres)

I.B.2. ATLAS Detector Research & Development

a) Overview of ANL ATLAS Tile Calorimeter Activities

The TileCal subsystem continued making good progress in the first half of 2004. Perhaps the highlight of the year was the installation of the lower 8 modules of the barrel in the Atlas cavern--the first elements of the detector proper (Fig. 1). In addition to this milestone, significant progress was made in engineering analysis associated with the calorimeter installation, services installation, and on the work being carried out in collaboration with Atlas Technical Coordination. These are discussed in more detail below.



Figure 1. The installation of the lower half of the barrel cylinder in the Atlas cavern.

I.B.3. Atlas Calorimeter Engineering Design and Analysis

Argonne engineering staff continued its work on engineering issues associated with the calorimeter installation in the cavern.

Argonne engineering staff participated in the barrel cryostat dummy load test, which was carried out in January 2004. An Argonne engineer carried out the FEA calculations used to determine the expected behavior of the calorimeter system under the load on the A-frames. In addition, strain gauges and readout were sent to CERN for use

in monitoring. Following the (successful) load test, the results of the test were compared to those of the FEA calculations. A cartoon showing the components used in this analysis is shown in Fig. 2.

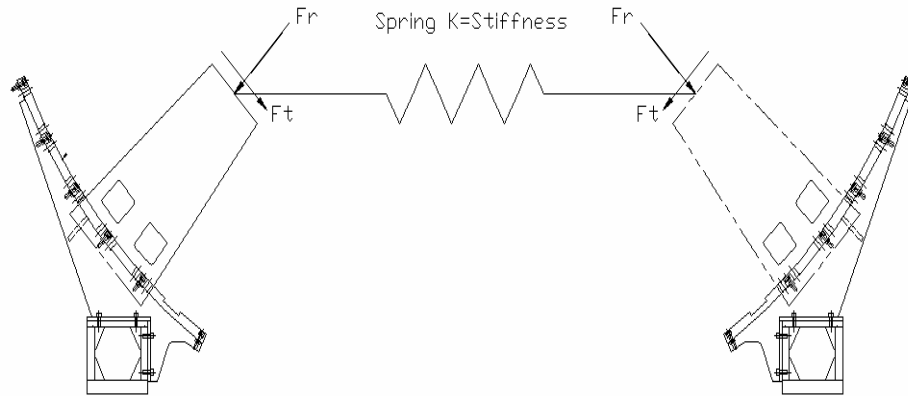


Figure 2. A sketch of the force diagram used to evaluate the barrel cylinder stability when the cryostat load is applied.

The main conclusion of this test (other than that the system was stable) was the observation that there must be friction at the supports in order for the FEA calculation to give the observed (almost negligible) deflections of the cylinder.

The FEA analysis of the support cradle to be used for transportation of the barrel cylinder to the cavern was completed. Argonne also had the responsibility for the fabrication and installation of brackets used to rigidly connect the modules to the cradle, as well as the specification for maximum accelerations during transportation. The lower 8 barrel modules were successfully lowered into the cavern and mounted on the HF truck in March 2004.

Argonne staff has also played a central role in monitoring the barrel cylinder shape for the final assembly of the first 30 modules. A model, whose parameters were empirically based on the pre-assembly geometry, was used to determine small modification to the shims to ensure that the cylinder would be open for the insertion of the last module. The comparison between the model, the geometry in the pre-assembly and the geometry in the cavern for the first 30 modules is shown in Fig. 3. All results are in excellent agreement and, as a result, we have confidence that the fully assembled cylinder will wholly be within its envelope.

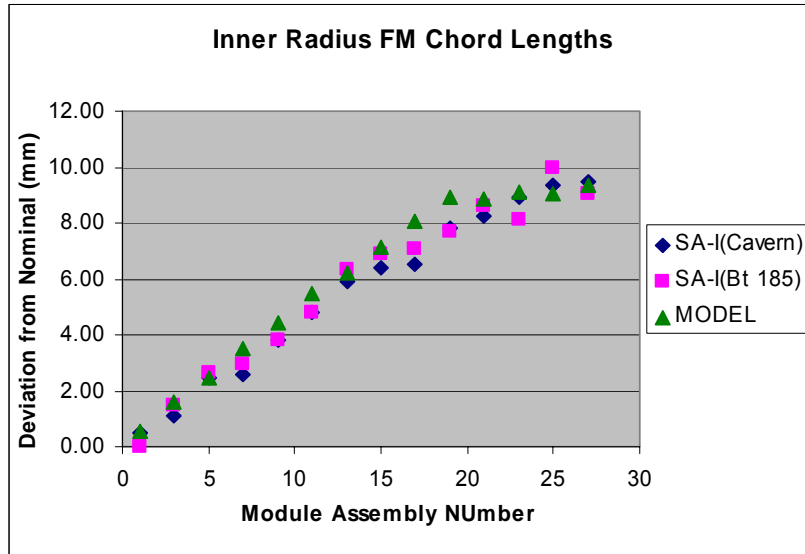


Figure 3. The barrel calorimeter envelope monitor (based on chord length between opposite modules) as a function of module number. The maximum deviation allowed for it to be within the envelope is 10mm.

a) Calorimeter EBA Pre-Assembly

Argonne technical and scientific staff have continued their participation in the ongoing preassembly of the EBA cylinder at CERN. J. Proudfoot is one of the three leaders of the pre-assembly team and is responsible for coordinating the shim plan used to control the assembly geometry. V. Guarino has the responsibility for the evaluation of the geometrical envelope and deformation of the cylinder under its static load. Finite Element calculations have been completed to determine the limit of stability when the cryostat load is applied (It should be noted here that the loading condition is significantly different from that of the barrel cryostat.). Although the calculations showed that the system would be completely stable with the cryostat dummy load applied, a chain restraint has been designed for use between the saddles (Fig. 4).

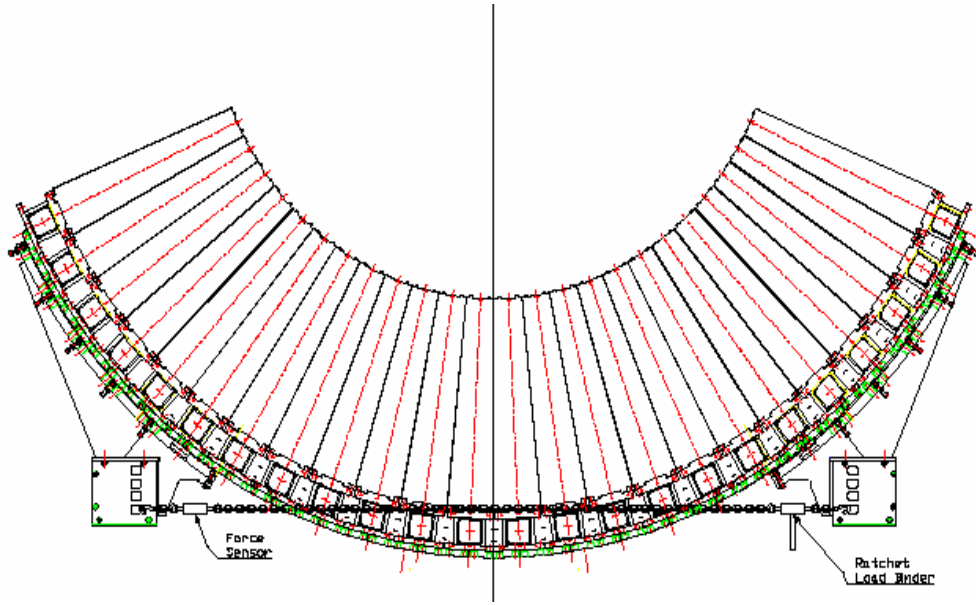


Figure 4. A sketch of the chain used to restrain the saddles on the extended barrel from separating in the event of an unexpected outward force.

The tension load in this chain will be monitored as the load is increased – just in case something untoward should happen.

(J. Proudfoot)

b) Work in Collaboration with ATLAS Technical Coordination

Argonne technical staff has established a strong collaboration with ATLAS Technical Coordination to design the guide and movement systems for the several components, which must be moved on the main rails to access the detector.

1. Bracket Design

After completion of the Extended Barrel (EB) X-bracket in late 2003, new spatial conflicts were found between the X bracket and the muon chamber mounting supports. This resulted in a significant redesign of the bracket in which one of the dominating previous criteria of withstanding the loads of a being driven by a single traction cylinder was removed. This allowed for the reduction in material that was needed to fit in the allotted space. A new design was developed, analyzed, and detailed, allowing the brackets to be sent into production by March of 2004.

2. Control System Design and Testing

As further development of the ATLAS movement control system took place, the vertical motion of the airpad cylinders was integrated into the PLC control system. A

hardware test-set-up for the airpads was set constructed at Argonne. The set-up (Fig. 5) consisted of the existing prototype control system, airpads, and 120 tons of concrete shielding blocks mounted on a steel frame.

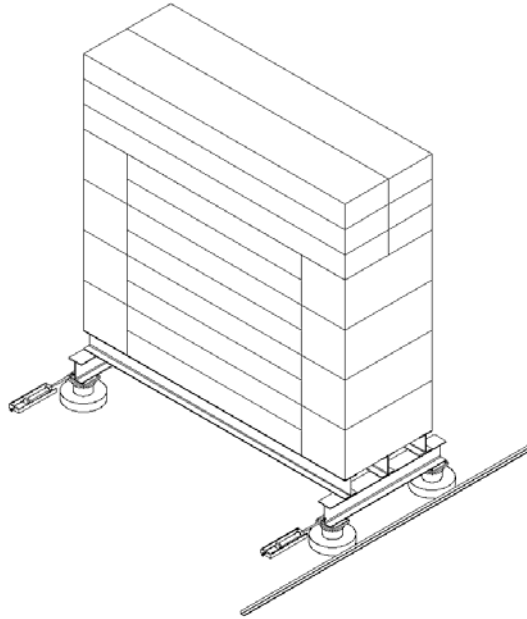


Figure 5. The ATLAS airpad test set-up; 120 tons of concrete shielding blocks stacked on steel frame supported with four airpads.

The resulting airpad test set-up at ANL was a major endeavor that required detailed design and planning, including structural design of the supporting frame, integration of the hydraulic, pneumatic, and electrical components into the system and, detailed safety analysis of all of these systems. The frame was designed to support the 120 tons with various accidental loading situations considered. A series of safety reviews were conducted for all aspects of the system before operation was begun.

Figure 6 shows the layout of the mechanical and sensor components, as well as the hydraulic schematic, as an illustration of the complexity of the system. Some of the components themselves are shown in Fig. 7.

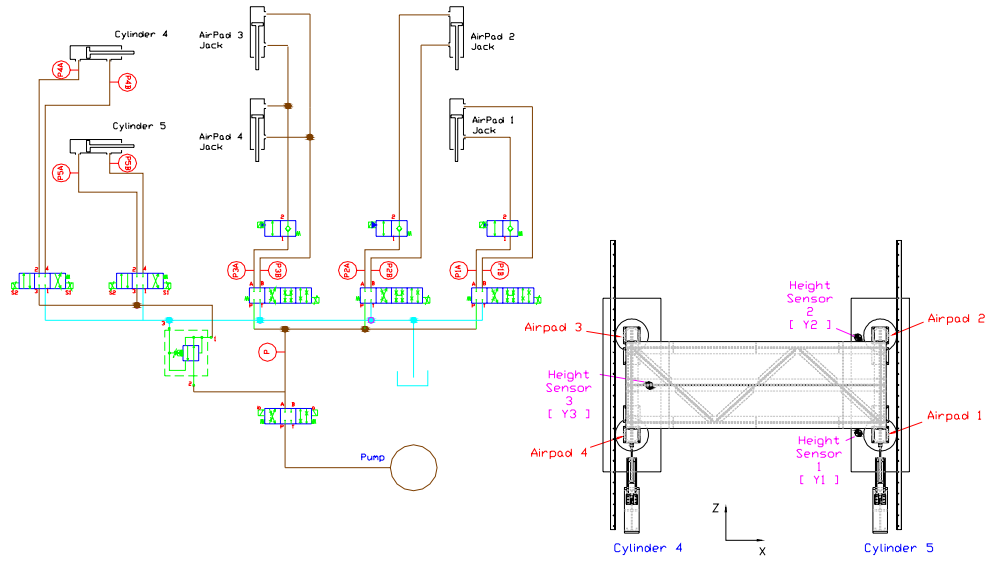


Figure 6. Layout of hydraulic, mechanical, and sensor components in test set-up. It comprises 6 cylinders, 10 valves, 5 position and height sensors, and 11 pressure sensors.

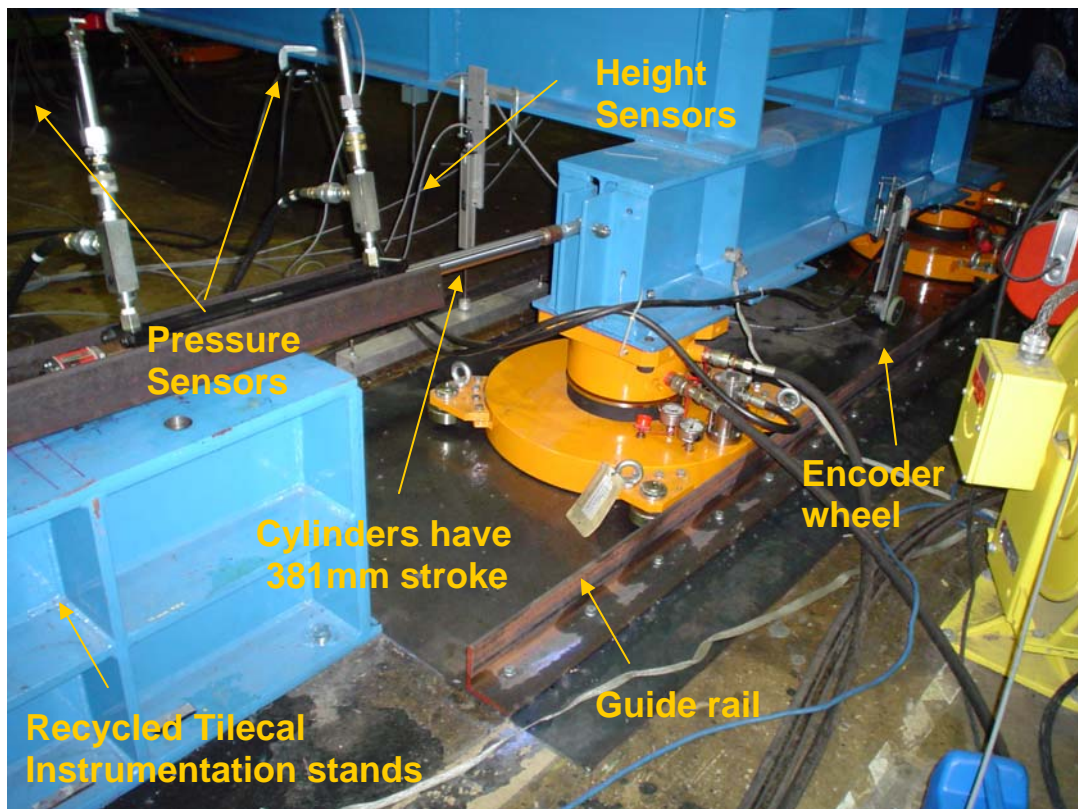


Figure 7. Detailed view of some of the varied components integrated into the test set-up.

Figure 8 shows a plot of the first test of the vertical motion control with the unloaded frame. The plot shows the system responding automatically to an initial height error for all three height sensors. The system properly responds, bringing the system smoothly to a state of small error (less than 0.5mm). In May, the system was energized with air and moved horizontally as a first test. Following this, the frame was loaded to 60 tons and additional tests carried out. The test and development program will continue in the fall and involve adding more automatic functions to the control system, then increasing the load to the full 120 tons.

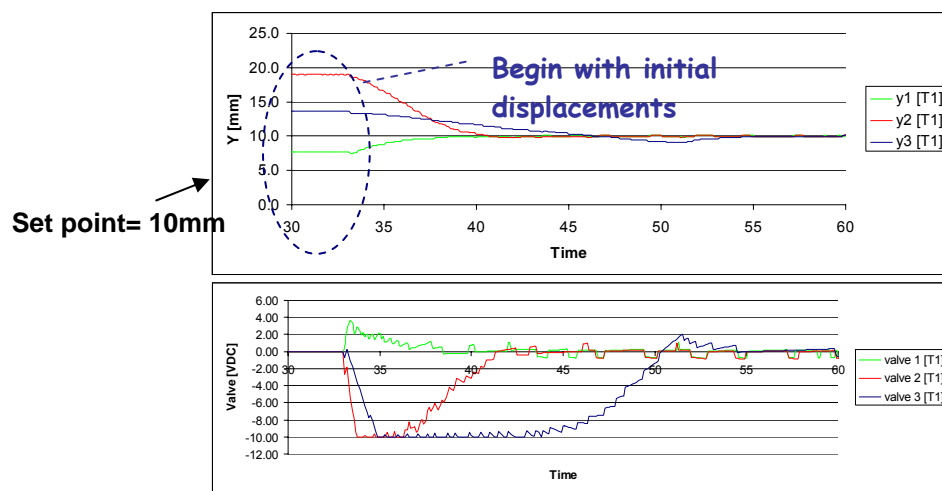


Figure 1. Plot of height change (y) and valve opening for leveling mode from initial displacement. Set point for control is 10mm. Inlet pressure at valves approximately 40 Bar. Maximum valve opening equates to +/- 10VDC.

Figure 8. Results of the first tests of vertical movement control.

(J. Grudzinski)

c) Services Design and Installation

R. Stanek from Argonne continued to be the co-coordinator for the Tile Calorimeter commissioning program, which includes services installation. With assistance from HEP personnel, we have progressed on defining the services and their installation. In particular, we have finished the following:

- Finished PRR2 for all cables;
- Purchased all cables and accepted delivery at CERN;
- Setup a cabling factory to assemble and test cables;
- Proposed readout and TTC fibers and their implementation;
- Designed and demonstrated the installation of on-detector cable trays and cooling;
- Designed and demonstrated cable routing, insertion and daisy chain feasibility.

The cabling procurement took several months of negotiations with suppliers, CERN TIS, and CERN procurement. Finally, we were the first ATLAS group to purchase all our needed cables.

Several trips were made to CERN to demonstrate the installation of services on the detector. Working with designers from TC, ANL staff designed the mounting system for cable trays and cooling tubes. ANL did the groundwork to find fittings, which were low-profile and non-magnetic. Samples were delivered to CERN for evaluation prior to proceeding with their procurement. In addition, we designed and fabricated brackets and inserts for fixing these elements to the calorimeter link plates. ANL technicians mounted the brackets to the surfaces of modules in the assembly area at CERN, then routed cables along the cable trays to the fingers.

At the finger end, we developed the method for neat cabling and power supply insertion and removal, as shown in Fig. 9. We also solved the problem of how the daisy chain cables would be fixed to the detector without interfering with the Inner Detector or LAr services. The lengths of these cables were defined during these trips, and the technicians were then able to construct all the daisy chain cables. ANL staff led much of the direction of these efforts in order to make progress on the cable tray design by TC and, to make progress on our cables by the Tile community. An example of the cable trays, cabling and daisy chains is shown in Fig. 10.



Figure 9. A demonstration of the installation and connection of services to one finger. The finger power supply is inserted directly in this opening.

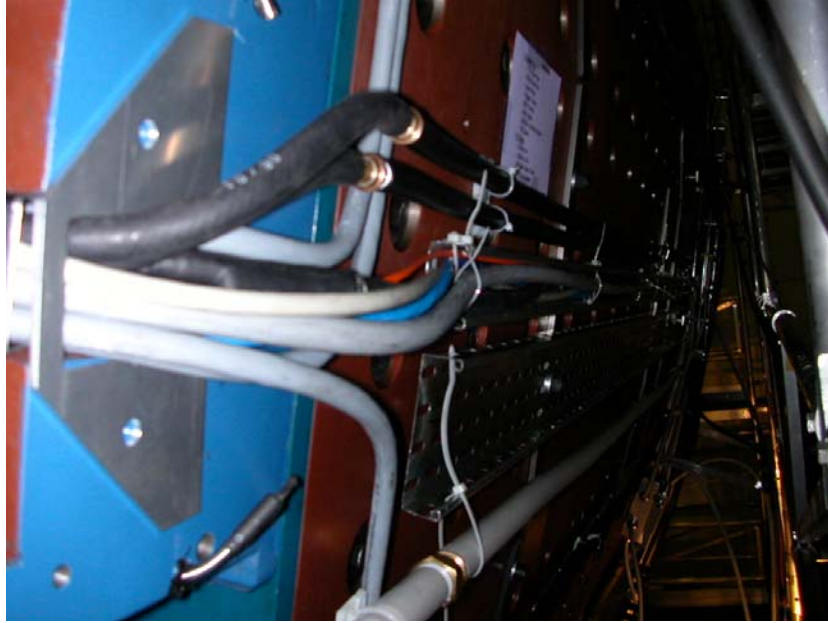


Figure 10. A demonstration of the installation of cable trays, cooling, daisy chains and cable routing to one finger.

(R. Stanek)

I.C. NEW PROJECTS AND DETECTOR DEVELOPMENT

I.C.1. Computational Projects

a) ATLAS Computing

Amid international ATLAS reorganization of its database effort in early 2004 to include Technical Coordination and Online work, Argonne continued to hold several leadership positions, particularly in offline data management. David Malon moved from the Computing Management Board to the Software Project Management Board and the Database Steering Group, remaining responsible for the multi-petabyte ATLAS event store, for core database software, and for framework integration of ATLAS data management infrastructure. David Malon was appointed to the ATLAS Computing Model Taskforce, which is responsible for the document that will provide the foundation for international ATLAS computing resource acquisition and deployment. Work on producing the ATLAS Computing Model document began.

Highlights of the ATLAS database coordination effort for which Argonne was responsible include design of Athena-based back navigation, design of the registration service that populates the event-level metadata system, construction of command-line tools, and integration of catalogs and collections infrastructure from the LHC-wide common computing project. In this reporting period, David Malon also wrote the

document that was to become the mandate for a newly-formed LHC-wide distributed database deployment project (LCG3D), and served as an invited member of a team charged by the DOE Office of Science with delivering a whitepaper on the data management needs of large-scale science.

Alexandre Vaniachine continued software development and support for the NOVA database. This database is now used as a primary source of the detector description parameters in all ATLAS offline software subsystems, and has been shown to work for LAr calibration parameters. He also provided support for both ATLAS main relational database prototyping server at CERN and the database development server for the LCG project at CERN. The use of relational databases in ATLAS continued to expand during this period.

Tom LeCompte continued in his roll as planning officer. In this period, ATLAS computing was fully integrated into the overall ATLAS project management structure. This was done at the request of the spokesperson, and is intended for use in scheduling the integration and commissioning efforts. Transparency in the planning process was substantially improved, as well as better integration between subprojects.

In February, Jack Cranshaw joined the group. Starting in May he took charge of a project to validate the Event Store tools needed for the 2004 ATLAS Data Challenge (DC2). The motivation was to spot problems and provide bug fixes before releasing the software to users. Serious work on this was kicked off at the software week in May. The group was composed of three people at Argonne (with Kristo Karr and David Malon), three people at Orsay, and one person at Brookhaven. This developed into the “DC2 Checklist” which was a critical component to the second data challenge and will be described in more detail in the next semiannual report.

(T. LeCompte)

I.C.2. Detector Development for the Linear Collider

In the first half of calendar year 2004, the Linear Collider Detector R&D group pursued their efforts aiming at the development of a design of the hadron calorimeter for the Linear Collider detector. Progress was made on both the detector simulation and the hardware development front.

a) Monte Carlo Simulation studies

Work on the ingredients to a complete Particle Flow Algorithm continued. A track-calorimeter deposit matching routine, based on the identification of the first interaction layer and using narrow cones to follow the hadronic showers from layer-to-layer, was

developed. Energy deposits in the calorimeter belonging to neutral hadrons were identified as the energy left over after subtraction of the charged particle energy and the energy belonging to electromagnetic showers as identified by the electromagnetic calorimeter. A photon finder was applied to identify the energy depositions in the calorimeter belonging to photons. Applying these algorithms to Z^0 decays at $\sqrt{s} = 91$ GeV, allowed to reconstruct the Z^0 mass via its decay into a pair of jets. The mass spectrum was fit to two Gaussians with widths $\sigma = 4$ and 7 GeV, respectively. Further tuning of the ingredients to the PFA will be necessary to reach the goal of $\sigma \sim 3$ GeV.

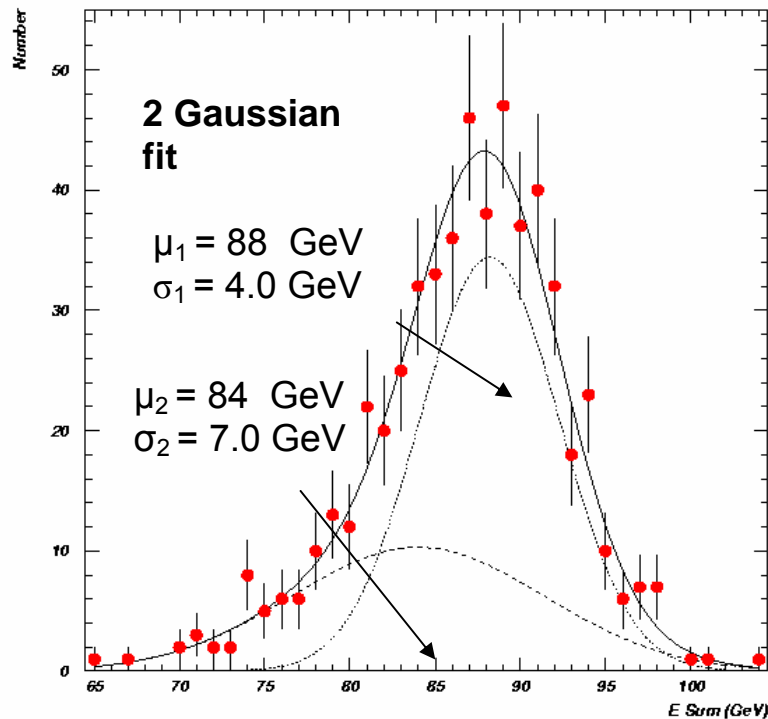


Figure 1. Reconstructed mass of the Z^0 boson.

b) *Development of Resistive Plate Chambers as active medium of a digital hadron calorimeter*

In the first half of 2004, the group continued its vigorous R&D program to develop Resistive Plate Chambers as an active medium of a digital hadron calorimeter. In the following, we briefly summarize the major highlights of the project:

b.1. Construction of chambers

Several chambers, each with an area of $20 \times 20 \text{ cm}^2$, were built. These chambers feature one single gas gap and two glass plates. The surface resistivity of the graphite layer was measured to be approximately $1 - 50 \text{ M}\Omega$. Additional chambers based

on somewhat exotic designs, such as using only one single glass plate or using copper tape instead of graphite, were built. All chambers were extensively tested and performed very well.

To gain experience with building larger chambers, a chamber using glass plates with an area of $30 \times 100 \text{ cm}^2$ was assembled. Its performance was measured to be similar to smaller chambers based on the same design.

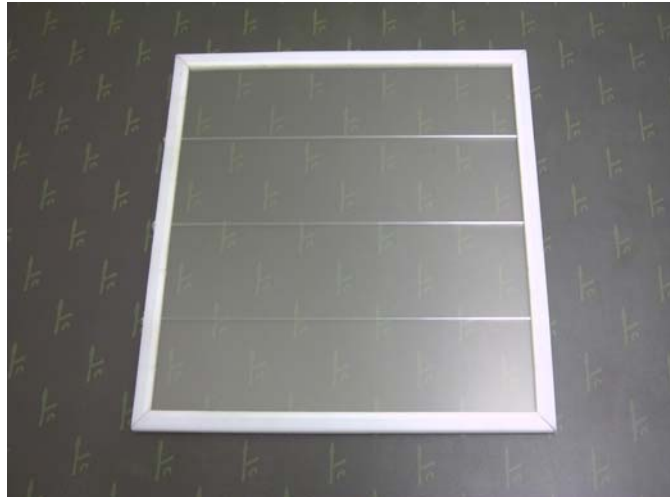


Figure 2. Photograph of one of the RPCs built at Argonne.

b.2. VME data collection system

We designed, built, and commissioned a VME-based readout system for the multiple pad studies. The system consists of 6U VME cards able to readout up to 64 input channels each. Each input channel consists of an amplifier, shaper and discriminator. The data acquisition runs in self-triggering mode. Each recorded event consists of the hit pattern and a time stamp with a 100 ns time resolution. The system works well with RPCs operating in streamer mode. Operation in avalanche mode requires additional amplification of the signal with the amplifier located close to the readout pad. The data acquisition software is based on the FISION library and was written by one of the members of the Argonne group.

b.3. Measurement of the noise rate

Using the VME data acquisition system, the noise rate as a function of threshold was measured. Figure 3 shows typical results for chambers built on the traditional design with two glass plates. With threshold settings at a fraction of the average avalanche signal, the noise rate is measured to be 0.1 Hz/cm^2 . The noise rate for the exotic designs is slightly more elevated, but still.

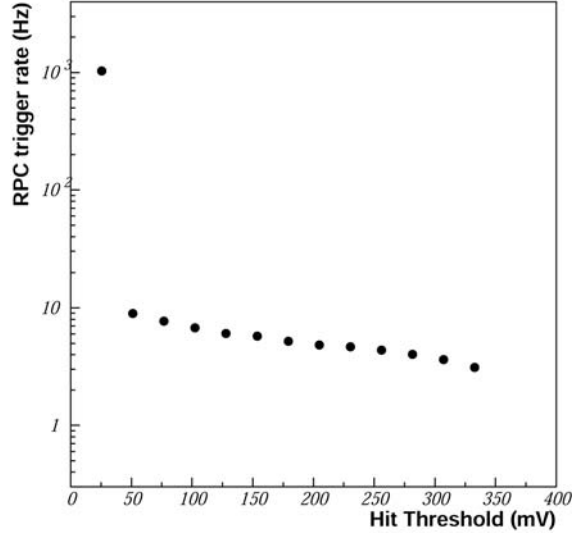


Figure 3. Rate of noise (random) hits as a function of discriminator threshold.

b.4. Measurements of the pad multiplicity.

Using the 64-channel VME data collection system, detailed measurements of the pad multiplicity and particle detection efficiency were performed. Figure 4 shows the pad multiplicity as a function of MIP detection efficiency. The measurements shown with

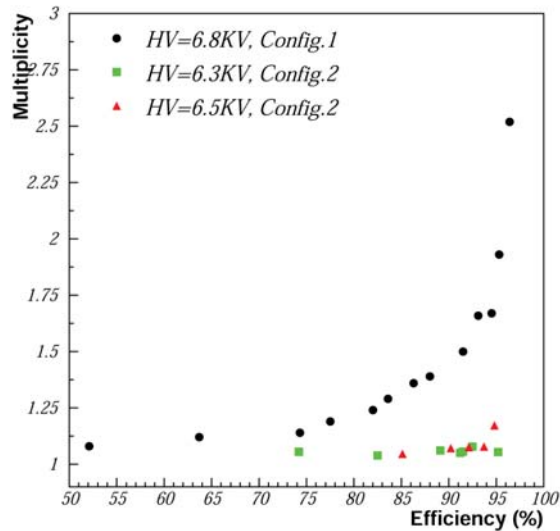


Figure 4. Average pad multiplicity as a function of MIP detection efficiency. The black dots (colored triangles and squares) correspond to measurements with a chamber based on the traditional (exotic) design.

black circles were obtained with a chamber based on the traditional RPC design, with two resistive plates. The colored triangles and squares were measured with a chamber based on the exotic design with only one glass plate.

b.5. Measurements of the rate capability

The rate capability of the chambers was determined using a radioactive source at varying distance from the chamber to provide the rates and cosmic rays to determine the MIP detection efficiency. Figure 5 shows the results obtained with a chamber based on an exotic design. Due to the special geometrical arrangement of these measurements, the purity of the cosmic ray triggers is not 100%, leading to a maximum apparent efficiency of 92%. The efficiency is seen to remain at the maximum level for rates up to 50 Hz/cm².

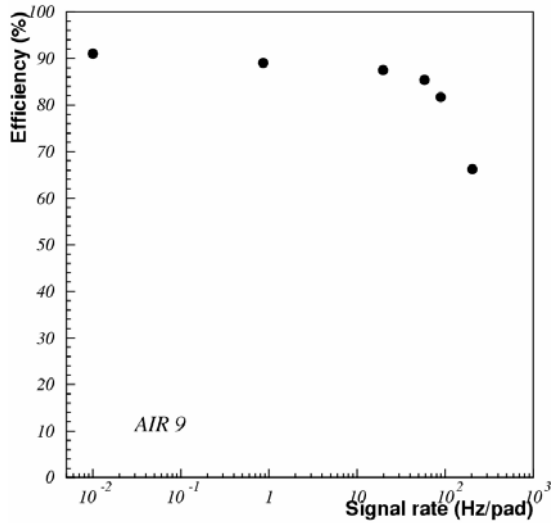


Figure 5. Measurement of the MIP detection efficiency as function of rate.

b.6. 1 m³ prototype section

The goal of the present effort is to build a 1 m³ prototype section to a) test the technological implementation of RPCs in a calorimeter and b) to measure hadronic jets with unprecedented spatial resolution. The latter is necessary to fine tune the existing models of hadronic showers to be used in the overall design of detector for the international linear collider. The section will consist of 40 layers, each with an area of 1 m². The active medium will be interleaved with 20 mm steel plates serving as absorber.

b.7. Conceptual design of the readout system for the 1 m³ prototype section

We developed a conceptual design of the readout system for the 1 m³ prototype section. With 40 layers of active medium, each with an area of 1 m², and 1 cm² lateral

segmentation, the prototype section will feature of the order of 400,000 readout channels. This large number of channels demands a novel approach to the electronic readout system. Our conceptual design consists of four parts: a front-end ASIC located on the readout boards of the RPCs, a data concentrator located on the side of the prototype section, a VME-based data collection system, and a timing and trigger system. See Figure 6 for more details.

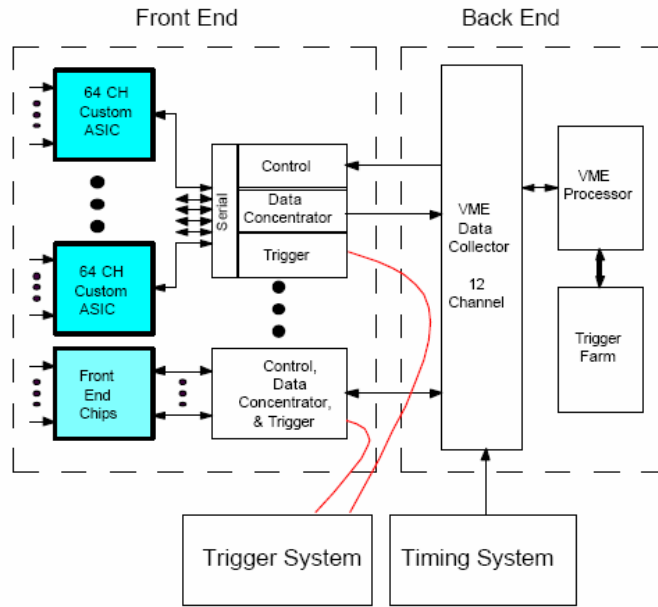


Figure 6. Schematic design of the electronic readout system for the 1 m³ prototype section.

b.8. Design of the front-end ASIC

We wrote a lengthy document to specify the details of the front-end ASIC. After a series of meetings with electronic engineers at Fermilab, design work on the chip initiated in June, 2004. By the end of the month, the layout of the chip had been worked out and is shown in Figure 7.

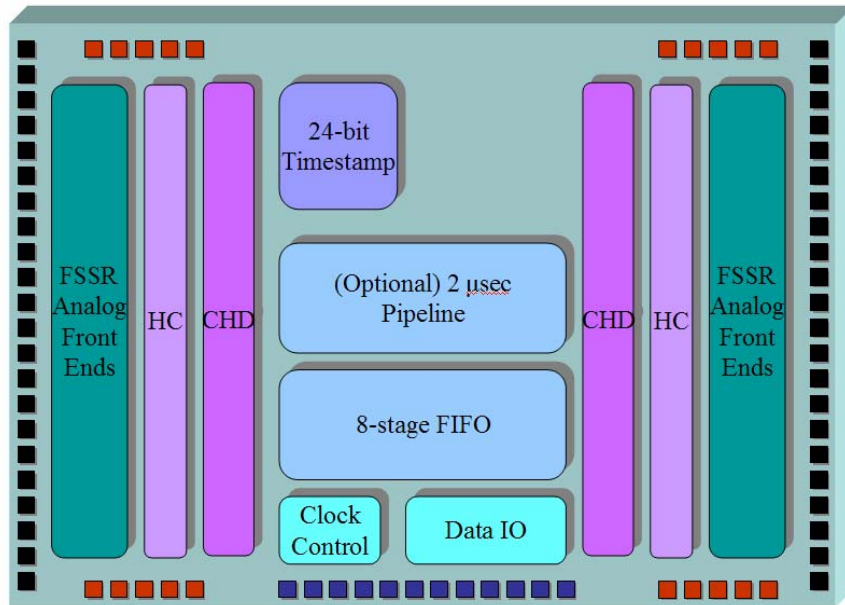


Figure 7. Schematic layout of the front-end ASIC being designed at Fermilab.

(J. Repond)

I.C.3. Electronics Support Group

ATLAS: We have major responsibilities in the development of electronics for the Level 2 Trigger of the ATLAS Detector at CERN. Working with colleagues from Michigan State University, we are responsible for the development of two parts of this system: the Level 2 Trigger Supervisor, and the Region of Interest (ROI) Builder.

The ROI Builder is the interface between the first level trigger and the second level trigger. When an event occurs in the detector, signals are sent from the front-end electronics to the Level 1 Trigger. The Level 1 Trigger collects event fragments from the front-end electronics over the entire detector, and stores them in a Readout Buffer. It evaluates the data, and identifies regions of the detector that could have an interesting event. The Level 1 Trigger boards then sends a list of addresses called pointers to the ROI Builder, identifying where the event data from the “Region of Interest,” can be found. The ROI Builder collects the pointers for the event, and “builds” the event using the pointer list. It then sends the result to the Trigger Supervisor for distribution to Level 2 processors. The selected Level 2 Processor then executes algorithms using the pointers, and can request information to be sent from the Readout Buffers as needed. The ROI

Builder is highly complex, using high-speed, highly complex Field programmable Gate Arrays (FPGAs) to implement the functionality.

In earlier reporting periods, we built the first version of ROI Builder. It has undergone extensive testing at Argonne and at CERN. In 2002, the module was reviewed by an internal ATLAS review committee, and certain improvements were recommended associated with error reporting and data slow control. In 2003, we created a new design document that incorporated the recommendations. We then proceeded with the design of a new version of the module. In this period, the new version was fabricated, assembled, and tested in the lab. The module has performed very well to date and meets all of the recommendations made by the review committee. The module will be sent to CERN for tests in the summer at the ATLAS testbeam.

MINOS: We have major responsibilities for the development of electronics for MINOS, the Neutrino Oscillation Experiment at Fermilab and the Soudan Mine. We are responsible for the design, development, and production of electronics Near Detector, one of the two major detectors for this experiment. One member of our group is the Level 3 Manager for the Near Detector Electronics.

The heart of the front-end electronics for the Near Detector is a custom integrated circuit designed at Fermilab, called the QIE. The QIE digitizes continuously at 53 MHz. The operations are pipelined so that there is no deadtime due to digitization. The digitized data will be stored in a local memory during the entire period of the beam spill. The data will be sent from the local memory to a read-out board after the spill is over. In between spills, the electronics will record data from cosmic rays.

The QIEs and associated circuitry will be built on small daughter boards called MENU Modules, which resemble memory SIMMs. The boards contain a high density of surface mount parts. The MENU Modules plug in to a motherboard called the MINDER Module. The MINDERS reside in front end crates called MINDER Crates, which are a semi-custom design. There is a crate controller in the MINDER Crates called the KEEPER, which controls all activity in the crate. When data is acquired, it is stored on the MENU Modules. After data is acquired, the MINDER then initiates a readout operation, where the data is sent from the MENUs to a VME readout board, called the MASTER Module. The MASTER resides in a 9U VME crate located some distance away from the MINDER Crates. All of the board designs contain a high level of programmable logic to do the complex processing of data and control of operations.

The chip design, and the development of the QIE daughter board, are responsibilities of Fermilab. Argonne is responsible for the design the MASTER Module, the MINDER Module, the KEEPER, the MINDER Crate, signal and data cables, and AUX cards for receiving signals in through the back of the VME Crates. We also

have overall responsibility for the design of the rest of the system for the Near Detector, including the specifications for the QIE performance. This is a major design and production project for our group.

In 2002, we completed the development stage of this project, including the building and testing of 200 channels of the read-out system. The system was sent to CERN for use in a test beam, which was set up to calibrate the detector. In early 2003, the final design changes were implemented on all parts of the system, and all sub-projects were signed off for production. Argonne is responsible for the production of 100 MASTERS, 600 MINDERS, and 60 KEEPERS. We have outside vendors do the printed circuit board fabrication and board assembly. We do the checkout work in-house with our staff technicians. In this period, we completed the production and checkout of all components. Installation and commissioning are in progress at Fermilab. We are assisting with the commissioning, which is expected to be completed in the fall. The experiment is scheduled to begin taking data in January, 2005.

Linear Collider Hadron Calorimeter: Argonne HEP physicists are leading an effort to develop a new detector based on Resistive Plate Chambers (RPCs) for an experiment that would be part of a new facility called the Linear Collider. The RPCs would form the hadron calorimeter, and is based on the concept of digital calorimetry. The electronics would have a discriminator on each channel to record hits in the detector, as opposed to measuring pulse-height information with an ADC. A technique known as a "Particle-Flow Algorithm" is then used to reconstruct the events. This experiment would have 50,000,000 channels in the final detector. As an intermediate step, it is proposed to build a "small" detector with only 400,000 channels, called the cubic-meter detector. This detector would be used for measurements in a test beam, perhaps operational around 2006. The Argonne group received an LDRD grant to fund work this year, and additional funding proposals are in progress.

In this period, we developed a conceptual design for the read-out system. In order to keep costs down, we intend to use a custom ASIC in the front-end electronics. We developed a conceptual design for this device, and wrote a complete specification. We have formed an alliance with the Fermilab ASIC Design Group, and work is in progress to realize the design. We will test the device at Argonne after it is fabricated. In addition, we are supporting the detector R&D that is in progress at Argonne. We built special instrumentation for this work, and provide support as the work progresses.

Veritas: Physicists at Argonne have joined Veritas, a telescope-based experiment to observe high-energy cosmic rays. The experiment is currently being built in Arizona using an array of four telescopes. We are working with the

University of Chicago to build high-speed electronics for the next phase of the project, which would add three more telescopes to the array, and also augment and enhance the capability of the current instrumentation. The system would have $\sim 10,000$ channels of high-speed, high-precision charge amplifiers in the final configuration. The Argonne group received a grant from the lab director to participate in this joint University of Chicago/Argonne project, primarily for us to work on electronics development.

In this period, the Argonne group began an R&D program involved with making measurements on multi-anode photodetectors. These would be new used in the upgraded experiment. We provided the data acquisition system and read-out software. We also began work on a teststand for reading out ~ 250 channels. A goal in the coming year is to set up a small telescope at on a site at Argonne and make measurements on the night sky, as a proof of principle for the photodetectors. Beyond that, we plan to build the electronics for the larger read-out system, which has a timescale of ~ 2 years.

(G. Drake)

I.C.4. Experiments to Measure the θ_{13} Neutrino Mass-mixing Parameter

a) NO ν A (NuMI Off-axis ν_e Appearance) Experiment

In 2002, Argonne physicists and engineers began serious work on the design of a next-generation long-baseline experiment in the NuMI neutrino beam. The experiment would take advantage of the narrow energy spectrum of neutrinos produced a few degrees away from the beam axis to perform a high sensitivity search for $\nu_\mu \rightarrow \nu_e$ oscillations. The observation of $\nu_\mu \rightarrow \nu_e$ would allow a measurement of the θ_{13} neutrino-mass mixing parameter. The peak energy depends on the off-axis angle, which would be chosen to give an energy close to the first maximum of the oscillation probability distribution. The reduced flux of high-energy neutrinos in the off-axis beam significantly lowers the background from neutral current events. Measurement of a nonzero value of θ_{13} could eventually lead to the construction of an even larger off-axis detector to resolve the neutrino “mass hierarchy” problem and to search for CP violation effects. If the NuMI beam intensity can be increased sufficiently and the neutrino-mass mixing parameter is large enough, it is even possible that the NO ν A experiment itself could see the first evidence for CP violation. Figures 5 and 6 show the ambiguities involved in these measurements and the sensitivity of the experiment for two different levels of incident proton intensity.

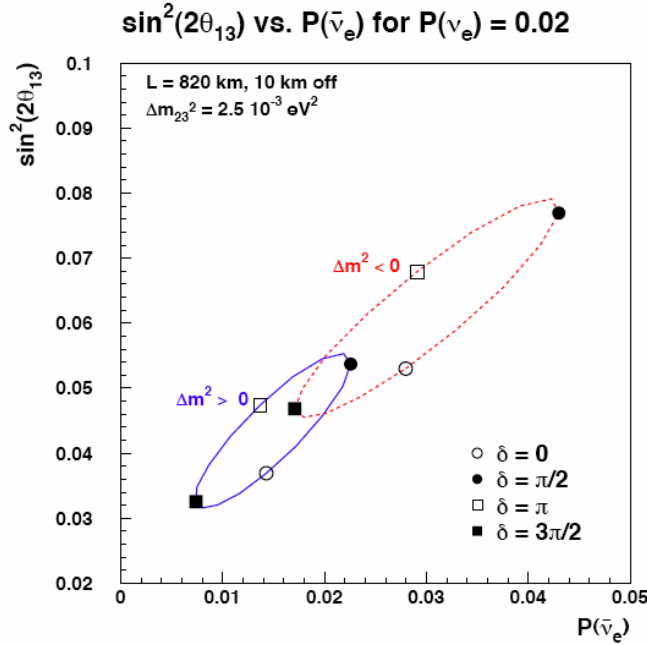


Figure 5. Measurement ambiguities in the NOvA experiment. The graph illustrates the possible interpretations of a NOvA measurement of a 2% $\nu_\mu \rightarrow \nu_e$ oscillation probability, as a function of the $\sin^2(2\theta_{13})$ mixing angle and the antineutrino oscillation probability. The solid ellipse shows the possible values for these two quantities, for the indicated values of the CP-violating phase δ , for the “normal” mass hierarchy ($\Delta m^2 > 0$). The dashed ellipse shows the situation for the “inverted” mass hierarchy ($\Delta m^2 < 0$). For example, a sufficiently accurate measurement of a 4% antineutrino oscillation probability would resolve the mass hierarchy, determine $\sin^2(2\theta_{13})$ and measure δ within a two-fold ambiguity.

In March 2004, the NOvA Collaboration, including Argonne and 33 other institutions, submitted a formal proposal (P-929) for the off-axis experiment to Fermilab. In response to a request from the Fermilab Physics Advisory Committee in April, the Collaboration submitted three Appendices to the proposal for discussion at the June PAC meeting. Argonne physicists and engineers played major roles in writing the proposal and producing engineering designs and cost estimates. The NOvA proposal requests approval to build a 50,000-ton detector to search for $\nu_\mu \rightarrow \nu_e$ oscillations, about 12 mrad off the axis of the NuMI beamline in Minnesota or Canada. Although the PAC did not recommend Stage 1 approval for NOvA, it did urge Fermilab to put the experiment on a “fast track” and to provide the R&D funds needed to finalize the detector technology choice.

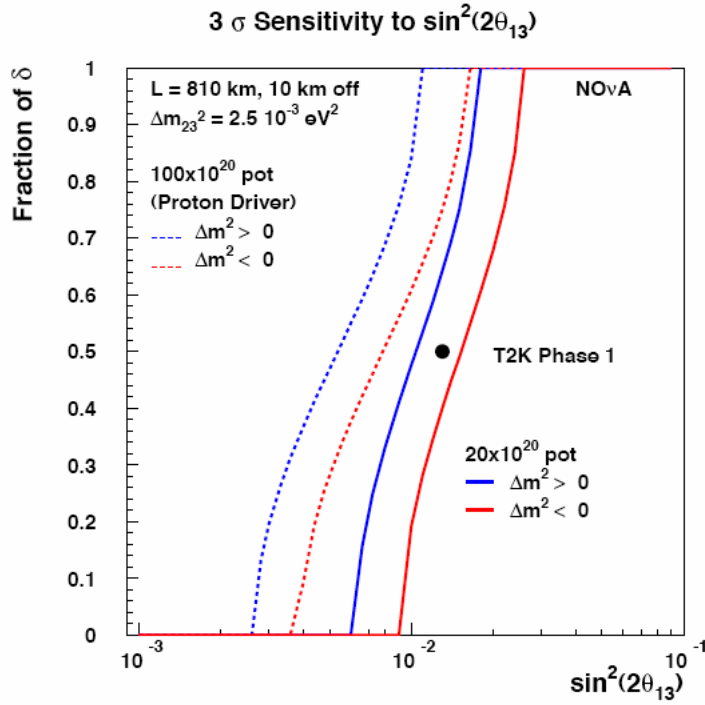


Figure 6. Discovery sensitivity of the NOvA experiment. The graph shows how NOvA 3- σ discovery limits for the observation of $\nu_\mu \rightarrow \nu_e$ oscillations depend on the CP-violating phase δ . The vertical axis shows the fraction of possible δ values for which a 3- σ discovery could be made (e.g., zero represents the limit for the most favorable value of δ). Limits are shown for two different proton-intensity levels. The left-hand line for each value of proton intensity shows the case for the normal mass hierarchy ($\Delta m^2 > 0$); the right-hand line is for the inverted hierarchy ($\Delta m^2 < 0$). The 3- σ sensitivity claimed for the T2K experiment (JPARC phase 1) is plotted at $\delta = 0.5$.

Initially, the Argonne group worked with Fermilab on a detector design using resistive plate chambers (RPCs). However, we have now decided to stop work on RPCs in favor of the liquid scintillator “baseline” technology chosen for the proposal. The baseline detector has planes of horizontal and vertical liquid scintillator strips (liquid-filled tubes in PVC extrusions, read out with wavelength-shifting fibers) interleaved with wood (particleboard) absorber material. The design of the liquid-scintillator design has continued to evolve since the proposal was submitted. A recent optimization, which is still under development, makes the detector “totally active” by removing the passive absorber entirely. This improves the detection efficiency and background rejection for ν_e events so much that the detector mass can be reduced by a factor of two (to 25,000 tons) with no loss of event rate. It seems likely that advanced simulations, with detailed event reconstruction software, will show this totally active design to have even higher efficiency and background rejection. Figure 7 shows a sketch of the totally active detector and a simulated electron neutrino event.

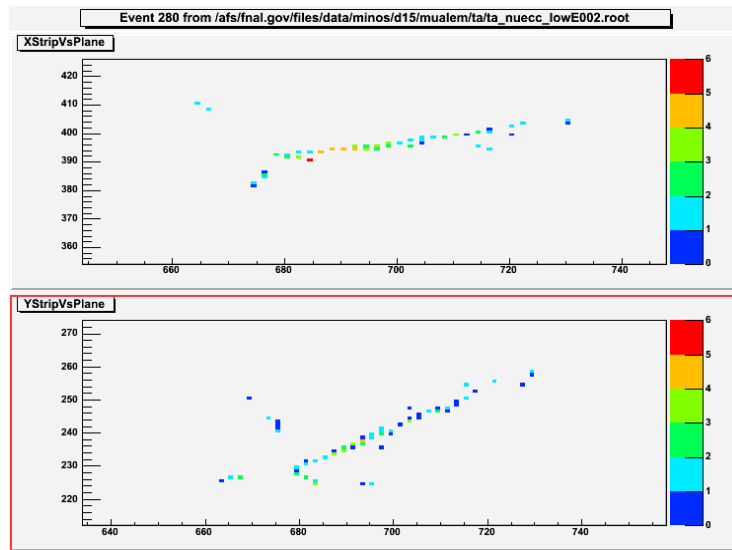
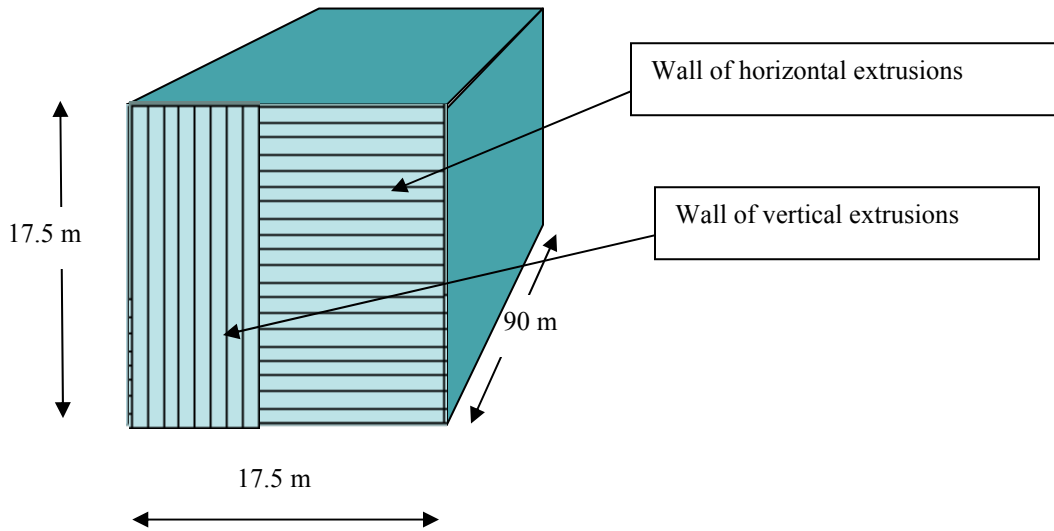


Figure 7. Design of the totally active detector for the NOvA experiment. The top diagram is a sketch of the detector, which is composed of 1845 “walls” of 17.5-meter long by 1.2-meter wide PVC extrusions filled with liquid scintillator. Each extrusion has 2-mm thick external walls, 1-mm thick internal walls, and contains 32 cells, each 3.9 cm wide by 4.9 cm deep. Each cell is filled with liquid scintillator and read out at one end through a double wavelength-shifting fiber (looped at the far end of each cell) by an avalanche photodiode. The detector mass consists of 85% liquid scintillator and 15% PVC. The bottom graphs show horizontal and vertical views of a charged-current electron neutrino event, $\nu_e + A \rightarrow p + e^- + \pi^0$, where the long track is the electron, the short track on the right-hand side of the vertex is the recoil proton and other hits are associated with the π^0 .

During the first half of 2004 the Argonne physicists and engineers have devoted a substantial effort to studying mechanical engineering issues associated with the totally active design. These include handling, machining and bonding of the 57-foot long PVC

extrusions, in addition to structural engineering considerations. The group has already built and tested a number of small prototype structures and expects to intensify its efforts in the second half of the year. Figure 8 is a photograph of the very promising PVC welding technique that might be used to bond the vertical “walls” of scintillator extrusions into a rigid, free-standing structure.



Figure 8. Welding of PVC extrusion walls for the NOvA experiment. The Argonne mechanical support group performed this test welding of a PVC extrusion with horizontal cells (bottom of photo) to attach it to a “wall” of extrusions with vertical cells. The dual-tipped tool melts (at 300 deg C) the surfaces of both extrusions and a PVC “welding” rod (long white object held in the operator’s hand). The group is also studying various gluing techniques for attaching detector walls to each other to form a rigid, stable structure.

(D.S. Ayres)

b) A New Reactor Neutrino Experiment

In the presently accepted paradigm to describe the neutrino sector, there are three mixing angles ($\theta_{12}, \theta_{23}, \theta_{13}$) that quantify the mixing of the neutrino mass and flavor states. θ_{12} has been measured by solar neutrino experiments and the KamLAND reactor experiment. θ_{23} has been measured by atmospheric neutrino experiments and the K2K long-baseline experiment, and will be precisely measured by the MINOS experiment. The third angle θ_{13} has not yet been measured but has been constrained to be smaller than the other two. The best current limit on θ_{13} comes from the CHOOZ experiment. It is a function of Δm^2 and has been measured to be $\sin^2 2\theta_{13} < 0.12$ to 0.17 .

In order to improve on the CHOOZ experiment, a new reactor experiment needs more statistics and better control of systematic errors. Increased statistics can be achieved by running longer, using a larger detector, and judicious choice of a nuclear reactor. The dominant systematic errors in an absolute measurement of the reactor neutrino flux, such as cross sections, flux uncertainties, and the absolute target volume, will be largely eliminated in a relative measurement with two or more detectors. Good understanding of the relative detector response and the backgrounds is required for a precise relative measurement of the reactor neutrino flux and spectrum. Experiments are being considered which increase the luminosity from the CHOOZ value of 12 GW-ton-year to 400 GW-ton-year or more. This will allow a mixing angle sensitivity increase by a factor of 10. The ability to phase upgrades to achieve a luminosity of 8000 GW-ton-year is also being considered. For example, Double CHOOZ has sensitivity to $\sin^2 2\theta_{13} < 0.03$; ANGRA or Braidwood could reach $\sin^2 2\theta_{13} < 0.01$, and experiments with larger detectors could improve another factor of 2 or 3.

Argonne has been instrumental in the establishment of an International Working Group of physicists who believe that a timely new experiment at nuclear reactors sensitive to θ_{13} has a great opportunity for discovery. Physicists from Russia, Europe and Japan agreed to work together on a document to present to the physics community. That group produced a white paper which was edited at Argonne, "A New Nuclear Reactor ν Experiment to Measure θ_{13} ", which was published in January 2004.

A next generation reactor experiment will be designed to make a precision measurement of the reactor electron anti-neutrino survival probability at different distances from the reactor. A measurement at the (O) 1% level will require careful control of possible systematic errors. While it is clear that a two detector experiment can improve the limit set by CHOOZ, it remains to be demonstrated that systematic errors can be controlled at the level necessary to take advantage of the statistics from the most ambitious reactor detector proposals. Thus a concerted program of detector R&D needs to take place, some of which can be part of an early experiment. Some of the open questions under consideration are the following: Liquid scintillator loaded with 0.1% of Gadolinium has been used in the past, but there are concerns regarding its stability in solution and possible attenuation length degradation. New scintillators have been identified which offer greater stability, but their suitability for this kind of experiment needs to be demonstrated. Moveable detectors offer a way to directly measure the relative calibration, but they present new challenges. If movable detectors are chosen, there must be confidence that moving the detector does not introduce additional time-dependent effects. Another interesting and time-critical challenge is the accurate estimation and reduction of cosmic ray associated backgrounds such as neutrons and ${}^9\text{Li}$ spallation. This will affect the ability to reduce the threshold to below 1 MeV, which is the minimum energy release from positron annihilation.

An illustration of how a reactor experiment could measure θ_{13} is shown in Figure 1. In that plot, the disappearance of reactor neutrinos is shown for the approximately known values of θ_{12} , Δm_{31}^2 and Δm_{21}^2 and a hypothetical value of θ_{13} . The large wiggle on the right comes from the solar neutrino parameters and has been confirmed by KamLAND, using reactor neutrinos and an average baseline of 180 km. The hypothetical smaller wiggle at $L/E \sim 0.5$ km/MeV could be tested by a precision reactor experiment using a baseline of 1.5 km.

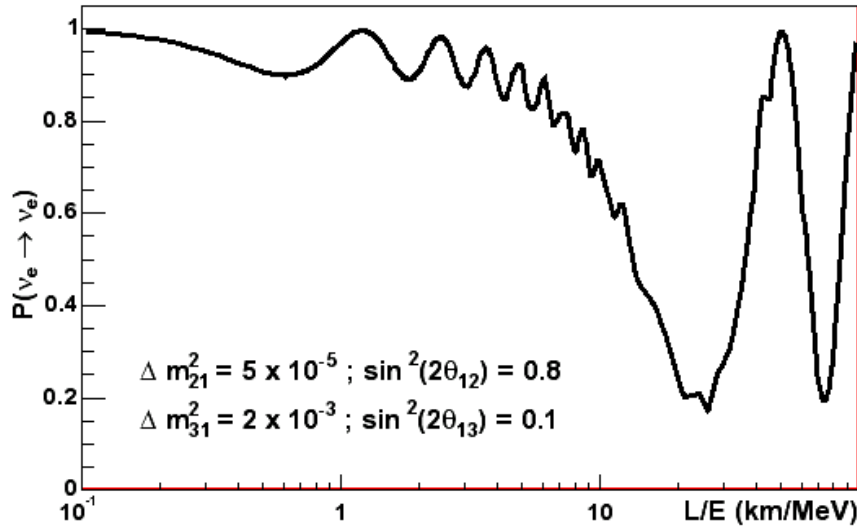


Figure 1. Illustrative plot of the L/E distribution for a hypothetical value of θ_{13} . Note that θ_{12} and both values of Δm^2 are approximately known, and that a large value of θ_{13} has been used. The huge dip at $L/E \sim 25$ km/MeV is what has been measured by the KamLAND reactor experiment with an average distance 180 km. The new reactor experiments would go back to $L/E \sim 0.5$ km/MeV and look for the smaller disappearance effect

Since the White Paper was published, four American Physical Society divisions have sponsored a study which is expected to give a report about future neutrino experiments in the United States in the fall of 2004. One of the six study groups will conclude that a measurement or stringent limit on θ_{13} would be crucial as part of a long term program to measure CP violation effects at accelerators, even though a reactor disappearance experiment does not measure any CP violation. A sufficient value of θ_{13} measured in a reactor experiment would strongly motivate the investment required for a new round of accelerator neutrino experiments. A reactor experiment's unambiguous measurement of θ_{13} would also strongly support accelerator measurements by helping to resolve degeneracies and ambiguities. The combination of measurements from reactors and neutrino results from accelerators will allow early probes for CP violation without the necessity of long running at accelerators with anti-neutrino beams.

The Reactor Neutrino White Paper identified seven possible sites for a new reactor antineutrino disappearance experiment. Argonne is currently helping to develop three of these possible projects: Angra (Brazil), Braidwood (Illinois) and Double CHOOZ (France). The Angra idea was initiated at Argonne and is now receiving some support from funding agencies in Brazil.

The principle of the proposed experiment is simple. One detector would be located about 100-200 m from a reactor core, and the other would be about 1400 m away. The detectors would measure inverse beta decay, the same process that was used to both discover the neutrino in the 1950's, and to solve the solar neutrino problem using KamLAND in 2002. If θ_{13} is large enough, the far detector will see a deficit of 1-5% in events compared to a $1/L^2$ extrapolation of the near detector, and there will be corresponding oscillations in the measured energy spectrum. The challenge is to keep differences in the response of the two detectors below 1%. There is increased recognition that this level of precision is achievable.

The measurement of reactor neutrinos in a reactor experiment is also straightforward. The inverse beta decay reaction is $\bar{\nu}_e p \rightarrow e^+ n$, followed by neutron capture. The positron annihilates with an energy release of 1-8 MeV. The reaction takes place on Hydrogen, which is a component of all scintillators. The neutron will capture on Hydrogen giving gamma rays with an energy of 2.2 MeV. Smaller experiments found it advantageous to add 0.1% Gd, which has a huge neutron capture cross section and gamma rays with an energy of 8 MeV. In CHOOZ 87% of the neutrons were captured on Gd. The early design of an acrylic sphere for a new reactor experiment is shown in Figure 2.

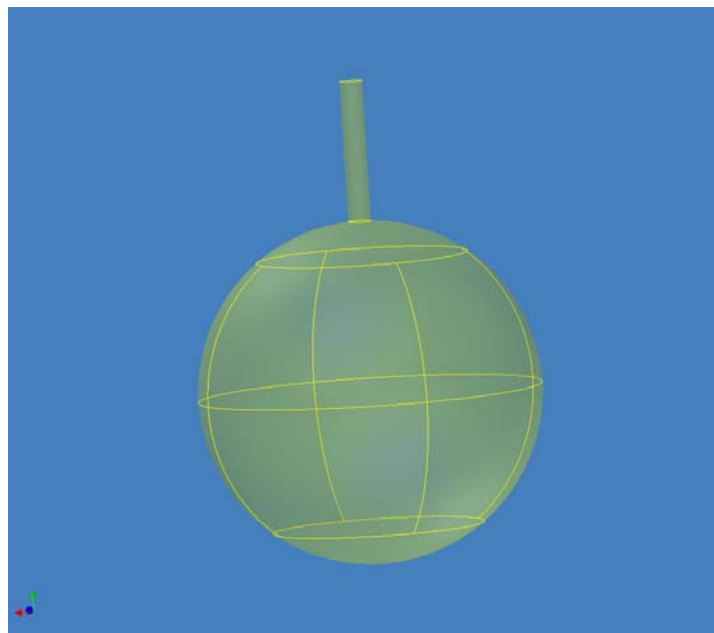


Figure 2. Preliminary design of an acrylic sphere in eleven segments.

The French Double CHOOZ proposal, taking advantage of an existing laboratory 1000 m from a powerful complex of nuclear reactors, can be the cheapest and fastest way forward. A pair of detectors can be constructed for about \$15M. A group of US institutions including Argonne has submitted a letter of intent to join the European Double CHOOZ collaboration, and could participate for about \$5M. However due to the location and size of the lab, Double CHOOZ can only reach a sensitivity of $\sin^2 2\theta_{13} < 0.03$ in three years. While this improves the current reach by about a factor of 5, it is considered possible and important to probe another factor of at least three. The Angra site in Brazil can use a single reactor site with two detectors dug into the nearby hills and improve the measurement of the backgrounds. The Braidwood site in Illinois can use two shafts located under the Illinois prairie. Each experiment can put large enough detectors and control backgrounds to reach $\sin^2 2\theta_{13} < 0.015$ with 5 years of running, but due to the need for civil construction together with larger detector costs, it is likely that funding and construction will be significantly later than Double CHOOZ. Thus a reasonable scenario is to help construct and operate the Double CHOOZ experiment from 2008-2010, and then shift attention to a more sensitive experiment after that.

The Double CHOOZ experiment together with Angra or Braidwood can be considered a single program. Experience related to backgrounds and systematic errors on the Double CHOOZ project can be applied towards assuring that the larger and more sensitive experiment can fully exploit its statistics.

A measurement of anti ν_e disappearance at the O (1%) level will require a new level of control of systematic errors compared to what has been done before. Most of the technical requirements of a new experiment are understood, but the details of the detector design still need to be optimized. Some of the open questions under consideration are the following: liquid scintillator loaded with 0.1% Gadolinium has been used in the past, but there are concerns regarding its stability in solution and attenuation length degradation needs to be understood. If movable detectors are chosen, there must be confidence that moving the detector does not introduce additional time-dependent effects. The use of a second detector will be used to control many systematic errors, but the relative energy calibration and efficiencies will need to be controlled and understood. A major challenge is the reduction of cosmic ray associated backgrounds, such as neutron spallation products and ^9Li spallation and their accurate estimation, particularly if the near detector and far detector are at different depths. The reduction of gamma ray background is also important because it will affect the ability to put the threshold below 1 MeV, the minimum energy expected from the positron.

Future searches for θ_{13} are a compelling part of the Department of Energy's 20 year program. The \$150M NOvA off-axis experiment, whose major goal is to measure θ_{13} , is being considered at Fermilab. A reactor experiment could make this measurement sooner (5 years rather than 10 years) and more economically. In the long run, both

experiments may be needed, but there are strong reasons to run a reactor experiment first. The early price estimates for participation in reactor experiments vary widely. The Double-CHOOZ experiment has a price estimate of 7.5M€, (not including locally provided site preparations or contingency) with an expected US contribution of no more than 1/3rd or \$5M (including contingency). An experiment done in Brazil or China would require large US contributions for the two detector costs of about \$20M, assuming the local funding agencies pay for the civil construction. A site in the US would probably cost \$50M - \$100M. ANL is well positioned to be the US host lab for any of these possibilities.

(M.C. Goodman)

I.C.5. Cosmic Ray Experiments

a) VERITAS

The Very Energetic Radiation Imaging Telescope Array System (VERITAS) is a high energy gamma-ray telescope array with sensitivity in the range 50 GeV - 50 TeV to study extreme astrophysical processes in the universe. The array VERITAS is being built at Kitt Peak in Arizona and is based on the ground-based detection techniques of its predecessor, the Whipple-10 meter optical gamma ray telescope, to explore the universe at the highest photon energies known to be emitted from cosmic sources. The emission of high-energy gammarays from cosmic objects always implies the presence of exotic and extreme physical conditions and the detection of this radiation offers a direct probe into these exciting phenomena.

The first phase of VERITAS (VERITAS-4) will be completed in 2006 when four telescopes are operating. These identical telescopes, each of aperture 12m, will be deployed in a filled hexagonal pattern of side 80m; each telescope will have a camera consisting of 499 pixels with a field of view of 3.5 degrees. It will have improved flux sensitivity over the Whipple telescope, a lower threshold energy, improved optics and camera and new technology where appropriate. An upgrade of 3 additional telescopes is planned after completion of VERITAS-4.

Four Argonne physicists, Karen Byrum, Steve Magill, Richard Talaga one electrical engineer, Gary Drake and one post-doctoral physicist, Elizabeth Hays have become involved with the VERITAS experiment. We received a joint University of Chicago-Argonne National Laboratory R&D grant to build the Track Imaging Cherenkov Experiment (TrICE) telescope to attempt to detect primary Cherenkov radiation of charged particles, which can be used to distinguish the composition of cosmic hadrons. But the primary purpose of TrICE is to study the feasibility of using multi-channel

photodetectors, to develop front end electronics to be used in conjunction with highly-pixellated future telescopes (VERITAS-7) in order to improve night sky background discrimination and to obtain angular resolution. We have constructed an electronics teststand, a dark box and have started developing a DAQ system. We have already performed initial gain, uniformity and crosstalk measurements on several candidate multi-channel photodetectors, the Hamamatsu H8500 and the Hamamatsu M64. We have chosen a site for TrICE after evaluating several candidate sites at ANL.

Argonne was accepted as an associate member of the VERITAS-4 collaboration in the spring 2004. Several of us took shifts in June running the Whipple telescope and in building the VERITAS-4 first prototype. Three of us also attended a collaboration meeting held in Arizona in January 2004.

b) Auger

The Pierre Auger Observatory is an experiment to study the highest energy cosmic rays with both fluorescence detectors, similar to those used in the Fly's Eye experiment, and an array of water Cerenkov detectors. This hybrid approach to observing the cosmic ray showers is believed to be essential to minimize systematic errors in the energy measurement and to accurately identify the arrival directions of the showers. The southern site for the observatory is under construction near Malargue, Argentina with expected completion in 2006, and the northern site is planned for Colorado or Utah.

Three Argonne physicists, S. Kuhlmann, H. Spinka, and R. Talaga, have begun to investigate a possible role for Argonne in the Auger experiment. One possibility is to tag muons traversing the water Cerenkov tanks with plastic scintillators located beneath the tank, after most of the electromagnetic part of the shower has been attenuated in the water. The use of spare MINOS scintillator strips to build a prototype muon detector is being considered. Another possibility would be to detect radio emission from cosmic ray showers. An ANL physicist attended an Auger upgrades meeting in Orsay, France where this possibility was discussed, as well as revised electronics for the northern site detectors.

(K. Byrum, R. Talaga, S. Magill, R. Wagner))

II. THEORETICAL PHYSICS PROGRAM

II.A. THEORY

II.A.1. Higgs Boson Production in Weak Boson Fusion at Next-to-Leading Order

Ed Berger and John Campbell investigated the weak boson fusion process for production of the neutral Higgs boson H at the CERN Large Hadron Collider (LHC). They focused on the accuracy with which the Higgs boson coupling to weak bosons may be determined from data. An important and, in fact, controlling aspect is the extent to which events produced by the weak-boson-fusion (WBF) subprocess may be separated from events in which a Higgs boson is produced by other mechanisms. A hallmark of the WBF subprocess is that the Higgs boson is accompanied in the final state by two jets that carry large transverse momentum and relatively large rapidity. However, purely strong interactions subprocesses also produce Higgs bosons accompanied by two jets. To extract the couplings reliably, a good understanding is required of both the production and the background processes. Berger and Campbell used hard QCD matrix elements in order to represent the signal and the H plus 2 jet background reliably. They did an independent calculation of the fully differential next-to-leading order QCD corrections to the WBF signal process and examined in detail the effects of the WBF selection cuts on these NLO QCD corrections. Among the goals in this study were to evaluate the effectiveness of different prescriptions for defining the WBF sample and to estimate the expected WBF signal purity P , by which they mean the fraction of real Higgs boson events produced by weak boson fusion.

Berger and Campbell found that purities of 60% to 70% can be expected if a selection of greater than 40 GeV is made on the two tagging jets. They derived an expression for the expected uncertainty on the effective Higgs-boson-to-weak-boson coupling strength g in terms of the signal purity, the expected statistical accuracy of the LHC experiments, and the theoretical uncertainties on the signal and the background processes. Numerical predictions for the uncertainty as a function of purity are shown in Fig. 1, for two choices of the statistical uncertainty. Signal purities of 0.65 or greater permit determinations of $\delta g/g$ of 10% or better after 200 inverse femtobarns have been accumulated at the LHC. On a cautionary note, however, they remarked that the WBF signal purity and the uncertainties are obtained in a very well controlled situation in which there is an identified Higgs boson in a sample of H plus 2 jet events produced by both the WBF mechanism and the QCD background processes. In an experimental context, there will be additional sources of background from final states that mimic a Higgs boson. The effects of these additional backgrounds presumably only increase the expected uncertainties on the couplings.

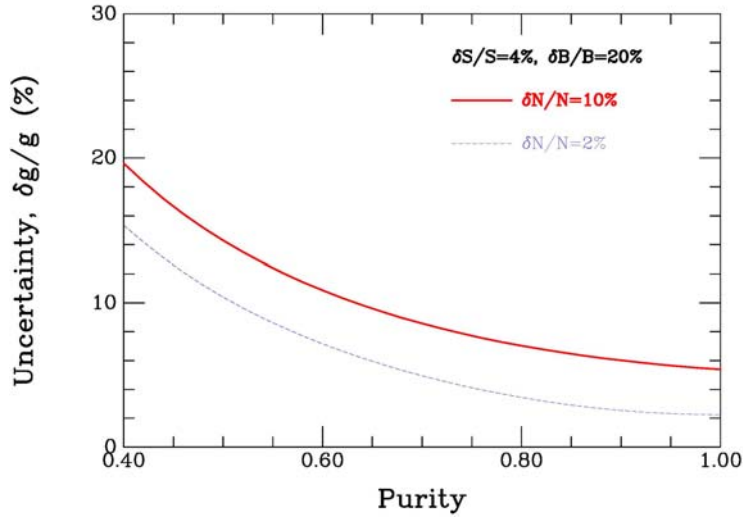


Figure 1. The predicted uncertainty $\delta g/g$ in the coupling of the Higgs boson to a pair of W bosons is shown as a function of signal purity $P = S/(S + B)$ for expected statistical accuracies $\delta N/N$ of 10% and 2%. The uncertainties in knowledge of the signal S and background B are assumed to be 4% and 20%, respectively.

The theoretical uncertainties on the signal and on both the size and uncertainty of the background dominate the uncertainty in the coupling. Current estimates of signal uncertainty are in the 5% range, and, since differential NLO calculations exist, this uncertainty is controlled by uncertainties in the parton densities and by the residual renormalization and factorization scale dependence. In order to reduce the estimated uncertainty in the coupling, the next major step would be a fully differential NLO calculation of the background applicable in the region of interest for WBF investigations, an undertaking that Berger and Campbell have begun.

The paper “Higgs Boson Production in Weak Boson Fusion at Next-to-Leading Order” by Berger and Campbell, hep-ph/0403194, was accepted for publication in Physical Review D, and is currently in press. Berger spoke on aspects of this work in seminars at the Kavli Institute for Theoretical Physics, Santa Barbara; the 12th International Conference on Supersymmetry and Unification of Fundamental Interactions (SUSY 2004), Tsukuba, Japan; the Victoria Linear Collider Workshop, Victoria, British Columbia; and the TeV4LHC Workshop, Fermilab.

(E. L. Berger and J. Campbell)

II.A.2. Constraints on the Light Gluino Mass from a Global Analysis of Hadronic Data

Light strongly interacting superpartners appear in certain supersymmetric models. Such particles would influence the running of the strong coupling strength α_s and would modify the evolution of the quark and gluon parton distribution functions (PDFs). It is important to ascertain how small a SUSY particle mass is tolerable within the constraints of present experiments. A global analysis of hadronic data is a powerful probe of strong interactions in which a simultaneous analysis is done of a large sample of data (about 2000 points) from a variety of scattering experiments at different momentum scales. The processes include deep-inelastic lepton scattering, production of Drell-Yan pairs, inclusive prompt photon production, and jet production at large values of transverse momentum. To describe the existing global analysis data set, it is necessary to account for the distributions of gluinos in the initial hadrons, which have different renormalization group properties from those of the quark and gluon distributions. An obvious question is whether the hadronic data are consistent with the existence of light superpartners.

Ed Berger, Pavel Nadolsky, Fred Olness of Southern Methodist University, and Jon Pumplin of Michigan State University, devised a set of parton densities for protons in which a gluino is included along with standard model quarks, antiquarks, and gluons. They used the methodology of the recent CTEQ6 analysis to explore the compatibility of the light gluino scenario with the world sample of hadronic data. Since the gluinos are fermions in the color-octet representation, their contributions are strongly enhanced when compared to the contributions from the color-triplet squarks. Therefore, Berger *et al.* included contributions from the gluino and neglected contributions from squarks. They found that the discriminating power of their analysis depends crucially on the inclusion of the Tevatron jet data in the fit, which allows them to better constrain the gluon distribution. The major results of their study are presented in the two-dimensional contour plot in Fig. 2 that shows the values of chi-squared of the global fit as a function of the gluino mass along one axis, and the value of the strong coupling strength evaluated at the scale M_Z , the mass of the neutral weak boson, along the other. Berger, Nadolsky, Olness, and Pumplin conclude that the possibility remains open for the existence of gluinos with mass above 10 to 20 GeV along with a moderately increased value (e.g., > 0.119) of the strong coupling strength at the scale M_Z . The scenario with light gluinos and bottom squarks is entirely consistent with their global analysis. Tighter constraints can be obtained in the future, after new data from HERA and the Tevatron become available.

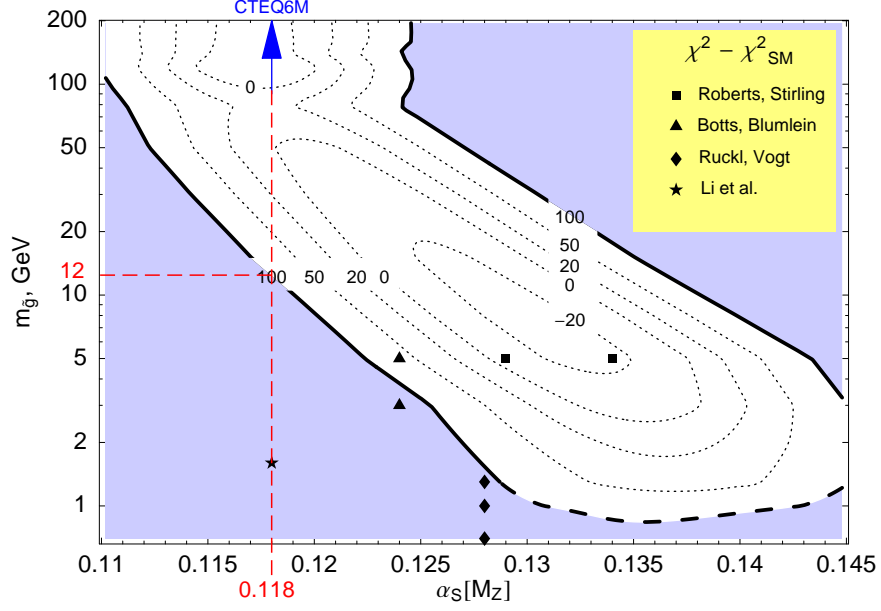


Figure 2. A contour plot of the change in χ^2 as a function of the strong coupling $\alpha_s(M_Z)$ and gluino mass $m_{\tilde{g}}$. The values of χ^2 are shown by labels on the corresponding isolines. The shaded region is excluded by the CTEQ6 tolerance criterion. The solid line marks the $\Delta\chi^2 = 100$ isoline.

This work appeared as “Light Gluino Constituents of Hadrons and a Global Analysis of Hadron Scattering Data”, hep-ph/0406143, submitted for publication in Physical Review D.

(E. L. Berger and P. Nadolsky)

II.A.3. Transverse Momentum Distribution of Upsilon Production

Ed Berger, working with Jianwei Qiu and Yi-li Wang of Iowa State University, calculated the transverse momentum distribution for production of the Upsilon states in hadronic reactions, applicable over the full range of values of transverse momentum. The Upsilon states are the spin-1 bound states of a pair of bottom quarks. Their results are in excellent agreement with Fermilab Tevatron data from the CDF and D0 collaborations. The starting assumption is that the transverse momentum distribution of Upsilon production may be derived from the transverse momentum distribution for the production of a pair of bottom quarks. Berger, Qiu and Wang expressed the differential cross section in terms of a two-step factorization procedure. They justified the validity of an all-orders soft-gluon resummation approach to compute the transverse momentum distribution in the region of small and intermediate values. Resummation is necessary to deal with the perturbative singularity and the large logarithmic enhancements

that arise from initial-state gluon showers. They demonstrated that the transverse momentum distribution at low values of transverse momentum is dominated by the region of small impact parameter and that it may be computed reliably in perturbation theory. They expressed the cross section at large values of transverse momentum by the lowest-order non-vanishing perturbative contribution. Their results and comparison with data, shown in Fig. 3, confirm that the resumable part of the initial-state gluon showers provides the correct shape of the transverse momentum distribution in the region of small transverse momentum. The work appeared in “Transverse Momentum Distribution of Upsilon Production in Hadronic Collisions”, hep-ph/0404158, submitted for publication in Physical Review D.

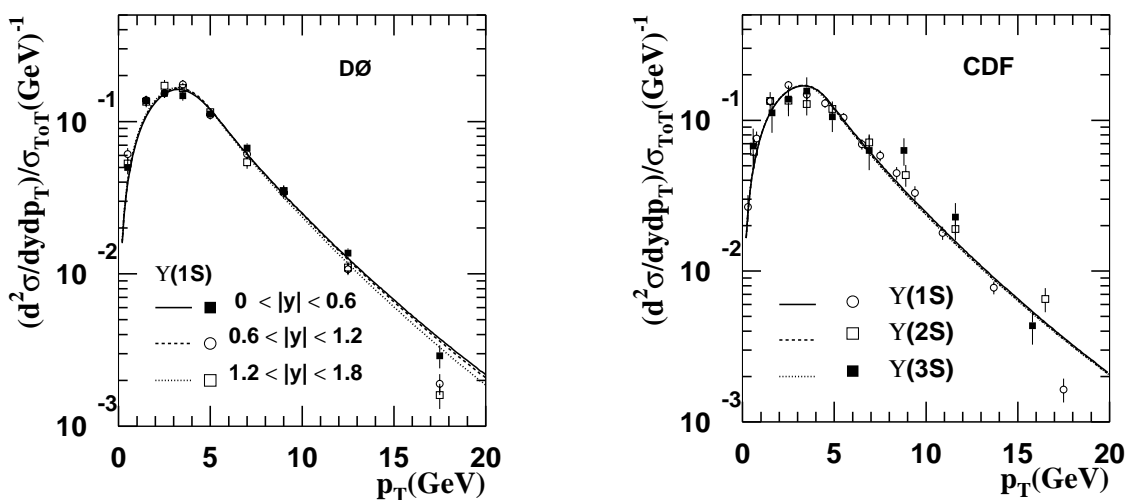


Figure 3. Normalized transverse momentum distribution for Υ production at a) $\sqrt{S} = 1.8$ TeV along with published Run 1 data and b) $\sqrt{S} = 1.96$ TeV along with preliminary D0 Run 2 data.

(E. L. Berger)

II.A. 4. Aspen Winter Meeting, 2004

Ed Berger was the principal scientific organizer of the 2004 Aspen Winter Conference on Particle Physics in February 2004, <http://gate.hep.anl.gov/berger/Aspen04/>. The responsibilities included the definition of a theme for the meeting, “Where We Are and Where We Are Going”, the appointment of a diverse Scientific Program Committee and an International Advisory Committee, construction and maintenance of the web page, preparation of a successful proposal for funding to DOE, and the choice and persuasion of Frank Wilczek (subsequent 2004

Nobel laureate) to deliver the Aspen evening public lecture. (At the final minute, Frank was prevented by a snow storm from arriving, and Berger had to be resourceful and persuasive in finding a replacement so that the public lecture in the Wheeler Opera House would go on.)

The winter conference was aimed at the full range of important topics in particle physics, theory and experiment, related to accelerator-based, underground, and space-based approaches, with emphasis on the “big picture” to which these all contribute. Speakers reported on lepton and quark flavor physics, hadronic and electroweak interactions, neutrino oscillations, the particle physics aspects of dark matter and dark energy, Higgs bosons, and new directions in supersymmetry, technicolor, and extra space-time dimensions. Presentations addressed future opportunities at the Large Hadron Collider, a new linear collider, new neutrino sources and experiments, and the other facilities under consideration. Connections to particle astrophysics and cosmology were explored. Berger gave an introductory overview talk on the first day of the meeting and a talk to introduce the speaker at the public lecture. In selecting members of the Program and Advisory Committees and in constructing the scientific program, he successfully involved new people who had not served previously on these committees or spoken at a recent Aspen winter conference. Circumstances left him with more than his share of the responsibility for the experimental, as well as the theory, parts of the program. A good mix was achieved of more senior speakers and young individuals, some of whom gave plenary talks for the first time in their careers. The full list of topics and speakers may be found on the web site. There was considerable praise both at the meeting and many times since for the high quality of the program and stimulating environment of the meeting.

(E. L. Berger)

II.A.5. Theory Workshop on Supersymmetry, Higgs Bosons, and Extra Dimensions

For the fifth year in a row, Ed Berger, Carlos Wagner, and the contingent of theory postdocs organized an Argonne Theory Workshop on the Physics of Supersymmetry, Higgs Bosons, and Extra Dimensions, May 24-28, 2004, <http://gate.hep.anl.gov/berger/ANLWorkshop2004/>. The goal was to examine outstanding issues in theory and phenomenology and their implications for future experiments. Seven talks were scheduled per day. Intense informal discussion was facilitated and encouraged among external participants and Argonne theory staff. The workshop was open to participation by all in the Division. A sixth similar workshop is planned in 2005. This series of meetings is valued highly in the national particle physics theory community and has come to be an expected event in the spring, with young theorists looking forward eagerly to participation.

(E. L. Berger and C.E.M. Wagner)

II.A.6. Lattice Computation of Spin Correlations in NRQCD Color-Octet Matrix Elements

The motivation for this study and previous work on the subject were described in the report for the period July 1, 2003--December 30, 2003.

G. Bodwin, J. Lee, and D. Sinclair have now completed and debugged two independent sets of code for calculating S -wave color-octet matrix elements. Preliminary results have been obtained for charmonium and bottomonium based on 400 gauge-field configurations on $12^2 \times 24$ lattices at a lattice coupling of $\beta = 5.7$. At this value of the coupling, the lattice spacing is $a = 0.81 \text{ GeV}^{-1}$ for charmonium and $a = 0.73 \text{ GeV}^{-1}$ for bottomonium. Since the radius of the charmonium is about 1.1 GeV^{-1} and the radius of the bottomonium is about 0.6 GeV^{-1} , the quarkonia are well contained in the lattice volume. However, the lattice spacing is rather coarse, and, so, order- a^2 improvements have been implemented in the part of the heavy-quark lattice action that is of leading order in v . Tadpole improvement of the action has been employed. This is a technique for redefining the lattice action so that its perturbation series is close to continuum perturbation series and, hence, converges well. Since the lattice and continuum matrix elements can be related through perturbation theory, the use of this technique gives some assurance that the lattice matrix elements that are obtained are not very different from the corresponding continuum matrix elements.

The preliminary results indicate that the hierarchy of matrix elements that is suggested by the velocity-scaling rules is realized in the computed matrix elements. If anything, the expansion parameter that governs the sizes of the matrix elements appears to be smaller than v . The values of the matrix elements that have been obtained may suggest that, in addition to the factors of v that are associated with a matrix element, one should associate a factor $1/\pi$ for each loop in the perturbative expansion for the matrix element.

The spin-triplet-to-spin-singlet transition is large compared with the triplet-to-triplet transition, suggesting that the production rate of η_c 's at large transverse momentum at the Tevatron may be comparable to the production rate of J/ψ 's.

The triplet-up-to-triplet-longitudinal rate is small compared with the triplet-up-to-triplet-up rate. This supports the expectation that there should be substantial transverse polarization of J/ψ 's at large transverse momentum at the Tevatron.

The computed decay matrix elements are somewhat smaller than the production matrix elements that have been extracted from phenomenology. In the case of the J/ψ , the computed decay matrix element is about a factor of two smaller than the smallest

phenomenological value for the production matrix element. In the case of the Υ , the computed decay matrix element is about a factor of ten smaller than the smallest phenomenological value for the production matrix element. However, it should be noted that the error bars on the phenomenological matrix elements are very large and that, in the case of the Υ , multiple gluon emission, which is known to reduce the size of the matrix elements drastically, has not been taken into account. Furthermore, decay matrix elements and production matrix elements need not be equal, even if they scale in the same way with v , and lattice matrix elements are not equal to continuum matrix elements, although, in the present case, the differences are not expected to be large.

There are some anomalies in the computed matrix elements. For example, the triplet-up-to-triplet-down rate is comparable to the triplet-up-to-triplet-up rate, even though it is nominally suppressed by v^2 . At $\beta = 5.7$, the lattice cutoff is $\Lambda = \pi/a \approx 4.1$ GeV. Hence, in the case of charmonium, the cutoff is substantially larger than the heavy-quark mass, and the matrix elements may be contaminated by spurious contributions that originate from momenta that lie beyond the region of validity of NRQCD. Such spurious contributions do not satisfy velocity scaling. A perturbative analysis indicates that the leading spurious contributions scale as $[a_s(\Lambda)]^2 (\Lambda/m_c)^4$ and $[a_s(\Lambda)]^2 (\Lambda/m_c)^2 \log(\Lambda/m_c)$. Work on controlling these contributions by reducing the effective value of Λ is in progress. Techniques that are being explored include the use of point-split operators, the use of different formulations of the lattice action, and computation at a coupling of $\beta = 5.5$. Preliminary results indicate that lowering Λ does indeed reduce the deviations of the matrix elements from expectations based on velocity scaling.

II.A.7. Lattice QCD

We perform lattice QCD simulations to study the properties of hadrons and their interactions, and to study the properties of hadronic matter, nuclear matter and the quark-gluon plasma.

One ongoing project involves the study of Lattice QCD at a finite isospin chemical potential μ_I (finite isospin density). Most recently we have been simulating this theory at finite temperatures and small μ_I close to the transition from hadronic matter to a quark-gluon plasma. We have collected evidence to support the indications that this is closely related to the more interesting case of finite quark-number chemical potential μ_q and temperature, which cannot be simulated directly because of a sign problem (complex fermion determinant). Our now-completed work with 2 flavours

showed that the dependence of the transition temperature transition on μ_l and μ_q is identical for $\mu_l = 2\mu_q$, but showed no sign of the expected critical endpoint.

In this time period we have extended these simulations to the more physical case of 3 flavours, where it is believed that the critical endpoint can be tuned to be as close to $\mu_l = 2\mu_q = 0$ as we desire. Very preliminary results (Fig. 1) suggested that we might indeed be seeing evidence for a critical endpoint. For this analysis, we have applied a powerful analysis tool developed in condensed matter physics, the Binder cumulant. However, we have seen in our 2-flavour analyses that such fluctuation quantities are very sensitive to the molecular-dynamics ‘time’ increment dt used in our simulations. This means an analysis of the dt dependence of these cumulants will be needed to determine whether this critical point will survive in the physical $dt \rightarrow 0$ limit.

We have continued our project to test the NRQCD velocity scaling rules for spin dependent colour-octet matrix elements for charmonium and bottomonium. For this we are using 400 quenched lattice configurations with inverse lattice spacing $\alpha^{-1} \sim 1$ GeV, and a lattice NRQCD action correct through next-to-leading order in v^2 (v is the quark velocity in the quarkonium state). Since production matrix elements are difficult, if not impossible, to define in such a way as to admit a lattice calculation, we are concentrating on decay matrix elements, in the belief that if velocity scaling works for decays, it should also work for production. Preliminary calculation of these matrix elements on 100 configurations show that they are indeed suppressed, as velocity scaling would suggest, but more work is required to make this observation quantitative.

We are continuing to collect statistics in a study of the properties of the finite temperature chiral transition for 2 flavours of massless quarks. These simulations are being performed on $12^3 \times 8$, $16^3 \times 8$ and $24^3 \times 8$ lattices. Here we are using a lattice QCD action, modified by the addition of irrelevant 4-fermion interactions, which allow zero-mass simulations. Preliminary estimates of the critical exponent describing the dependence of the chiral condensate on temperature close to the critical point are consistent with the expectation that the critical scaling is in the universality class of 3-dimensional $O(4)$ or $O(2)$ spin models. More work is needed to exclude other possibilities.

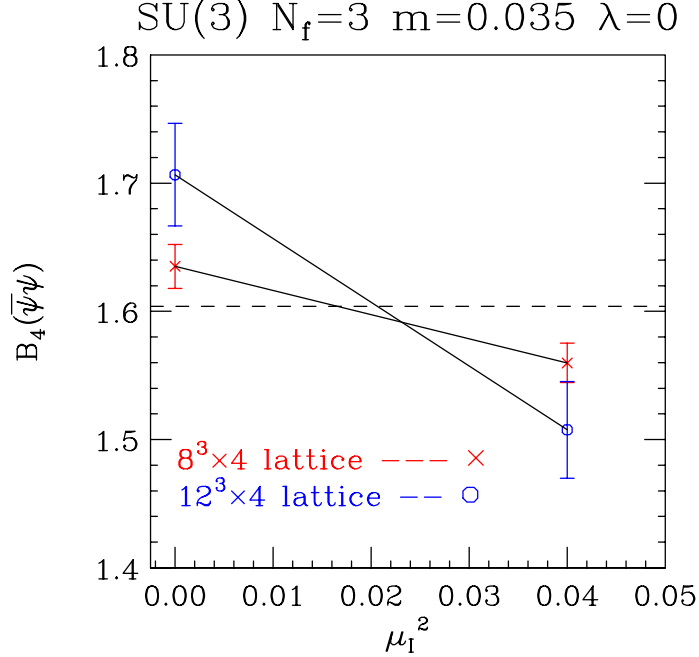


Figure 1. Preliminary measurements of the Binder cumulant as a function of μ_I at finite temperature $T = 1/4a$. $B_4 \approx 1.604$ at a critical endpoint.

Finally, we have been generating configurations with 2 flavours of massless dynamical quarks using the aforementioned action at zero temperature on a $16^3 \times 32$ lattice, on which we will make a first measurement of the low-lying hadron spectrum in the chiral limit.

(D. K. Sinclair)

II.A.8. Electroweak Baryogenesis and Dark Matter in the nMSSM

The Standard Model (SM) provides an excellent description of all elementary particle interactions up to energies of order 100 GeV. However, there are several reasons to expect that an extension of the Standard Model description is needed at energies slightly above this scale. The most important of these is that the scale of electroweak symmetry breaking in the SM is unstable due to large quantum mechanical corrections. The Standard Model description also fails to answer two of the most important questions at the interface of particle physics and cosmology: the nature of the dark matter and the origin of the baryon asymmetry. All of these problems can be resolved by invoking supersymmetry (SUSY). SUSY forces the most dangerous quantum corrections to vanish thereby stabilizing the electroweak scale. In models of low-energy supersymmetry with conserved R-parity, the lightest supersymmetric particle (LSP) provides a natural source

for the observed dark-matter density. Supersymmetric models can also explain the origin of the matter-antimatter asymmetry in several ways.

Electroweak baryogenesis is a particularly attractive mechanism to generate the baryon asymmetry, which relies on anomalous baryon violating processes at the weak scale. For electroweak baryogenesis to be successful, these processes must out of equilibrium in the broken phase at the critical temperature of the electroweak symmetry breaking phase transition. This is possible only if the phase transition is strongly first order, or equivalently,

$$\frac{\varphi(T_c)}{T_c} \gtrsim 1, \quad (1)$$

where $\varphi(T_c)$ is the Higgs vacuum expectation value in the broken phase at the critical temperature T_c . Such a strongly first order transition cannot be achieved within the SM framework. This condition is also difficult to fulfill in the minimal supersymmetric extension of the SM, the MSSM.

The electroweak phase transition can be made more strongly first order by adding a gauge singlet superfield to the MSSM. Unfortunately, such a field may also generate new problems such as cosmologically unacceptable domain walls or a destabilization of the weak scale. However, there exists a particular singlet extension of the MSSM, the nMSSM, which is free of such problems. In [arXiv:hep-ph/0404184], we demonstrated that within the nMSSM, a strong, first order electroweak phase transition, necessary for electroweak baryogenesis, may arise. Furthermore, we found that in the regions of parameter space for which this is true, it is also possible to obtain a neutralino LSP with the correct relic abundance to explain the observed dark matter. Figure 1 shows the relic density obtained for parameter sets consistent with electroweak baryogenesis. We also investigated the phenomenology of the parameter space in which these two properties are fulfilled. In particular, we found that there are always two light CP-even and one light CP-odd Higgs bosons with masses smaller than about 250 GeV. Moreover, in order to obtain a realistic relic density, the lightest neutralino mass tends to be smaller than $M_Z/2$, in which case the lightest Higgs boson decays predominantly into neutralinos.

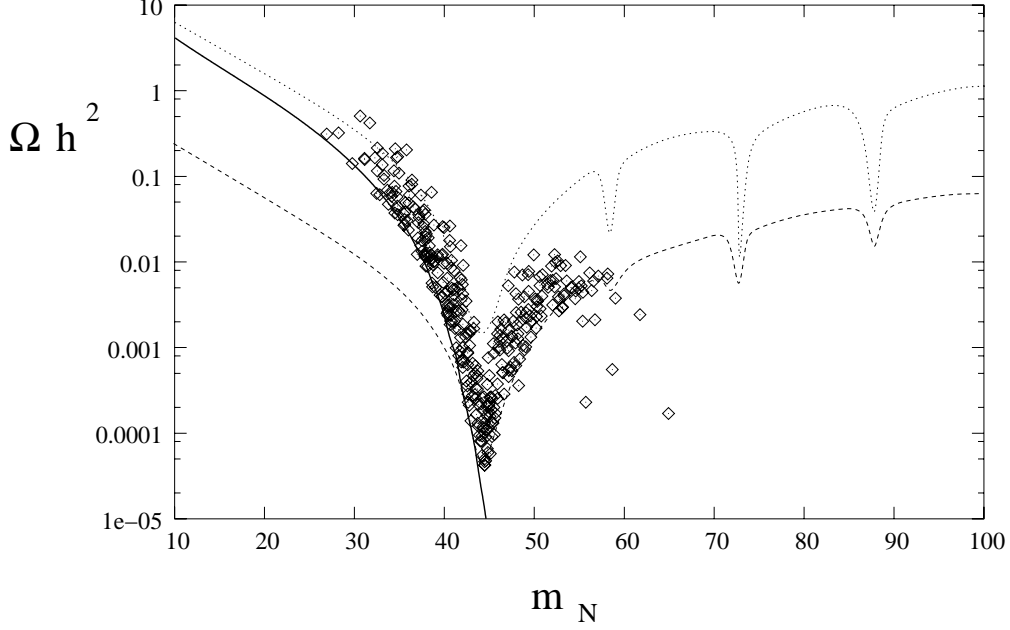


Figure 1. Neutralino relic density as a function of mass for two values of the mixing parameter, $\left| |N_{13}|^2 - |N_{14}|^2 \right| = 0.1$ (dotted), 0.5 (dashed) and typical values of the Higgs mixing parameters. The region to the right of the thick solid line is consistent with the observed Z width. The scattered points correspond to parameter sets that give a strong first order phase transition, and are consistent with perturbative unification.

(A. Menon, D. E. Morrissey, and C.E.M. Wagner)

II.A.9. Noncommutativity and the Ultrahigh-Energy Cosmic Ray & TeV Photon Paradoxes

Extragalactic cosmic rays with $E > 4 \times 10^{19}$ eV (exceeding the GKZ cutoff) should be stopped by microwave background ($10^{-3} - 10^{-4}$ eV) photons, $p + \gamma \rightarrow p + \pi$.

Likewise, ultra-energetic photons, with $E \sim 10 - 20$ TeV from BL Lac blazars, 157 Mpc away, are claimed to be necessarily absorbed by IR background (10^{-1} eV) photons, $\gamma + \gamma \rightarrow e^+ + e^-$.

Yet, there are multiple reports of experimental observation of both types of such events, which are thus deemed paradoxical. Tiny hypothesized violations of Lorentz invariance (*e.g.*, in noncommutative and q -deformed settings) might shift the relevant

thresholds and thereby allow such paradoxical events, by modifying Einstein's energy-momentum dispersion law, $E = \sqrt{m^2 + p^2}$.

C Zachos [Mod Phys Lett **A19**, 1483-1487 (2004)] demonstrated that an entire class of such models (Chen & Yang) cannot possibly work. He showed that the underlying noncommutative theory invoked does not really dictate the modified dispersion law proposed, because it has been misunderstood and its implications have been misinterpreted. Moreover, even if the novel dispersion law investigated was simply postulated, independently of any theory, it would still be plagued by tachyonic (superluminal) propagation, and would thus violate causality/positivity.

Furthermore, such modified dispersion photons would decay in flight by themselves, $\gamma \rightarrow e^+ + e^-$, with no need for IR photons to absorb them. As a result, Zachos showed the proposed dispersion law to be untenable. The proponents of the modified dispersion attempted to subsequently save it, by complexifying the hypothesized relevant parameters, but this 'fix' has proven worse than the original affliction, leading to a proliferation of unforgiving constraints, and merely displacing the tachyonic behavior from high to low energies.

Interestingly, vigorous discussion with experts, in response to archive posting of this comment paper, led to the conclusion that the data themselves need not be that paradoxical, after all, despite widespread claims to the contrary. Indeed, intergalactic absorption can account for survival of TeV photons; while, for cosmic rays, even if there is anomalous punch-through, the relevant thresholds are not really displaced, as required by the unrealistic dispersion law.

(C. Zachos)

III. ACCELERATOR RESEARCH AND DEVELOPMENT

III.A. ARGONNE WAKEFIELD ACCELERATOR PROGRAM

III.A.1. The Argonne Wakefield Accelerator Facility Status

We continued to commission the new gun and perform beam physics studies on it. The beam energy from the gun has now reached 8 MeV, with a minimum of dark current. Using a Mg photocathode, an electron beam charge ranging from 1 nC to 100 nC was produced. The electron bunch length was measured using Cherenkov light emitted from an electron beam passed through a thin quartz plate. The measured rms bunch length is in a good agreement with the design and a FWHM < 13 ps was measured for a 70 nC beam charge.

For the anticipated series of high-gradient wakefield experiments that we have planned, including our goal for the 100 MeV demonstration, the drive beam energy needs to be at least doubled from 8 to >16 MeV by adding a linac tank from the original AWA beamline. During this period, we commissioned the new linac tank with 12 MW of RF power input. This is expected to yield beam energy of more than 18 MeV and detailed beam energy measurement are underway.

During this period, we have performed additional high-brightness electron beam measurements by using a modified 3-screen technique to measure the emittance (Figure 1 shows the experimental setup). To our surprise, detailed analysis of the data showed that the 1 nC beam emittance is so low and that the space charge is so high that emittance

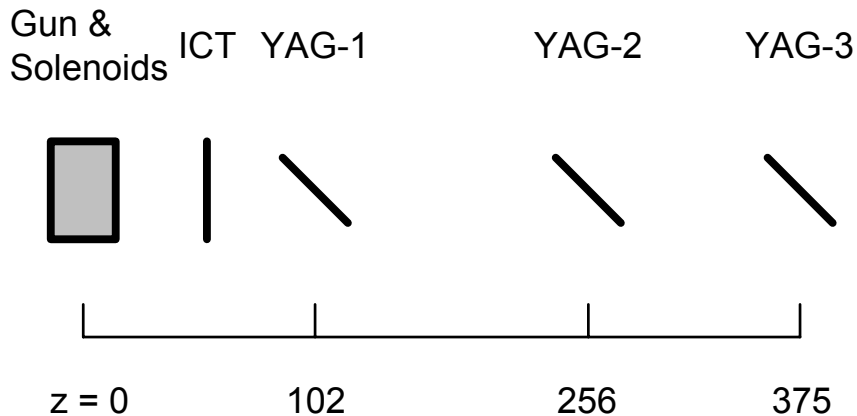


Figure 1. A simplified diagram of the AWA Gun Test Stand beamline. Charge is measured by the ICT and beam images are measured by inserting the phosphor screens YAG-1, YAG-2, or YAG-3. ($z = 0$ is the location of the photocathode; all distances are in cm)

could not be accurately determined with our technique due to the uncertainty in the spot size. Even so, we were still able to fit the data with TRACE 3-D and found that the fitted emittance value is bounded between 1 and 20 mm mrad at ~ 8 MeV. The large fit range is a result of the resolution with which we measure the beam size. In addition to the emittance determination, we also compared the measured spot sizes to predictions from PARMELA (Figure 2) and found reasonably good agreement.

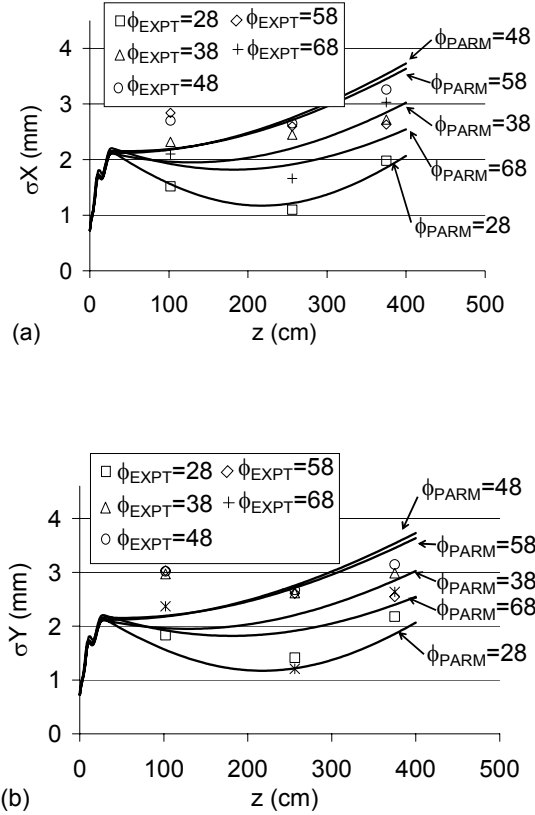


Figure 2. Comparison of the PARMELA beam envelope (solid lines) and the measured spot sizes (symbols) shows relatively good agreement.

We have also performed another experiment that has the potential to impact high-brightness electron beam generation. The scheme is based on Schottky enabled photoemission from the AWA photoinjector and uses photons with energy lower than the cathode work function. The single-photon photoemission process is possible due to the lowering of the effective work function by the RF electric field (E-field) on the cathode (Schottky effect). This effect can be used to significantly lower the thermal emittance of an electron beam, opening up new possibilities in the quest for high brightness beam.

Figure 3 shows the schematic experimental setup. Where the experimental parameters are: A frequency-doubled Ti:Sapphire laser 372 nm (3.3 eV), 1 – 4 mJ, 8ps as the light source; The photocathode: Mg, $\Phi = 3.6$ eV. In Figure 4, we show the measured electron beam charge for the example of Schottky effect on the cathode with at $E = 60$ MV/m, $\Delta\phi \sim 0.3$ eV.

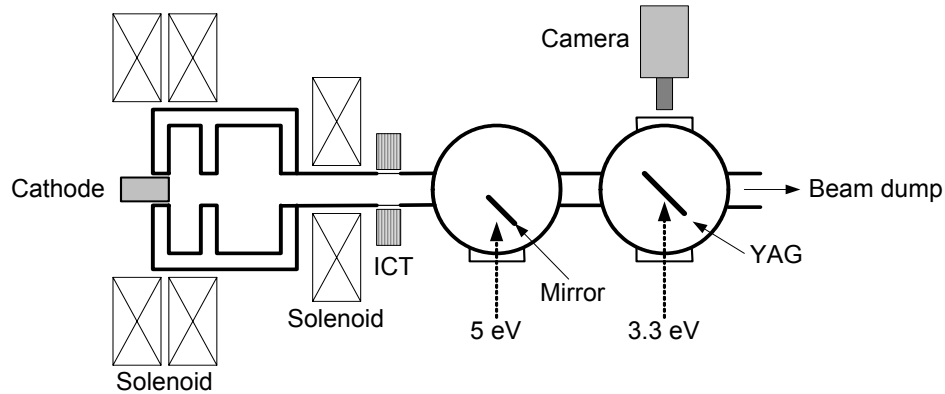


Figure 3. Experimental setup for the Schottky-enabled emission.

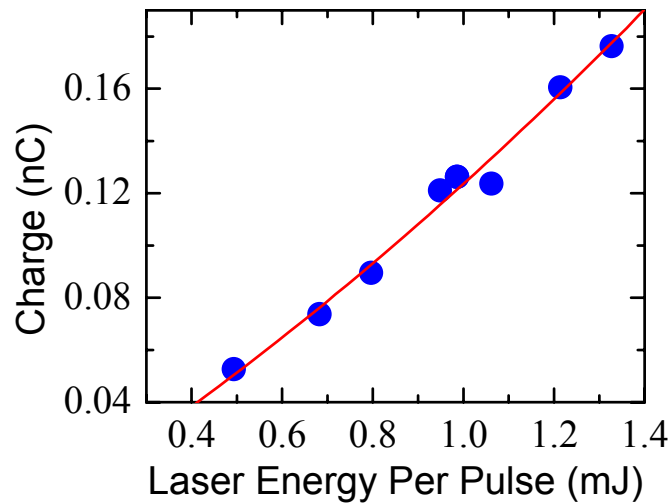


Figure 4. Measured photoemission via Schottky effect. As we increase the laser intensity, we detect more charge.

III. A. 2. Development of externally-driven, 11.424 GHz, dielectric-loaded structures and high-power tests at NRL.

A series of high power tests were conducted at NRL during this period, and a number of significant physics results were obtained that may impact the eventual use of these devices for future high energy accelerators.

Once the modulator RF coupling structure developed, the experimental development period has been much reduced. We have been testing two dielectric materials, Alumina (dielectric constant of 9.4) and $\text{Mg}_x\text{Ca}_{1-x}\text{TiO}_3$ (dielectric constant of 20). Progress has been made and new physical phenomena observed. The problems observed in each experiment were investigated, understood and solutions are under development. Better performance is expected for the coming new experiments.

In order to suppress the multipactor in the alumina based DLA structure that we discovered in the previous experiment, a thin layer of TiN coating was applied on the inner surface of alumina tube. The initial indications are that the coating was partially effective in reducing multipactoring. For instance, multipactor initiated at 1.6 MV/m accelerating gradient compared to 1 MV/m for the uncoated structure. Furthermore, when the incident power reached 1 MW, then finally 5MW, which is equivalent to an increase in gradient from 3.7MV/m to 8MV/m, the multipactoring effect appeared to saturate. A second method to suppress multipactor was to apply a uniform, longitudinal, magnetic field to the dielectric tube by use of a solenoid installed outside the structure during the experiment. In both the non-multipactor region (incident power below 200 kW) and the saturation region (incident power above 1 MW) the RF power transmission did not show a significant change, but to our surprise, it slightly reinforced the multipactor process in the central region.

The other two high-power RF tests were performed on the $\text{Mg}_x\text{Ca}_{1-x}\text{TiO}_3$ (MCT) based DLA structure in January and June 2004. In the January experiment, the dielectric taper in the output end had a small defect at the small end surface that caused a strong local field enhancement to occur. (This is the same 'air gap' effect observed in the test of August 2003.) The maximum RF power applied to the tube was only 1.2 MW due to the appearance of an arc that started at an incident power level of 1 MW. This is equivalent a local field of more than 65 MV/m at the output dielectric joint with the field enhancement effect factored in, but not considering the standing wave ratio. In the June 2004 experiment, a new set of dielectric pieces were used in the structure. The power reflection and transmission coefficients measured on the bench were very close to the simulation results; indicating a well made structure. However, the dielectric joint breakdown happened again but this time at a different location; the dielectric joint at input end. The incident power was still limited to 1 MW before breakdown, which is equivalent to 5.7 MV/m accelerating gradient at the input end and 100 MV/m at the input

dielectric joint. It is apparent that there will always exist a vacuum gap between the dielectrics with the current design. New schemes are currently being investigated to overcome such problems.

(W. Gai)

III. B. MUON COLLIDER EFFORT

As part of the MICE rebaselining effort there was continuing study of the background levels in the MICE experimental area. We have also been working to try to generate an experimental program using the high voltage field ion microscope in the David N. Seidman group in the Materials Science and Engineering Department of Northwestern University.

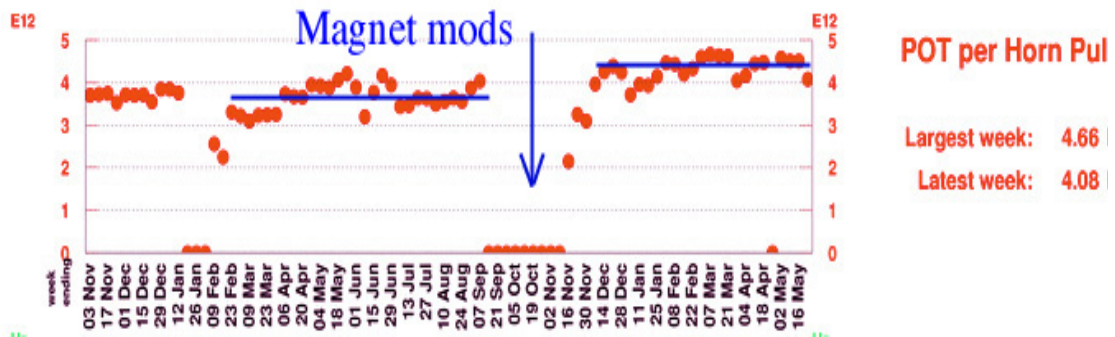
a) Development of the Breakdown Model

We have continued to improve our model of breakdown, which we are expanding to include high pressure gas, small gaps and a variety of special circumstances such as coulomb explosions, cluster emission, dusty plasmas and backbombardment of the wall surface. We submitted a short outline of our method to Nuclear Instruments and Methods. The powers involved in field emission heating of fragments are enormous, on the order of 10^{14} W/cm³, one of the highest natural power densities in the universe, and comparable to those in nuclear weapons. We submitted a proposal to DOE to do a systematic study of this subject.

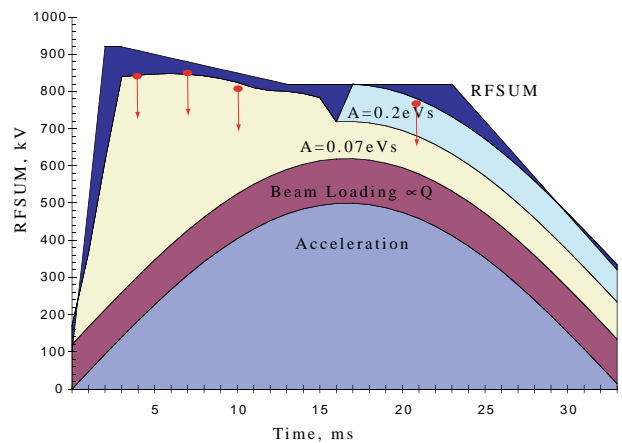
b) Booster Improvements at Fermilab

A group consisting of J. Dooling, IPNS, K. Harkay ASD and J. Norem directed some effort at the Fermilab Booster, in response to a general request, and funding, from the Lab Director.

In September '03, FNAL was unable to proceed with planned improvements in beam optics due to funding problems. With the promise of LDRD funds, we fabricated and helped install components for a modification to the injection dogleg chicane. This modification, made in a shutdown in October 03, was the major change in the shutdown which was able to **raise the intensity of the accelerator by ~20%**, a remarkable achievement for a 30 year old accelerator. The data below, showing protons on target, is from the MiniBoone experiment website. This effort required some managerial, but very little intellectual, effort.



We have also been active in looking at beam losses at transition and overall rf voltage requirements. We have proposed a new (to them) picture of beam loading and longitudinal phase space requirements. This original picture shows how longitudinal beam emittance growth at transition, causes losses that limit the beam intensity. A program of beam loss measurements led by Argonne has quantified this effect. One FNAL-TM has been written on this subject. We have also lead a study of causes for longitudinal longitudinal emittance growth that cannot be eliminated, such as the recapture of asymmetrical bunches after transition. They are using this data to reconfigure their voltage program.



(J. Norem)

IV. PUBLICATIONS

IV. A. Books, Journals And Conference Proceedings

A DK Molecule or Other $4q$ Model for the $D_s\pi$ Resonance at 2.32 GeV

H. J. Lipkin

Published in *New York 2003, Proceedings of the Conference on Intersections of Particle and Nuclear Physics (CIPANP 2003)*, Vol. 698, (AIP, February 2004) pp. 493-496.

Anomaly Mediated Supersymmetry Breaking and the Ancillary U(1) Formalism

B. Murakami

Published in *Boston 2003, Proceedings of the International Conference on 20 Years of SUGRA and Search for SUSY and Unification (SUGRA20)*, ed. by P. Nath (Rinton, Princeton, 2004) pp. 214-227.

Associated Production of a Z Boson and a Single Heavy Quark Jet

J. Campbell, R. K. Ellis, F. Maltoni, and S. Willenbrock

Phys. Rev. **D69**, 074021 (April 2004).

Azimuthal anisotropy at RHIC: the first and fourth harmonics

R. V. Cadman, K. Krueger, H. M. Spinka and D. G. Underwood

Phys. Rev. Lett **92**, 062301, (Feb. 2004).

Azimuthally sensitive HBT in Au+Au collisions at $\sqrt{s_{NN}} = 200$ GeV

R. V. Cadman, K. Krueger, H. M. Spinka and D. G. Underwood

Phys. Rev. Lett. **93**, 012301 (June 2004).

Beautiful Mirrors, Unification of Couplings and Collider Phenomenology

D. E. Morrissey and C.E.M. Wagner

Phys. Rev. **D69**, 053001 (March 2004).

Beauty Photoproduction Measured Using Decays into Muons in Dijet Events in ep Collisions at $\sqrt{s} = 318$ GeV

S. Chekanov, M. Derrick, D. Krakauer, J. H. Loizides, S. Magill, S. Miglioranza,

B. Musgrave, J. Repond and R. Yoshida

Phys. Rev. **D70**, 012008 (December 2003). (*not previously reported*)

Charmless $B \rightarrow VP$ Decays Using Flavor SU(3) Symmetry

C.-W. Chiang, M. Gronau, Z. Luo, J. L. Rosner, and D. A. Suprun

Phys. Rev. **D69**, 034001 (February 2004).

Cross Sections and Transverse Single-Spin Asymmetries in Forward Neutral Pion Production from Proton Collisions at $\sqrt{s} = 200$ GeV

R. V. Cadman, K. Krueger, H. M. Spinka and D. G. Underwood
Phys. Rev. Lett. **92**, 171801 (April 2004).

Comment on “Noncommutativity as a Possible Origin of the Ultrahigh-energy Cosmic Ray and the TeV Photon Paradoxes

C. Zachos
Mod. Phys. Lett. **A19**, 1483-1487 (June 2004).

CP^H : A Computational Tool for Higgs Phenomenology in the Minimal Supersymmetric Standard Model with Explicit CP Violation

J. S. Lee, A. Pilaftsis, M. Carena, S. Y. Choi, M. Drees, J. Ellis, and C.E.M. Wagner
Comput. Phys. Comm. **156**, 283-317 (January 2004).

Deformation Quantization, Superintegrability and Nambu Mechanics

C. K. Zachos and T. L. Curtright
Acta Physica Hungarica **19**, 199-203 (April 2004).

Evidence of a Narrow Baryonic State Decaying to $K_s^0 p$, $K_s^0 \bar{p}$ and $K_s^0 p \bar{p}$ in Deep Inelastic Scattering at HERA

S. Chekanov, M. Derrick, D. Krakauer, J. H. Loizides, S. Magill, S. Miglioranzi, B. Musgrave, J. Repond and R. Yoshida
Phys. Lett. **B591**, 7-22 (2004).

Exclusive Electroproduction of J/ψ Mesons at HERA

M. Derrick, S. Chekanov, D. Krakauer, J. H. Loizides, S. Magill, S. Miglioranzi, B. Musgrave, J. Repond, R. Yoshida
Nucl. Phys. **B695**, 3-37 (2004).

Finite Density Lattice Gauge Theories with Positive Fermion Determinants

J. B. Kogut, D. K. Sinclair, and D. Toublan
Prog. Theor. Phys. Suppl. **153**, 40-50 (2004).

High Q^2 Neutral Current Cross Sections in e+p Inelastic Scattering at $\sqrt{s} = 318$ GeV

M. Derrick, S. Chekanov, D. Krakauer, J. H. Loizides, S. Magill, S. Miglioranzi, B. Musgrave, J. Repond, R. Yoshida
Phys. Rev. **D70**, 052001 (2004).

Identified particle distributions in $p\bar{p}$ and Au+Au collisions at $\sqrt{s_{NN}} = 200$ GeV

R. V. Cadman, K. Krueger, H. M. Spinka and D. G. Underwood
Phys. Rev. Lett. **92**, 112301 (March 2004).

Lattice QCD at Finite Isospin Density and/or Temperature

J. B. Kogut and D. K. Sinclair

Nucl. Phys. Proc. Suppl. **129**, 542-544 (March 2004).

Lower Limits on R-Parity-Violating Couplings in Supersymmetric Models with Light Squarks

E. L. Berger and Z. Sullivan

Phys. Rev. Lett. **92**, 201801 (May 2004).

Measurement of Beauty Production in Deep Inelastic Scattering at HERA

M. Derrick, S. Chekanov, J. H. Loizides, S. Magill, B. Musgrave, J. Repond, R. Yoshida

Phys. Lett. **B559**, 173-189 (2004).

New Predictions for Multiquark Hadron Masses

H. J. Lipkin

Phys. Lett. **B580**, 50-53 (January 2004).

Nonleptonic Λ_b Decays to $D_s(2317)$, $D_s(2460)$ and Other Final States in Factorization

A. Datta, H. J. Lipkin, and P. J. O'Donnell

Phys. Rev. **D69**, 094002 (May 2004).

Observation of Multipactor in an Alumina-Based Dielectric-Loaded Accelerating Structure

J. G. Power, W. Gai, S. H. Gold, A. K. Kinkead, R. Konecny, C. Jing, W. Liu, and Z. Yusof

Phys. Rev. Lett. **92**, 164801-164804 April (2004).

Overcoming an Intrinsic Depolarizing Resonance with a Partial Siberian Snake

H. Spinka, D. Underwood, et al

Published in Phys. Rev. Special Topics – Accelerators and Beams, Vol. 7, 071001 (2004).

Photoproduction of $D^{*\pm}$ Mesons Associated with a Leading Neutron

S. Chekanov, M. Derrick, D. Krakauer, J. H. Loizides, S. Magill, S. Miglioranzi, B. Musgrave, J. Repond and R. Yoshida

Phys. Letts **B590**, 143-160 (2004).

ANL-HEP-PR-04-13

Relativistic Corrections to Gluon Fragmentation into Spin-Triplet S-wave Quarkonium

G. T. Bodwin and J. Lee

Phys. Rev. **D69**, 054003 (March 2004).

Search for Contact Interactions, Large Extra Dimensions, and Finite Quark Radius in ep Collisions at HERA

M. Derrick, S. Chekanov, D. Krakauer, J. H. Loizides, S. Magill, S. Miglioranzi, B. Musgrave, J. Repond, R. Yoshida
Phys. Lett. **B591**, 23-41 (2004).

Search for QCD-instanton Induced Events in Deep Inelastic ep Scattering at HERA

M. Derrick, S. Chekanov, D. Krakauer, J. H. Loizides, S. Magill, S. Miglioranzi, B. Musgrave, J. Repond, R. Yoshida
Eur. J. of Physics, **C34**, 255-265 (2004).

Seesaw Induced CMSSM Lepton Flavour Violation Post-WMAP

B. Campbell, D. Maybury, and B. Murakami
JHEP 0403:**052** (April 2004).

Substructure Dependence of Jet Cross Sections at HERA and Determination of α_s

M. Derrick, S. Chekanov, J. H. Loizides, S. Magill, B. Musgrave, J. Repond, R. Yoshida
Nucl. Physics. **B700**, 3-50 (2004).

Squark Mixing in Electron-Positron Reactions

E. L. Berger, J. Lee, and T.M.P. Tait
Phys. Rev. **D69**, 055003 (March 2004).

The Dependence of Dijet Production on Photon Virtuality in ep Collisions at HERA

M. Derrick, S. Chekanov, D. Krakauer, J. H. Loizides, S. Magill, S. Miglioranzi, B. Musgrave, J. Repond, R. Yoshida
Eur. J. Physics, **C35**, 487-500 (2004).

The Grid2003 Production Grid: Principles and Practice

I. Foster, J. Gieraltowski, E. May, A. Vaniachine, *et al.*
Published in the *13th IEEE International Symposium on High Performance Distributed Computing (HPDC-13)*, (OmniPress, June 2004) p. 236.

The Narrow Width of the Θ^+ --A Possible Explanation

H. J. Lipkin
Phys. Lett. **B586**, 303-306 (April 2004).

What is Coherent in Neutrino Oscillations

H. J. Lipkin
Phys. Lett. **B579**, 355-360 (January 2004).

IV.B. Major Articles Submitted For Publication

A Digital Hadron Calorimeter with Resistive Plate Chambers

J. Repond

Proceedings of the VII Workshop on Resistive Plate Chambers and Related Detectors, Clermont-Ferrand, France, 2004.

ANL-HEP-CP-04-1

A Mass Inequality for the Ξ^* and Θ^+ Pentaquarks

M. Karliner and H. J. Lipkin

Phys. Letts.

ANL-HEP-PR-04-5

An Inclusive Search for Anomalous Production of High- p_T like-sign Lepton Pairs in $p\bar{p}$ Collisions at $\alpha_s = 1.8$ TeV

W. Ashmanskas, R. E. Blair, K. L. Byrum, S. E. Kuhlmann, T. LeCompte, L. Nodulman, J. Proudfoot, M. Tanaka, R. Thurman-Keup, R. G. Wagner and A. B. Wicklund

Phys. Lett.

ANL-HEP-PR-04-16

Associated Production of a Z Boson and a Single Heavy Quark Jet

J. Campbell, R. K. Ellis, F. Maltoni, and S. Willenbrock

Phys. Rev. D

ANL-HEP-PR-03-104

$B_s - \bar{B}_s$ Mixing in Z' Models with Flavor-Changing Neutral Currents

V. Barger, C.-W. Chiang, J. Jiang, and P. Langacker

Phys. Lett. B

ANL-HEP-PR-04-39

Comment on “Noncommutativity as a Possible Origin of the Ultrahigh-energy Cosmic Ray and the TeV Photon Paradoxes”

C. Zachos

Mod. Phys. Lett. A

ANL-HEP-PR-04-11

Dark Matter, Light Stops and Electroweak Baryogenesis

C. Balazs, M. Carena, and C.E.M. Wagner

Phys. Rev. D

ANL-HEP-PR-04-27

Direct Photon Cross Section with Conversions at CDF

W. Ashmanskas, R. E. Blair, K. L. Byrum, E. Kovacs, S. E. Kuhlmann, T. LeCompte,
L. Nodulman, J. Proudfoot, M. Tanaka, R. Thurman-Keup, R. G. Wagner and A. B. Wicklund
Phys. Rev. D
ANL-HEP-PR-04-36

Electroweak Baryogenesis and Dark Matter in the MSSM

A. Menon, D. E. Morrissey, and C.E.M. Wagner
Phys. Rev. D
ANL-HEP-PR-04-38

Higgs Boson Production in Weak Boson Fusion at Next-to-Leading Order

E. L. Berger and J. M. Campbell
Phys. Rev. D
ANL-HEP-PR-04-4

Light Gluino Constituents of Hadrons and a Global Analysis of Hadron Scattering Data

E. L. Berger, P. M. Nadolsky, F. I. Olness, and J. Pumplin
Phys. Rev. D
ANL-HEP-PR-04-59

Measurement of the $t\bar{t}$ Production Cross Section in $p\bar{p}$ Collisions at $\sqrt{s}=1.96$ TeV
using Dilepton Events

W. Ashmanskas, R. E. Blair, K. L. Byrum, E. Kovacs, S. E. Kuhlmann, T. LeCompte,
L. Nodulman, J. Proudfoot, M. Tanaka, R. Thurman-Keup, R. G. Wagner and A. B. Wicklund
Phys. Rev. Lett. (2004).
ANL-HEP-PR-04-44

Method 2 at NLO

J. M. Campbell and J. Huston
JHEP
ANL-HEP-PR-04-58

Production of Charged Pions and Hadrons in Au+Au Collisions at $\sqrt{s}_{NN} = 130$ GeV

R. V. Cadman, K. Krueger, H. M. Spinka and D. G. Underwood
Phys. Rev. C
ANL-HEP-PR-04-25

Quantum Mechanics in Phase Space (an Overview and Reprint Volume)

C. Zachos, D. Fairlie, and T. Curtright
World Scientific
ANL-HEP-PR-04-49

Search for $B_s^0 \rightarrow \mu + \mu^-$ and $B_d^0 \rightarrow \mu + \mu^-$ Decays in $p\bar{p}$ Collisions at $\sqrt{s} = 1.96$ TeV

W. Ashmanskas, R. E. Blair, K. L. Byrum, E. Kovacs, S. E. Kuhlmann, T. LeCompte,
L. Nodulman, J. Proudfoot, M. Tanaka, R. Thurman-Keup, R. G. Wagner and A. B. Wicklund
Phys. Rev. Lett. March (2004).
ANL-HEP-PR-04-28

Search for Doubly-Charged Higgs Bosons Decaying to Dileptons in $p\bar{p}$ Collisions at
 $\sqrt{s} = 1.96$ TeV

W. Ashmanskas, R. E. Blair, K. L. Byrum, E. Kovacs, S. E. Kuhlmann, T. LeCompte,
L. Nodulman, J. Proudfoot, M. Tanaka, R. Thurman-Keup, R. G. Wagner and
A. B. Wicklund
Phys. Rev. Lett. June (2004).
ANL-HEP-PR-04-78

Seesaw Induced CMSSM Lepton Flavour Violation Post-WMAP

B. Campbell, D. Maybury, and B. Murakami
JHEP
ANL-HEP-PR-03-100

Sextet Quark Physics at the Tevatron?

A. R. White
Phys. Lett. B
ANL-HEP-PR-04-47

Study of Pion Trajectory in the Photoproduction of Leading Neutrons at HERA

M. Derrick, Chekanov, D. Krakauer, J. H. Loizides, S. Magill, S. Miglioranza,
B. Musgrave, J. Repond, R. Yoshida
Phys. Lett. B
ANL-HEP-PR-04-26

SUSY Les Houches Accord: Interfacing SUSY Spectrum Calculators, Decay Packages,
and Event Generators

P. Skands, B. C. Allanach, H. Baer, C. Balazs, *et al.*
JHEP
ANL-HEP-PR-04-51

The Narrow Width of the Θ^+ --A Possible Explanation

H. J. Lipkin
Phys. Lett. B
ANL-HEP-PR-04-2

Transverse Momentum Distribution of Upsilon Production in Hadronic Collisions

E. L. Berger, J.-W. Qiu, and Y. Wang

Phys. Rev. D

ANL-HEP-PR-04-29

Triggers for RF Breakdown

J. Norem, Z. Insopov and I. Konkashbaev

Nucl. Instr. & Methods in Phys. Research A, 1/29/04.

ANL-HEP-PR-04-9

The Underlying Event in Hard Interactions at the Tevatron $p\bar{p}$ Collider

W. Ashmanskas, R. E. Blair, K. L. Byrum, E. Kovacs, S. E. Kuhlmann, T. LeCompte, L.

Nodulman, J. Proudfoot, M. Tanaka, R. Thurman-Keup, R. G. Wagner and A. B. Wicklund

Phys. Rev. D (2004).

ANL-HEP-PR-04-37

Warped Unification, Proton Stability and Dark Matter

K. Agashe and G. Servant

Phys. Rev. Lett.

ANL-HEP-PR-04-19

Why the Θ^+ is Seen in Some Experiments and Not in Others—A Possible Explanation

M. Karliner and H. J. Lipkin

Phys. Rev. D

ANL-HEP-PR-04-45

IV.C Papers Or Abstracts Submitted To Conference Proceedings

A Comparison of Predictions for SM Higgs Boson Production at the LHC

C. Balazs, M. Grazzini, J. Huston, A. Kulesza, and I. Puljak

Les Houches 2003 “Physics at TeV Colliders” Les Houches, France,

26 May—6 June 2003.

ANL-HEP-CP-04-50

Ancillary Abelian Symmetry Solution to the AMSB Slepton Problem

B. Murakami

In: *11th Annual International Conference on Supersymmetry and Unification of the Fundamental Interactions (SUSY 2003: Supersymmetry in the Desert)*, Tucson, AZ, June 5-10, 2003.

ANL-HEP-CP-04-3

ATLAS Detector Description Database Architecture

A. Vaniachine, D. Malon, et al.

In: *Computing in High Energy and Nuclear Physics (CHEP) Conference, Interlaken, Switzerland, 27 September—1 October 2004.*

ANL-HEP-CP-04-95

Determining the Extra-Dimensional Location of the Higgs Boson

A. Aranda, C. Balazs, J. L. Diaz-Cruz, S. Gascon-Shotkin, and O. Ravar

Les Houches 2003 “Physics at TeV Colliders” Les Houches, France, 26 May—6 June 2003.

ANL-HEP-CP-03-112

Experimental Study of Mutipactor Suppression in a Dielectric-Loaded Accelerating Structure

J. G. Power, W. Gai, S.H. Gold, A.K. Kinkead, R. Konecny, C. Jing and W. Liu

In: *Advanced Accelerator Concepts 2004.*

ANL-HEP-CP-04-73

Hard Probes in Heavy Ion Collisions at the LHC: Heavy Flavor Physics

M. Bedjjidian, D. Blaschke, G.T. Bodwin, Jungil Lee and et al.

In: *3rd Workshop on Hard Probes in Heavy Ion Collisions at the LHC, CERN, Geneva, Switzerland, October 7-11, 2002, Yellow Book.*

ANL-HEP-CP-04-12

Higgs Boson and Diphoton Production at the LHC

P. Skands, B. C. Allanach, H. Baer, C. Balazs, et al.

Les Houches 2003 “Physics at TeV Colliders” Les Houches, France, 26 May—6 June 2003.

ANL-HEP-CP-03-111

High Power rf Test on X-band $\text{Mg}_x\text{Ca}_{1-x}\text{TiO}_3$ Based Dielectric-Loaded Accelerating Structure

C. Jing, R. Konecny, W. Gai, S. H. Gold, J. G. Power, A. K. Kinkead, and W. Liu

In: *AIP Conference*, Stony Brook, NY, June 2004.

High Power rf Test on X-band $\text{Mg}_x\text{Ca}_{1-x}\text{TiO}_3$ Based Dielectric-Loaded Accelerating Structure

C. Jing, R. Konecny, W. Gai, S. H. Gold, J. G. Power, A. K. Kinkead, and W. Liu

In: *AIP Conference*, Stony Brook, NY, June 2004.

Pin-Hole Luminosity Monitor with Feedback

J. Norem

In: *5th International Workshop on Electron-Electron Interactions at TeV Energies*, Santa Cruz, California,

ANL-HEP-CP-04-46

Plans for Experiments to Measure θ_{13}

M. Goodman

In: *2003 Coral Gables Conference*, Ft. Lauderdale, Florida.
ANL-HEP-CP-04-43

Proton Stability and Dark Matter: Are They Related?

G. Servant

In: *39th Rencontres de Moriond on QCD and High-Energy Hadronic Interactions*, La Thuile, Italy, March 28—April 4, 2004.
ANL-HEP-CP-04-62

Results of the Searches for Narrow Baryonic States with Strangeness in DIS at HERA

S. Chekanov

In: *XII International Workshop on Deep Inelastic Scattering*, Strbske Pleso, High Tatras, Slovakia, April 14-18, 2004.
ANL-HEP-CP-04-48

Search for Narrow Baryonic States in DIS at HERA

S. V. Chekanov

In: *YITP Workshop on Multi-quark Hadrons: Four, Five and More?*
Kyoto, Japan, February 17-19, 2004.
ANL-HEP-CP-04-034

Simulating Lattice QCD at Finite Temperature and Zero Quark Mass

J. B. Kogut and D. K. Sinclair

Workshop on QCD in Extreme Environments, ANL-HEP, Argonne, IL,
June 29—July 3, 2004.
ANL-HEP-CP-04-72

Summary of the Argonne workshop of High Gradient RF

J. Norem

In: *Conference LINAC 2004*, Lubeck, Germany, Aug. 16-20, 2004.
ANL-HEP-CP-04-80

The Argonne Wakefield Accelerator Facility: Capabilities and Experiments

Manoel E. Conde, Sergey Antipov, Wei Gai, Chunguang Jing, Richard Konecny,
Wanming Liu, John G. Power, Haitao Wang, and Zikri Yusof

In: *AIP Conference*, Stony Brook, NY, June 2004.

The Grid2003 Production Grid: Principles and Practice

ATLAS Collaboration, I. Foster, J. Gieraltowski, E. May, A. Vaniachine, *et al.*

In: *13th IEEE International Symposium on High Performance Distributed Computing (HPDC-13)*, Honolulu, HI, June 4-6, 2004.
ANL-HEP-CP-04-84

The Sensitivity of the LHC for TeV Scale Dimensions in Dijet Production

C. Balazs, M. Escalier, S. Ferrag, B. Laforge, and G. Polesello

Les Houches 2003 “Physics at TeV Colliders” Les Houches, France,

26 May—6 June 2003.

ANL-HEP-CP-03-110

The WEB Interface for the ATLAS/LCG MySQL Conditions Databases and Performance Constraints in the Visualisation of Extensive Scientific/Technical Data

A. Vaniachine, *et al.*

Computing in High Energy and Nuclear Physics (CHEP) Conference,

Interlaken, Switzerland, 27 September—1 October 2004.

ANL-HEP-CP-04-96

Triggers for RF Breakdown

J. Norem, Z. Insepav

In: *9th European Particle Accelerator Conference (EPAC'04)*

ANL-HEP-CP-04-68

IV D. Technical Reports And Notes

Technical Reports

High Energy Division Semiannual Technical Report of Research Activities (July 1, 2003-December 31, 2003).

H.M. Spinka, L.J. Nodulman, M.C. Goodman, J. Repond, D.S. Ayres, J.

Proudfoot, R. Stanek, T. LeCompte, G. Drake, E.L. Berger, G.T. Bodwin, D.K.

Sinclair, C. Zachos, W. Gai and J. Norem

ANL-HEP-TR-03-120

Proposal for a Shift Register Approach to RPC Calorimeter Readout for Test Beam, Cosmics, and Sources.

D. Underwood

ANL-HEP-TR-04-35

Stability of EB When Cryostat Load is Applied

V. Guarino

ANL-HEP-TR-04-65

CDF Notes:

CDF 6919

Reduced Tracking for Calibration,
L. Nodulman, CDF//TRACKING//6919.

CDF 6971

Curvature Corrections for 5.3.1,
L. Nodulman, CDF/DOC/ELECTRON/CDFR/6971.

CDF 7037

Measurement of the J/psi Meson and b Hadron Production Cross > Sections,
M.Bishai, Y.Gotra, J.Kraus, T.LeCompte, J.Lewis, D.Litvintsev, P.Lukens,
T.Miao, R.St.Denis, R.Tesarek, S.Tkaczyk, S.Waschke, T.Yamashita,
CDF/PUB/BOTTOM/CDFR/7037.

WF Notes:

WF-219

Measurements of High Brightness Electro Beam
H. Wang, J. Power, W. Liu, W. Gai
January 24, 2004.

V. COLLOQUIA AND CONFERENCE TALKS

Csaba Balazs

Neutralino Dark Matter and Baryogenesis in the MSSM
12th International Conference on Supersymmetry and Unification of
Fundamental Interactions (SUSY 2004), Tsukuba, Japan, June 17-23, 2004.

Super-, Anti- and Dark Matter
ANL Workshop on the Physics of SUSY, Higgs Bosons, and Extra Dimensions,
Argonne, IL, May 24, 2004.

Baryogenesis and Dark Matter in the MSSM
Physics Department, Michigan State University, East Lansing, May 11, 2004.

Super-, Anti- and Dark Matter
Pheno 2004, Madison, WI, April 26, 2004.

Electroweak baryogenesis and dark matter in the MSSM
High Energy Theory Seminar, Michigan State University, East Lansing MI,
May 11, 2004

Baryogenesis and Dark Matter in the MSSM
Fermilab HEP Theory Seminar, Batavia, IL, April 8, 2004.

Supersymmetric Dark Matter
Physics Department, Purdue University, West Lafayette, IN, February 24, 2004.

Dark Matter
ANL's 2nd Theory Afternoon, Argonne, IL, February 16, 2004.

Supersymmetric Dark Matter
ANL-HEP Theoretical Physics Seminar, Argonne, IL, January 12, 2004.

Edmond L. Berger

Bounds on the Mass of a Light Gluino from a Global PDF Analysis of Hadron Scattering Data
12th International Conference on Supersymmetry and Unification of
Fundamental Interactions (SUSY 2004), Tsukuba, Japan, June 21, 2004.

Higgs Boson plus 2 Jet Production: WBF Signal and QCD Backgrounds
12th International Conference on Supersymmetry and Unification of
Fundamental Interactions (SUSY 2004), Tsukuba, Japan, June 17, 2004.

Higgs Boson Plus Two Jet Production at Next to Leading Order in QCD
Kavli Institute for Theoretical Physics, U California, Santa Barbara, March 23, 2004.

John Campbell

NLO Tools for Colliders
CTEQ Summer School, U Wisconsin, Madison, June 25, 2004.

W and Z + Jet Production
15th Topical Conference on Hadron Collider Physics (HCP 2004), MSU, East
Lansing, MI, June 15, 2004.

Collider Physics at NLO and the Monte Carlo MCFM
Physics Department, Purdue University, West Lafayette, IN, March 30, 2004.

Next-to-Leading Order QCD Tools: Status and Prospects
Collider Physics Conference, Kavli Institute of Theoretical Physics, Santa
Barbara, CA, January 12-16, 2004.

Wei Gai

High Power Rf Testing Of Dielectric Loaded Accelerating Structures
Power Modulator Conference 2004, San Francisco, CA, May 23, 2004.

Development of Dielectric Based Accelerating Structures
Wei Gai, 2004 OCPA Meeting, Shanghai, China, June 30, 2004.

Jing Jiang

Charged Higgs Boson Searches at Hadron Colliders
Physics Department, Purdue University, West Lafayette, IN, February 10, 2004.

Jungil Lee

Belle $J/\psi + \eta_c$ Anomaly

Physics Department, Ohio State University, Columbus, OH, January 14, 2004.

Harry J. Lipkin

The Theory of Pentaquarks

Heavy Quarks and Leptons (HQ&L 2004), San Juan, Puerto Rico, June 2, 2004.

New Results in Hadron Spectroscopy

26th Annual Montreal-Rochester-Syracuse-Toronto Conference (MRST 2004 from Quarks to Cosmology), Montreal, Quebec, Canada, May 13, 2004.

What Does the Pentaquark Teach Us About QCD and Vice Versa?

Physics Division, Argonne National Laboratory, IL, March 9, 2004.

What Does the Pentaquark Teach Us About QCD and Vice Versa?

University of California, Irvine, March 3, 2004.

What Does the Pentaquark Teach Us About QCD and Vice Versa?

University of California, Los Angeles, March 1, 2004.

Experimental Challenges for the Pentaquark

Experimental Group, SLAC, Stanford, CA, February 24, 2004.

What Does the Pentaquark Teach Us About QCD and Vice Versa?

Theory Group, SLAC, Stanford, CA, February 20, 2004.

David Morrissey

Cosmological Properties of the MSSM with a Minimal Singlet Sector

Pheno 2004, Madison, WI, April 26, 2004.

Brandon Murakami

Differentiating Solutions to the Gauge Hierarchy Problem through Rare Muon Decays

12th International Conference on Supersymmetry and Unification of Fundamental Interactions (SUSY 2004), Tsukuba, Japan, June 17, 2004.

Expectations from Forthcoming Lepton Flavor Violation Experiments
Pheno 2004, Madison, WI, April 27, 2004.

Differentiating Solutions to the Gauge Hierarchy Problem through Rare Muon Decay
Department of Physics, Northwestern University, Evanston, IL, March 1, 2004.

Differentiating Solutions to the Gauge Hierarchy Problem through Rare Muon Decays
Lake Louise Winter Institute: Fundamental Interactions, Alberta, Canada,
February 17, 2004.

James Norem

The Limits of RF Acceleration in Metal Structures,
Enrico Fermi Institute, Univ. of Chicago, April 26, 2004.

Jose' Repond

Testing Calorimeter Prototypes with Particle Beams
American Linear Collider Workshop, SLAC, Stanford, January 2004

Geraldine Servant

Gauged Baryon Number in Warped GUT
Department of Physics, U Washington, Seattle, June 18, 2004.

Warped Unification, Proton Stability and Dark Matter
Department of Physics, Caltech, Pasadena, CA, May 10, 2004.

Proton Stability and Dark Matter: Are They Related?
Physics Department, University of Wisconsin, Madison, April 22, 2004.

Proton Stability and Dark Matter: Are They Related?
39th Rencontres de Moriond on QCD and High-Energy Hadronic Interactions,
La Thuile, Italy, March 21-28, 2004.

Baryon Number and Dark Matter in Warped SO(10)
Lawrence Berkeley National Laboratory, Berkeley, CA, February 3, 2004.

Donald K. Sinclair

Simulating Lattice QCD at Finite Temperature and Zero Quark Mass

Workshop on QCD in Extreme Environments, ANL-HEP, Argonne, IL
June 29—July 3, 2004.

The Finite Temperature Transition for 3-Flavor Lattice QCD at Finite Isospin Density

22nd International Symposium on Lattice Field Theory (Lattice 2004), FNAL,
Batavia, IL, June 21-26, 2004.

David Underwood

BNL: “A Few Polarimeter Studies” (Analysis by H. Spinka with a few interpretations by D.U.)

RHIC SPIN Meeting, Sept 02, 2004.

Plans for RPC – DHCAL Prototype,

Presented at American Linear Collider Physics Group Workshop, ALCPG2004,
SLAC, Pasadena, CA, 7-10 January, 2004.

RPC R&D for DHCAL at ANL

LCWS2004, April 21, 2004 Paris, France:

Some Recent Developments: Amplifiers for Reading Systems, Electrostatics, Source tests, etc,
Fermilab RPC meeting, February 13, 2004.

Carlos Wagner

Phenomenology of Higgs with CP Violation

12th International Conference on Supersymmetry and Unification of
Fundamental Interactions (SUSY 2004), Tsukuba, Japan, June 17-23, 2004.

New Results in Electroweak Baryogenesis

April Meeting of the American Physical Society, Denver, CO, May 4, 2004.

Supersymmetry, Dark Matter and Electroweak Baryogenesis

Department of Physics, Ohio State University, Columbus, OH, April 19, 2004.

Cosmology and Phenomenology of the nMSSM

39th Rencontres de Moriond on QCD and High-Energy Hadronic Interactions,
La Thuile, Italy, March 21-28, 2004.

Dark Matter and Electroweak Baryogenesis in SUSY Models

Department of Physics, University of Colorado, Boulder, CO, March 12, 2004.

Introduction to Cosmology

Lecture Series, U Chicago, IL, March-May 2004.

Supersymmetry and the Matter-Antimatter Asymmetry

Northwestern University, Evanston, IL, February 2004.

Supersymmetry, Dark Matter and Electroweak Baryogenesis

Graduate students, U Chicago, IL, February 2004.

Extra Dimensions—Large, Small and Universal

2004 Aspen Winter Conference on Particle Physics, “Where We Are and Where We Are Going”, CO, February 2, 2004.

Cosmas Zachos

Branes, Quantum Nambu Brackets, and the Hydrogen Atom

XIII International Colloquium on Integrable Systems and Quantum Groups (ISQS-13), Prague, Czech Republic, June 18, 2004; also, Session Chair, June 17, 2004.

Deformation Quantization: QM Lives and Works in Phase Space

Physics Department, Virginia Technical Institute, Blacksburg, March 26, 2004.

Membranes and Consistent Quantization of Nambu Mechanics

Physics Department, California Institute of Technology, Pasadena, March 12, 2004.

VI. HIGH ENERGY PHYSICS COMMUNITY ACTIVITIES

Csaba Balazs

Co-Organizer, Argonne Theory Institute on the Physics of Supersymmetry, Higgs Bosons, and Extra Dimensions, High Energy Physics Division, Argonne, IL, May 24-28, 2004.

A Referee of Physical Review D.

Edmond L. Berger

Co-Chair, International Linear Collider Summer Study, Snowmass, CO, August 13-27, 2005.

Advisory Board, FRONTIERS IN CONTEMPORARY PHYSICS - III, Vanderbilt University, Nashville, TN, May, 2005.

Advisory Committee, 2005 Aspen Winter Meeting on Particle Physics, CO, February 13-19, 2005.

Organizing Committee, Workshop on QCD, SURA, Washington, DC, February 10-12, 2005.

International Advisory Committee, International Conference on Flavor Physics, Taiwan, 2005.

International Advisory Committee, HADRON 2005, Rio de Janeiro, Brazil, 2005.

Organizing Committee, 9th Conference on the Intersections of Particle and Nuclear Physics (CIPANP 2005), 2005.

Scientific Program Committee, Vth Rencontres du Vietnam, Hanoi, Vietnam, August 6-11, 2004.

Co-Organizer, Argonne Theory Institute on the Physics of Supersymmetry, Higgs Bosons, and Extra Dimensions, High Energy Physics Division, Argonne, IL, May 24-28, 2004.

Scientific Program Organizing Committee, XXXIXth Rencontres de Moriond, QCD and High Energy Hadronic Interactions, La Thuile, March 28—April 4, 2004.

Organizer, ANL 2nd Lab-Wide Theory Afternoon, Argonne, IL, February 16, 2004.

Co-Chair, Aspen Winter Conference on Particle Physics, “Where We Are and Where We Are Going”, Aspen Center for Physics, CO, February 1-7, 2004.
(<http://gate.hep.anl.gov/berger/Aspen04>)

Scientific Advisory Board, Argonne Theory Institute, 2004
(<http://www.anl.gov/OPA/theoryinstitute/index.html>)

Co-Principal Investigator, Argonne Theory Institute, 2003—

Member, Committee on International Scientific Affairs, American Physical Society, 2003—

Member, Andrew Gemant Award Committee, American Institute of Physics, 2002—

Member, American Linear Collider Working Group, 2002—

Adjunct Professor of Physics, Michigan State University, East Lansing, MI, 1997—present.

Member, Coordinated Theoretical-Experimental Project on QCD (CTEQ) Collaboration.

Geoffrey T. Bodwin

Member, International Advisory Committee and Convener for the Heavy Quarks (and Gluonia) Section, Sixth International Conference on Quark Confinement and the Hadron Spectrum, Sardinia, Italy, September 21-25, 2004.

Member, Local Organizing Committee, XXII International Symposium on Lattice Field Theory (LATTICE 2004), Fermilab, Batavia, IL, June 21-26, 2004.

Convener, Production Section, Quarkonium Working Group QWNET Proposal to fund a Marie Curie Research Training Network on Heavy Quarkonium, 2003—present.

Member, Working Group for the Production Section of Quarkonium Working Group CERN Yellow Report, November 2002—present.

Member, Quarkonium Working Group, 2002—present.

John Campbell

Co-Organizer, ANL-HEP Theoretical Physics Seminars, 2002—2004.

Wei Gai

Advanced Accelerator Concept 2004, Stony Brook, NY, Member of Organizing Committee

Accelerator Safety Review Committee, Argonne National Lab.

Advanced Photon Source 20 years Study Committee, ANL

Jing Jiang

Co-Organizer, ANL-HEP Division Lunch Seminars, 2002—2004.

Edward May

Member of organizing committee for "ESnet Collaboration Services Workshop," Oct 27-29, 2005.

Invited presentation "What is the RCWG and Why Should I Care?" at the "ESnet Collaboration Services Workshop", Oct 27, 2004.

Meeting organization and general administration for the ESnet Steering Committee.

Brandon Murakami

Co-Organizer, ANL-HEP Theoretical Physics Seminars, 2002—2004.

James Norem

Muon Collaboration, Technical Committee

Jose' Repond

Convener of the American Linear Collider Calorimetry Working Group

Member of both the International Advisory and the Local Organizing Committee for DIS2005

Geraldine Servant

Co-Organizer, ANL-HEP Theoretical Physics Seminars, 2003—2004.

Donald Sinclair

Organizer, Argonne Workshop on QCD in Extreme Environments, Argonne, IL, June 29—July 3, 2004.

Carlos Wagner

Co-Organizer, 2004 TASI Lectures, "Physics in D Greater or Equal than 4", Boulder, CO, June 2004.

Co-Organizer, Argonne Theory Institute on the Physics of Supersymmetry, Higgs Bosons, and Extra Dimensions, High Energy Physics Division, Argonne, IL, May 24-28, 2004.

Head, Theory Committee, Argonne National Laboratory, 2003—

Head, Theory Group, HEP Division, Argonne National Laboratory, September 2002—

Associate Professor, Lecturer for Courses on "Supersymmetry and Advanced Electrodynamics" and "Introduction to Cosmology", EFI, U Chicago, IL, 2000—

Cosmas Zachos

Member, International Advisory Board, Ninth International Wigner Symposium [WIGSYM-9], Poznan, Poland, July 18-22, 2005.

Session Organizer, New Ideas/Developments, 2004 Coral Gables Conference: "Celebrating 40 Years of Quarks and Coral Gables Conferences" [CGC 2004], Key Biscayne, FL, December 15-19, 2004.

Member, Advisory Panel, J. Phys A: Math Gen (IOP).

VII. HEP DIVISION RESEARCH PERSONNEL

Administration

Price, L.

Hill, D.

Accelerator Physicists

Conde, M.

Norem, J.

Gai, W.

Power, J.

Yusof, Z.

Experimental Physicists

Ayres, D.

Proudfoot, J.

Blair, R.

Repond, J.

Byrum, K.

Reyna, D.

Cadman, R.

Spinka, H.

Chekanov, S.

Stanek, R.

Derrick, M.

Talaga, R.

Fields, T.

Tanaka, M.

Goodman, M.

Thron, J.

Kuhlmann, S.

Underwood, D.

LeCompte, T.

Wagner, R.

Magill, S.

Wicklund, A. B.

May, E.

Xia, L.

Musgrave, B.

Yokosawa, A.

Nodulman, L.

Yoshida, R.

Theoretical Physicists

Balacz, C.

Murakami, B.

Berger, E.

Servant, G.

Bodwin, G.

Sinclair, D.

Campbell, J.

Wagner, C.

Chiang, C. W.

Zachos, C.

Jiang, J.

Lee, J.

Engineers and Computer Scientists

Cranshaw, J.	Karr, K.
Dawson, J.	Kovacs, E.
Drake, G.	Malon, D.
Grudzinski, J.	Schlereth, J.
Guarino, V.	Vaniachine, A.
Gieraltowski, J.	

Technical Support Staff

Adams, C.	Kasprzyk, T.
Ambats, I.	Konecny, R.
Cox, G.	Nephew, T.
Cundiff, T.	Reed, L.
Farrow, M.	Rezmer, R.
Franchini, F.	Skrzecz, F.
Haberichter, W.	Wood, K.

Laboratory Graduate Participants

Korobkin, D.	Jing, C.
Loizides, J.	Morrissey, D.
Miglioranzi, S.	Wang, H.

Visiting Scientists

Kovacs, E. (Theory)	Lipkin, H. (Theory)
Liu, W (AWA)	Ramsey, G. (Theory)
	Uretsky, J. (Theory)